Characterization of *Staphylococcus aureus* peptidogylcan hydrolases and isolation of defined peptidoglycan structures

der Fakultät für Biologie

der Eberhard Karls Universität Tübingen

zur Erlangung des Grades eines Doktors

der Naturwissenschaften

von

Raja Biswas

aus

Bishnupur, Indien

vorgelegte

Dissertation

2006

Tag der mündlichen Prüfung:	27.07.2006
Dekan:	Prof. Dr. F. Schöffl
1. Berichterstatter:	Prof. Dr. F. Götz
2. Berichterstatter:	Prof. Dr. V. Braun

… for my parents

INDEX

ABBREVIATIONS

aa	amino acids
Amp	ampicillin
APS	ammonium persulphate
ATP	adenosine triphosphate
Bp	base pair
BSA	bovine serum albumin
C	centigrade
Cm	chloramphenicol
Da	dalton
DMSO	dimethyl sulfoxide
DNA	deoxyribonucleic acid
DNase	deoxy ribonuclease
dNTP	deoxyribonucleoside 5´-triphosphates
DTT	1,4-dithiothreitol
EDTA	ethylenediamine tetraacetic acid
Fig	figure
FPLC	fast protein liquid chromatography
g	gram
h	hour
HPLC	high performance liquid chromatography
HFA	hydro fluoric acid
6×His	hexahistidines
IPTG	isopropyl-β-thiogalactoside
l	liter
K	kilo
Kb	kilobase
kDa	kilodalton
M	molar
m	milli
MALDI-MS	Matrix assisted laser desorption ionization mass spectrometry
min	minute

MW	molecular weight
MS	mass spectroscopy
NaOH	sodium hydroxide
Ni-NTA	nickel-nitrilotriacetic acid
ORF	open reading frame
PCR	polymerase chain reaction
PEG	polyethylene glycol
PG	peptidoglycan
PGRP (s)	peptidoglycan receptor protein (s)
PAMP(s)	pathogen-associated molecular pattern(s)
PMSF	phenylmethylsulfonyl fluoride
PRR(s)	pattern recognition receptor(s)
RNase	ribonuclease
RP	reverse phase
rpm	rotation per minute
RT	room temperature
s	second
SDS	sodium dodecyl sulphate
PAGE	polyacrylamide gel electrophoresis
TCA	trichloroacetic acid
TEMED	N,N,N´,N´-tetramethylethylenediamine
TLR (s)	toll Like receptor (s)
Trisma	tris hydroxymethyl aminomethane
U	unit
UV	ultraviolet
wt	wild-type

SYMBOLS

Δ	deletion
°	degree
λ	lamda
µ	micro
::	insertion

A. SUMMARY

Peptidoglycan (PG) hydrolases or autolysins are a group of enzymes which catalyze the degradation of bacterial cell wall at specific sites. *Staphylococcus aureus* produces two major PG hydrolases: major autolysin (Atl) and Aaa, a autolysin/ adhesin protein. The major autolysins of *Staphylococcus aureus* (AtlA) and of *Staphylococcus epidermidis* (AtlE) are well-studied enzymes. But little is known about the Aaa protein. To analyse the possible role of these PG hydrolases we constructed the *atlA* and *aaa* deletion mutants in *S. aureus*.

SAΔ*atl*A formed large cell clusters and was biofilm-negative owing to a deficiency in adherence to the indwelling device surface. In electron micrographs, the mutant cells were distinguished by a rough outer cell surface. A high proportion of abnormally formed multicells that were septated but not separated from each other were observed, which suggested hampered cell separation. Both *atlA* and *atlE* complemented the mutant.

The *atl* gene product is a bifunctional protein that has an N-terminal N-acetyl L-alanine amidase (Ami) domain, three internal repeat domains ($R_{1, 2, 3}$) and a C-terminal endo-ß-N-acetylglucosaminidase (GL) domain which undergo proteolytic processing to generate the two extracellular lytic enzymes (62 kDa Ami-$R_{1, 2}$ and 51 kDa R_3-GL) found in the culture broth of *S. aureus*. In the mature protein repeats R_1 and R_2 are located at the C-terminal portion of the amidase (Ami-$R_{1, 2}$) and repeat R3 is located at N-terminal portion of the glucosaminidase (R_3-GL). To study the role of the repetitive sequences of *atlE,* we expressed in *Escherichia coli* the amidase domain encoded by the gene, carrying no repeat regions (*amiE*) or two repeat regions (*amiE*-$R_{1, 2}$), or the three repeat regions alone ($R_{1, 2, 3}$) as N-terminal His-tag fusion proteins. Only slight differences in the cell wall lytic activity between AmiE and AmiE-$R_{1, 2}$ were observed. The repetitive sequences have a good binding affinity to isolated peptidoglycan and might contribute to the targeting of the amidase to the substrate. AmiE and AmiE-$R_{1, 2}$ have a broad substrate specificity as shown by similar activities with peptidoglycan (PG) lacking wall teichoic acid, O-acetylation, or both. Since the amidase activity of AtlA and AtlE has not been proved biochemically, we used purified AmiE-$R_{1, 2}$ to determine the exact PG cleavage site. We provide the

first evidence that the amidase indeed cleaves the amide bond between *N*-acetyl muramic acid and L-alanine.

SAΔ*aaa* mutant did not differ from the wild type in its colony morphology, growth rate, cell cluster and biofilm formation, suggesting that Aaa does not play a vital role in cell separation or, more probably, that the function of Aaa in cell separation may have been taken over by the major autolysin Atl, which seemed to be more strongly expressed in the *aaa* mutant than in the wild type. Autolysin/adhesin protein Aaa is a 35 kDa protein containing two direct LysM (lysine motif) repeats at the N-terminal and catalytic domain in the C-terminus. The C-terminal catalytic domain of Aaa is homologous to the CHAP (cysteine, histidine-dependent amidohydrolases/ peptidases) domain. This domain is often found in PG hydrolysing enzymes.

This work also established a purification method for isolation of soluble defined staphylococcal peptidoglycan fragments (PGs). Compared to earlier methods, which were based on using insoluble purified peptidoglycan, we standardize the purification method soluble PGs using HPLC. Commercially available mutanolysin and lysostaphin can be used to cleave PG structures. Apart from these two lytic enzymes, we biochemically characterized the amidase, which provides an alternative tool for PG analysis. Mutanolysin, lysostaphin and amidase can be used individually or together to isolate muropeptides, stem peptides or sugar residues for studying host cell signaling activities.

B. INTRODUCTION

The major component of the Gram-positive bacterial cell wall is peptidoglycan composed of glycan strands cross-linked by oligopeptides forming the sacculus around the cell. The cell wall not only functions to protect bacteria from environmental stress and osmotic lysis, but also serves as a surface organelle that allows pathogens to interact with their environment, most notably the infected tissues of the host (Navarre *et al.*, 1999).

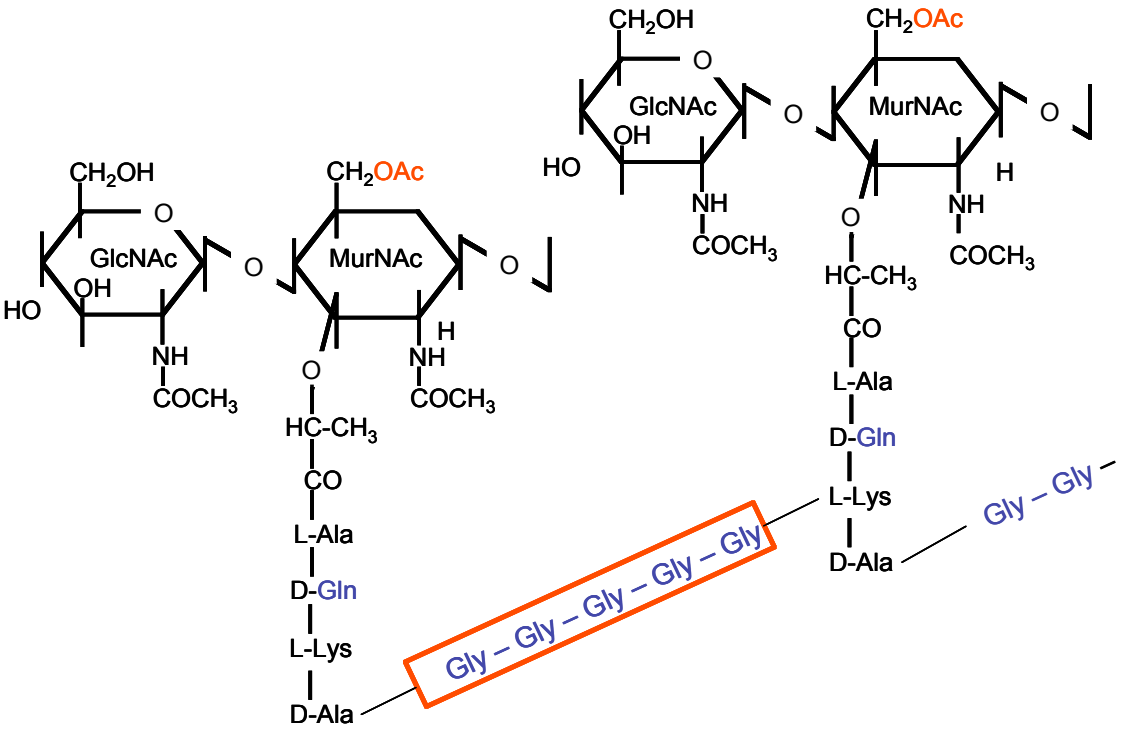

Fig. 1. Structure of *S. aureus* peptidoglycan (PG). Staphylococcal peptidoglycan is composed of glycan strands, peptide subunits, and penta glycine cross bridges. The repeating disaccharide, N-acetylmuramic acid (MurNAc) and N-acetylglucosamine (GlcNAc) are β, 1-4 linked with each other. The D-lactyl moiety of N-acetylmuramic acid is amide-linked to the short peptides L-Ala-D-Gln-L-Lys-D-Ala. These peptides are cross-linked with other peptides via penta glycine residues.

The peptidoglycan of *S. aureus* consists of a repeating disaccharide, N-acetylmuramic acid- (β, 1-4)-N-acetylglucosamine (MurNAc – GlcNAc) (Ghuysen and Strominger, 1963a, b). The D-lactyl moiety of N-acetylmuramic acid is amide-linked to the short peptide component of peptidoglycan. The peptide is unusual as it consists of both D- and L- amino acids forming unique L-D peptide bonds in the peptidoglycan (**Fig. 1 and 2**). These peptides are cross-linked with other peptides attached to neighbouring glycan strands, thereby generating a three-dimensional network that surrounds the staphylococcal cell (Navarre *et al.*, 1999). During cell wall synthesis the peptidoglycan precursor molecule, lipid II, C55-PP-MurNAc-(L-Ala-D-iGln-L-Lys-(NH2-Gly5)-D-Ala-D-Ala-COOH-GlcNAc (C55-PP is undecaprenyl pyrophosphate), is incorporated into the peptidoglycan network via transglycosylation and transpeptidation reactions. Whereas transglycosylation leads to the polymerization of the glycan strands, the transpeptidation reaction results in the cross-linking of the peptide backbone of the cell wall. During this reaction, the terminal D-Ala of the pentapeptide precursor (L-Ala-D-iGln-L-Lys-(NH2-Gly5)-D-Ala-D-Ala-COOH) is removed and the carboxyl of D-Ala at position four is linked to the free amino of the pentaglycine cross-bridge within cell wall peptides of neighboring peptidoglycan strands (Grundling and Schneewind, 2006; Navarre *et al.*, 1999).

Various peptidoglycan degrading enzymes with different action mechanisms have been isolated from animals, plants, and microorganisms and characterized. These enzymes are able to hydrolyse particular bonds in cell wall peptidoglycan and are generally classified into three groups: muramidases which hydrolyse the polysaccharide chain; endopeptidases which cleave the peptide moiety; and N-actetyl muramoyl L-alanine amidases which split the linkage between polysaccharides and peptides (Huard *et al.*, 2003; Jayaswal *et al.*, 1990; Schindler and Schuhardt, 1964; Strominger and Ghuysen, 1967). Through cell wall degradation, these hydrolytic enzymes may be involved in important biological processes such as cell wall turnover, cell separation, genetic transformation, formation of flagella and sporulation. Some of these enzymes are bactericidal, having the potential for use as antimicrobial agents.

Fig. 1 and 2 show the structure of the staphylococcal peptidoglycan and the cleavage sites of muralytic enzymes. Bacteria produce several peptidoglycan

hydrolases that are involved in the degradation of the peptidoglycan. The main physiological functions include cleaving the peptidoglycan for insertion of newly synthesized cell wall components during cell growth, division and separation. Some of these maintenance enzymes are autolysins disintegrating the peptidoglycan when cells are placed under unfavorable conditions that lead to autolysis.

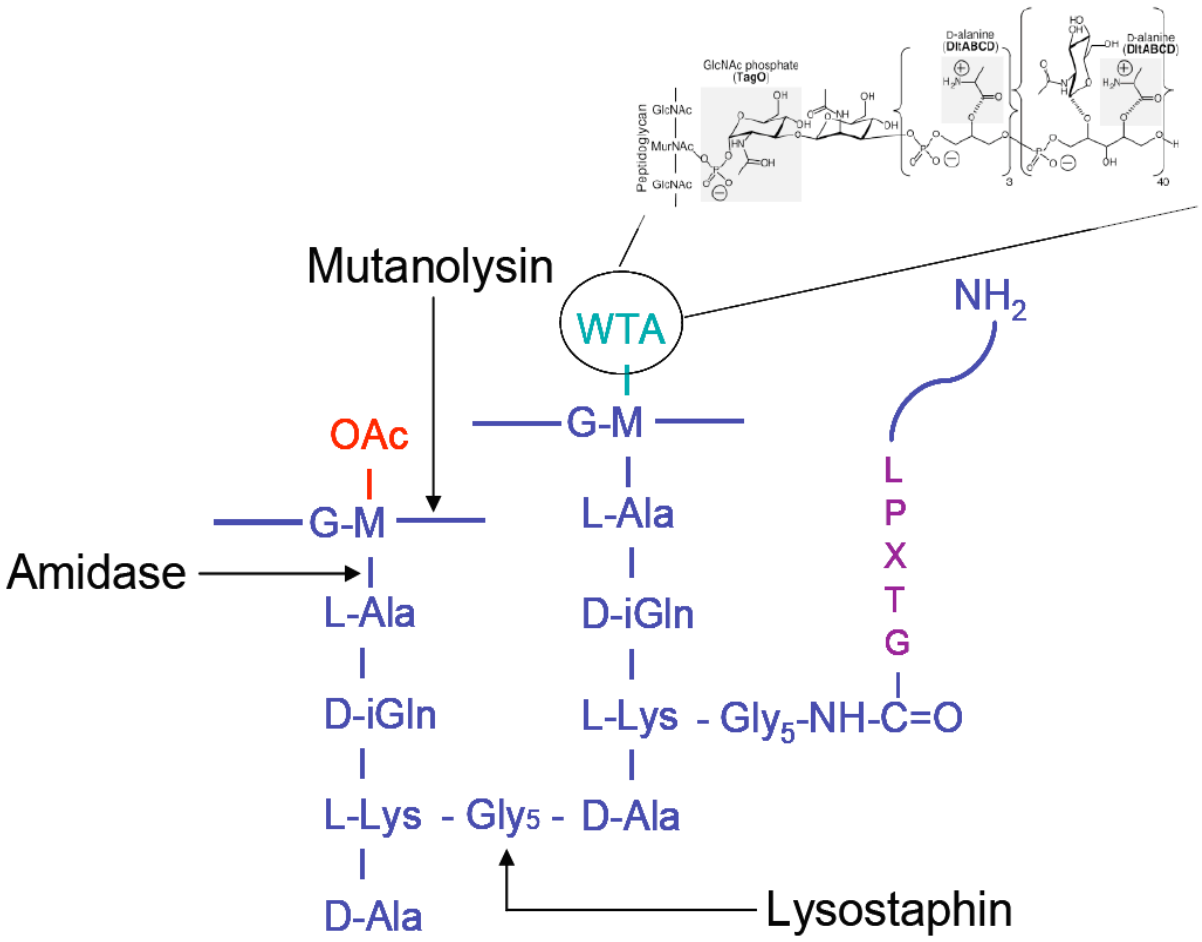

Fig. 2. Diagram of *Staphylococcus aureus* peptidoglycan, indicating the cleavage sites of mutanolysin, lysostaphin and amidase. *S. aureus* peptidoglycan is highly modified. The C6-OH group of muramic acid in staphylococci is modified by O-acetylation and also serves as an anchor for cell wall teichoic acid (WTA). The fifth glycine of the pentapeptide bridge of uncross-linked peptidoglycan is sometimes linked with covalently associated proteins via a LPXTG motif (Perry *et al.*, 2002).

The major peptidoglycan hydrolase of *S. aureus* was identified as a bifunctional autolysin called AtlA (Oshida et al., 1995). AtlA is initially produced as a 138 kDa

protein that possess an amidase domain and a glucosaminidase domain (Heilmann *et al.*, 1997a; Oshida *et al.*, 1995). It undergoes proteolytic processing to generate, the 62 kDa N-acetylmuramyl-l-alanine amidase (Ami) and the 51 kDa N-acetylglucosaminidase (GL). In *S. aureus* cells, more than 95% of the PG subunits are cross-linked. This extremely high degree of cross-linking is possible only because the long and flexible penta-glycine interpeptide bridges are able to span distances between peptides which otherwise are too far apart to be cross-linked.

PG of *S. aureus* is highly modified. It has almost no free carboxyl groups since the α-carboxyl group of D-glutamic acid is amidated (Pucci *et al.*, 1995; Sugai *et al.*, 1995; Tipper *et al.*, 1967) and about 50% of the muramic acid residues are 4-*N*, 6-*O*-diacetyl-derivatized (Sugai *et al.*, 1995; Tipper *et al.*, 1971). This latter substitution renders PG resistant to human and egg-white lysozyme. As has been shown recently, the major determinant for this high lysozyme resistance is the PG-specific *O*-acetyltransferase, OatA (Bera *et al.*, 2005b).

Moreover, peptidoglycan is also associated with surface proteins. *S. aureus* surface proteins (**Fig. 2**) can be classified into three major types: (i) surface proteins covalently linked to the peptidoglycan by their C-terminal domain (LPXTG proteins) (Carlin and Viitanen); proteins associated to the surface by ionic or hydrophobic interaction; (iii) proteins attached to the surface by their N-terminal region (lipoproteins) (Cabanes *et al.*, 2004). The two major peptidoglycan hydrolases (AtlA and Aaa) are associated with cell surface by hydrophobic interactions (Heilmann *et al.*, 2005).

AtlA of *S. aureus* (Oshida *et al.*, 1995) and AtlE of *S. epidermidis* (Heilmann *et al.*, 1997b) are quite similar in both sequence and domain organization. The enzymes are bifunctional, composed of an amidase and a glucosaminidase domain. Cells of SA∆*atlA* and SA∆*atlE* mutants form large clusters (Heilmann *et al.*, 1997b; Sugai *et al.*, 1995). The wild-type phenotype of *S. epidermidis* AtlE, i.e., moderate cell clustering, primary adhesion to polystyrene, and binding to vitronectin and fibronectin, is restored in *atlE* mutants carrying the DNA encoding the 60-kDa amidase domain and the two repeat sequences R1 and R2 (Heilmann *et al.*, 1997b).

These results identified a new function of AtlE as an adhesin involved in the primary attachment of the cells to a polystyrene surface, the first step in biofilm formation.

Recently, two very similar novel autolysin/adhesins in *S. epidermidis* (Aae) (Heilmann *et al.*, 2003) and *S. aureus* (Aaa) (Heilmann *et al.*, 2005; Sugai *et al.*, 1995) have been described. Both are 35-kDa surface-associated proteins and their N-terminal portion contains three repetitive sequences that might be putative PG-binding domains (LysM domain) found in a number of enzymes involved in cell-wall metabolism and also in some adhesins. In addition to their bacteriolytic activity, Aaa and Aae also bind to fibrinogen, fibronectin, and vitronectin.

Deletion of *aaA* does not inhibit cell separation, nor induce *S. aureus* to form clusters (Heilmann *et al.*, 2005). However, Aaa gets overexpressed in an *atl* mutant. It is assumed that overexpression of Aaa compensates the functional loss of the major autolysin. These results suggest that *S. aureus* uses two peptidoglycan hydrolases, Aaa and Atl, which are involved in cell separation after cell division.

Gram-positive bacteria trigger some of the most powerful inflammatory responses known to medicine (Dziarski, 2004; Takeuchi and Akira, 2001). The cell wall of these bacteria is a surface consisting of several layers of an insoluble network of peptidoglycan (PG) which are associated with teichoic acids, lipopeptides, as well as covalently or noncovalently linked proteins (**Fig. 3**). Recent studies have provided some information about the role of PG in cell signaling. In this context, Gram-positive PG has attracted much attention because more than 60% of a gram-positive bacterium is composed of PG. To detect microbial infection, multicellular organisms have evolved sensing systems for pathogen-associated molecular patterns (PAMPs) (Esen and Kielian, 2006). Staphylococcal peptidoglycan serves as PAMP that acts as an elicitor of innate immunity. During sepsis and endocarditis, *Staphylococcus aureus* can activate blood coagulation (Mattsson *et al.*, 2002). Similarly, LPS from gram negative bacteria and LTA and peptidoglycan of gram positive bacteria can induce expression of proinflamatory cytokines (Takeuchi *et al.*, 1999).

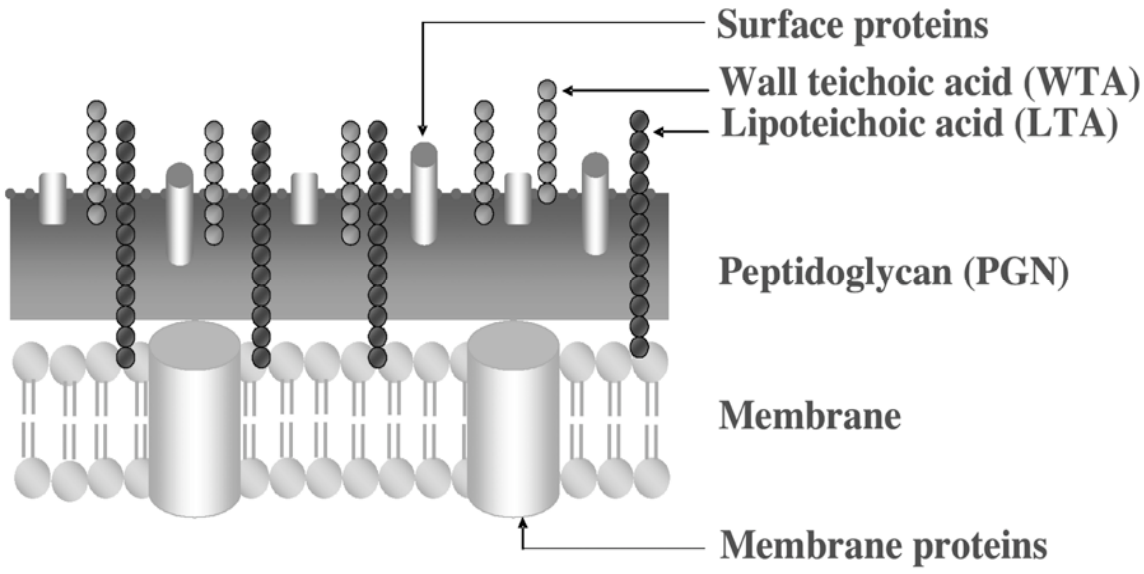

Fig. 3. Schematic representation of bacterial cell wall architecture in association with LTA, WTA, and proteins. The cell wall of *S. aureus* is composed mainly of peptidoglycan (PG) (50 to 60% by weight), wall teichoic acid (WTA), lipoteichoic acid (LTA), lipo-proteins and covalently or non-covalently associated proteins.

The host recognizes bacterial components known as pathogen associated molecular patterns (PAMPs) and regulates cellular responses. Toll like receptors (TLR), a type I transmembrane protein, has been found to act as a major signalling receptor for PAMPs (Kirschning and Schumann, 2002). To date, >10 members of the TLR family have been discovered and most of their ligands were identified (Akira and Sato, 2003; Barton and Medzhitov, 2002; Janssens and Beyaert, 2003). TLR4 is a well characterized member of the family which recognizes LPS (Fitzgerald *et al.*, 2003), an outer membrane component of gram-negative bacteria. TLR9 has been reported to be involved in immune responses to unmethylated CpG DNA (Bauer *et al.*, 2001; Chuang *et al.*, 2002), and TLR-3 and TLR7/8 sense viral double- and single stranded RNA (Crozat and Beutler, 2004). Activation of TLR-5 has been demonstrated to be mediated by bacterial flagellin (Tallant *et al.*, 2004). Bacterial lipoproteins have been found to be stimuli of the TLR-2 subfamily (TLR1, 2 and 6) (Hirschfeld *et al.*, 1999). TLR recognizes PAMPs through an extracellular leucine rich repeat domain and activates signal transduction cascades via a cytoplasmic TOLL/ IL-1 receptor domain (Yamamoto *et al.*, 2004). The cascades involve MyD 88, IRAK, TAK1 and TRAF 6 activate NF-κB which lead to expression of inflammatory

mediator genes. During infection, *S. aureus* activates cells and evokes serious inflammations in the host. TLR2 has been shown to play a crucial role in the host response to *S. aureus*. However, detailed information on molecular components of *S. aureus* cells interacting with TLR2 remains unclear. In recent years, a number of contradictory ideas developed in this field. For example, a recent report emphasize that TLR2 dependent bacterial sensing does not occur via peptidoglycan recognition (Travassos *et al.*, 2004). On the other hand, a number of other data shares the opposite (Dziarski and Gupta, 2005; Hadley *et al.*, 2005; Wang *et al.*, 2001; Yoshimura *et al.*, 1999). However, most of such ideas are based on results obtained from experiments using purified insoluble peptidoglycan or synthetic muramoyl dipeptide.

It must also be considered that Nod factors and peptidoglycan receptor proteins can recognise peptidoglycan. Nod1 and Nod2 (Girardin *et al.*, 2003; Strober *et al.*, 2006) are recently described proteins involved in innate immune defense (Chamaillard *et al.*, 2003). These intracellular surveillance proteins detect bacterial PGN. Nod1 and Nod2 initiate pro-inflammatory signaling via NF-κB activation, which is necessary for clearance of infecting pathogens from the host (Boneca, 2005). It was demonstrated that the naturally occurring PGN degradation product sensed by Nod1 is GlcNAc-MurNAc-L-Ala-D-Glu-meso-DAP (GM-triDAP) (Girardin *et al.*, 2003). However, the minimal PGN structure is comprised of the dipeptide D-Glu-meso-DAP, in which meso-DAP amino acid is in the terminal position. The presence of meso-DAP is a characteristic of most Gram-negative bacteria plus some Gram-positive bacteria. The specificity of Nod1 to detect this subset of bacteria might represent a selective advantage for the host in certain cases when Gram-negative bacteria represent the main threat, such as in the epithelial cells lining the intestinal mucosa.

In contrast, Nod2 has been implicated as a general sensor for both Gram-positive and Gram-negative PGNs. Biochemical and functional analysis have identified muramyl dipeptide MurNAc-L-Ala-D-isoGln (MDP), the minimal motif in all PGNs, as the essential structure recognized by Nod2. Apart from Nods and TLRs host cells also produce highly conserved peptidoglycan receptor proteins. They recognize unique cell wall components of bacteria. In humans four such proteins

were described, *viz*., PGRP-Iα, Iβ, L and S (Liu *et al*., 2001; Swaminathan *et al*., 2006). A list of bacterial PAMPs and their receptors are listed in Table1:

Table. 1. Bacterial PAMPs and their receptors.

PAMP	Bacteria	PRRs
LPS	Gram negative	TLR-4
Lipoprotein, lipopeptide	Eubacteria	TLR-2, TLR-6, CD-36
Lipoteichoic acid	Gram positive	TLR-2, TLR-6
Peptidoglycan	Bacteria	TLR-2, Nods, PGRPs
CpG	Nonmethylated CpG DNA	TLR-9
Flagellin	Most Bacteria	TLR-5

In plants, recognition-dependent disease resistance has been studied most thoroughly and most successfully in cases that depend on the presence of specific resistance-genes which confer immunity to particular races of plant pathogens (Dangl and Jones, 2001). Several of these resistance genes were shown to be involved in the chemoperception of factors specifically attributed with particular strains of pathogens (Felix and Boller, 2003). In addition, plants have a broader, more basal surveillance involving sensitive perception systems for patterns characteristic for entire groups, or classes of microorganisms, and they respond to these general elicitors with activation of signalling pathways that initiate defence mechanisms. This is highly reminiscent of innate immunity in animals and humans. Among the elicitors that represent patterns characteristic for fungi are cell wall components like glucans, chitin and chitosan oligosaccharides, peptides and proteins with fungal-specific N-glycosylation and the membrane component ergosterol. Similarly, cells of many plant species have a perception system for the common bacterial surface protein flagellin (Felix *et al.*, 1999), the building block of the flagella. Perception of general elicitors in plants resembles perception of PAMPs in the innate immune system of animals with respect to the type of molecules perceived, the characteristics of pattern recognition receptors (PRRs) involved, as well as some of the signalling mechanisms and

defence responses induced. In initial experiments we tested heat-killed cells of different Staphylococcal strains and mutants for induction of responses in Arabidopsis. Peptidoglycan has long been known as a PAMP signalling component of gram-positive bacteria in the innate immune systems of animals. However, the role of peptidoglycan in signalling plant response has not been experimentally proved. We used purified peptidoglycan to assess its role as an elicitor of defence response.

C. MATERIAL AND METHODS

1. Materials

1.1 Chemicals, kits and instruments

1.1.1 Chemicals and kits

Amersham (www.amersham.com)	Sepharyl 100 HR, SP sepharose, Phenyl sepharose
Biomer (www.biomers.net)	Synthetic oligonucleotide
Difco Laboratories (www.bd.com)	Tryptic soya broth, Antibiotic Medium -3
Hampton (www.hampton.com)	Crystallization screen
MBI Fermentas (www.fermentas.com)	DNA and Protein marker, Restriction enzymes, HiFidelity DNA polymerase
Novagen (www.emdbiosciences.com)	Cloning vector pBAD(b), pET28(a+)
Peqlab (www.peqlab.de)	Plasmid isolation kits, IPTG
Qiagen (www.qiagen.com)	Ni-NTA, Plasmid extraction kit, QIAquick gel extraction kit, pQE cloning vectors
Roth (www.carl-roth.de)	BCIP-NBT, 30% Acrylamid, Urea, Dithio threitol, Sucrose, Glucose, Antibiotics, Glutaraldehyde, Roti® phenol/ chloroform solution, Spectra Por Dialysis membrane, HPLC grade water, methanol, acetonitrile
Sigma-Aldrich (www.sigmaaldrich.com)	Trizma base, BSA, Anti-mouse IgG (Fab specific), Glycerol, L-arabinose, Triton X-100, Tween 20, Bradford assay kit, Endotoxin detection kit, Mutanolysin

Serva (www.serva.de)	Agarose, Ammonium per sulfate (APS), Coomassie Brilliant BlueR-250, TEMED, β-Mercaptoethanol
Stratagene (www.stratagene.com)	Strataclean® Resin
Genmedics (www.genmedics.com)	Lysostaphin
E.Merck AG (www.merck.de)	All other chemicals not mentioned above were from Merck AG

1.1.2 Instruments

Amersham Pharmacia Biotech	ImageMaster® VDS, Power Supply
Amersham Biosciences	Acta FPLC system
Bischoff	Preparative HPLC
Beckman	Ultra centrifuge
Eppendorf	Microcentrifuge
Leica	Confocal laser scanning microscope
Sartorius	Balances
MWG Biotech	LI-COR DNA-Sequencer, PCR
Milli pore	Water purification system, Centrifugal protein concentrator
Kontron	Analitical HPLC system
Revco	Refrigerator
Uni Equip	Rotary evaporator
Olympus	Microscope
Scotsman	Ice machine
American instrument Company	French press
Branson Sonic power supply	Sonicator, ultra sonic bath
Liebherr Premium	Freeze (-20°C)
Heraeus	Laminar air
Labortechnik	UV transluminator
Thermo spectronic	Spectrophotometer
Fischer	pH meter

1.2 Software

1.2.1 Purchased software

Geminics	Analatical HPLC
Mac DNasis	Tools for analyzing DNA and protein sequences

1.2.2 Sequence analysis websites

The protein sequences were compared with those of known proteins using the programs BLASTP and FASTA (http://www.ncbi.nih.gov). Multiple sequence alignments were done using the program ClustalW from the European Bioinformatics Institute (http://www.ebi.ac.uk/clustalw/). Homologous sequences were analyzed using official websites of The Institute for Genomic Research (http://www.tigr.org) and from The Wellcome Trust Sanger Institute (http://www.sanger.ac.uk). The signal peptides were predicted by using the SignalP http:://www.cbs.dtu.dk/services/SignalP/.

1.3 Nucleotide sequence accession numbers

The EMBL/GenBank/DDBJ accession number of the *atlA* DNA sequence is D17366, for *atlE* is SEU71377 and for *aaa* is AJ250906.

1.4 Antibiotics

Ampicillin (100 mg/ml): 5 g ampicillin (sodium salt) dissolved in 50 ml deionized water. Filter-sterilized and stored in aliquots at -20°C.

Kanamycin (30 mg/ml): 1.5 g kanamycin (monosulfate salt) dissolved in 50 ml deionized water. Filter-sterilized and stored in aliquots at -20°C.

Spectinomycin (160 mg/ml): 8 g spectinomycin (sodium salt) dissolved in 50 ml deionized water. Filter-sterilized and stored in aliquots at -20°C.

Chloramphenicol (20 mg/ml): 10 g chloramphenicol dissolved in 50 ml 80% ethanol and stored in aliquots at -20°C.

Erythromycin (5 mg/ml): 5 g erythromycin dissolved in 50 ml of 80% ethanol and stored in aliquots at -20°C.

1.5 Strains and plasmids

1.5.1 Strains

Escherichi coli: DH 5α (Hanahan, 1983), XI1 blue (Stratagene), M15 (Qiagen), BL-21(Stratagene).

Staphylococcus aureus: RN4220 (Kreiswirth *et al.*, 1983) , SA113 (Iordanescu and Surdeanu, 1976), SAΔ*dlt* (Peschel *et al.*, 1999), SAΔ*oat*A (Bera *et al.*, 2005a), SAΔ*tag*O (Weidenmaier *et al.*, 2005), SAΔ*oat*AΔ*tag*O (Bera *et al.,* in press J. Bacteriology), SAΔ*lgt* (Stoll *et al.*, 2005), SAΔ*srt*A (Dr. Günther Thümm, unpublished result).

Staphylococcus epidermidis: SE O-47 (Heilmann *et al.*, 1996).

Staphylococcus carnosus: TM300 (Schleifer, 1982).

Micrococcus luteus: Wild type.

1.5.2 Plasmids

***E. coli* specific vectors**: pEC2 (4.2 kb, Amp ^{R}) (Bruckner, 1997); pDG782 (4 kb, Amp ^{R}) (Guerout-Fleury *et al.*, 1995); pQE30 (3.4 kb, Amp ^{R}) (Qiagen) ; pET28a (5.3 kb, Kan ^{R}) (Novagen) ; pBADb (4.1 kb, Amp ^{R}) (Invitrogen).

***Staphylococcus* sp specific vectors**: pCX19 (5.8kb, Cm ^{R}) (Wieland *et al.*, 1995); pTX15(8.9kb, Tet ^{R}) (Peschel *et al.*, 1996).

***E. coli* and Staphylococcal shuttle vector**: pBT2 (6.9kb, Amp ^{R} in *E.coli* and Cm ^{R} in *Staphylococcus* sp) (Bruckner, 1997), pRB473 (5.7 Kb, Amp ^{R} in *E.coli* and Cm ^{R} in *Staphylococcus* sp) (Bruckner, 1997).

1.6 Oligo-neucleotides

1.6.1 Synthetic oligo-neucleotides for PCR

atlF NheI	:5'-aataagctagccgtaaagacttagaattatcacc-3'
atlR EcoRI	:5'-ttattgaattcggtactatcaaacg-3'
atlR BamHI	:5'-aataaggatccgctcgatgccttcctcaag-3'
atlE-BglII	:5'-attgaaacagatcttattaatgcgaggagtaagaaa-3'
atlE-PstI	:5'-aactgcagtcattatttgtatgttggaatttcgaag-3'
tufA F	:5'-tacattgaattcgttcggttatgcaacatcattacgttc-3'
tufA R	:5'-tatcatagtactctctcatgatagtttctcaccatc-3'
AM-BglII	:5'-caagatctgtatctagtcaaaaaacat-3'
AM-PstI	:5'- aactgcagatcattagccccaaggtgctacttgcttcg-3'
AR2-PstI	:5'-aactgcagttatcataaatagtatttactaatccaacc-3'
R1-BglII	:5'-caagatctacaacatctacaaaaccgtc-3'
AR3-PstI	:5'-aactgcagttatcataaatccttagcagcaatccatcc-3'
GL BglII	:5'-caagatctatccaaaacagtactgacg-3'
aaA NheI	:5'-aaattgctagcaaggcgcataaaggaacaaagatttcagc-3'
aaA EcoRI	:5'-aaattgaattccagcgcgtgtacttgtgattcc-3'
aaA HindIII	:5'-ccctacaaacataagcttgaactttgcttgtaggacgc-3'
aaA BamHI	:5'-aaattggatccaattttatggcgggc-3'
His aaA BamHI	:5'-aataaggatccgctacaactcacacagtaaaaccg-3'
aaA BamHI SD 990	:5'-aaattggatcccaagaggaggattttaaagtgc-3'
aaA SacI-2610	:5'-aaattgagctcatttaatcatctttgacacccc-3'

1.6.2 Synthetic oligonucleotides for DNA sequencing (5' labeled)

pRB473 HindIII	:5'-ccagtaatgacctcagaactcc-3'
pRB473 EcoRI	:5'-ccccaggcgtttaagggc-3'
Spec Down	:5'-gaaagaaattgttccttcgatag-3'

SpecUp	:5'-ctgttcaataaagctgaccgttagcg-3'
ErmKaH Dist	:5'-gttacacgttactaaaggg-3'
ErmKaH Prox	:5'-cacaatagagagatgtcacc-3'
pBT HindIII	:5'-cgcattgttagatttcatacacg-3'
pQE prom	:5'-ggcgtatcacgaggcccttttcg-3'
pQE rev	:5'-cattactggatctatcaacagg-3'
pET BglII	:5'-gtccggcgtagaggatcgagatctcg-3'
pBAD Do	:5'-gattatttgcacggcgtcacac-3'

1.7 Media

Unless otherwise stated, the media were prepared with distilled water and autoclaved for 20 min at 121°C. To obtain agar media, 1.5% (w/v) agar was added before autoclave. When necessary, sterile supplementary components like glucose and antibiotics were added in the sterile media prior to inoculation with bacteria. The media were stored at room temperature. The media used in this study were as follows:

Luria-Bertani Medium (LB medium): 10 g Tryptone, 5 g Yeast extract, 5 g NaCl in 1l water.

B-Medium: 10 g Tryptone, 5 g Yeast extract, 5 g NaCl, 1 g Glucose, 1 g K_2HPO_4 dissolved in 1l water

Tryptic soy broth (TSB): 17 g Peptone from casein, 3 g Peptone from soymeal, 2.5 g D(+)-Glucose, 5 g NaCl, 2.5 g K_2HPO_4 dissolved in 1l water.

B-Agar: B-medium containing 15 g Agar/l.

1.8 Buffers of Molecular Cloning

1.8.1 Plasmid extraction buffers

Buffer P1 (resuspension buffer): 50 mM Tris-HCl, pH 8.0; 10 mM EDTA; 100 µg/ml RNase A, stored at 4°C.

Buffer P2 (lysis buffer): 200 mM NaOH, 1% SDS, stored at 15–25°C.

Buffer P3 (neutralization buffer): 3.0 M potassium acetate, pH 5.5, stored at 4°C.

Buffer FWB2 (QIAfilter wash buffer): 1 M potassium acetate, pH 5.0, stored at RT.

Buffer QBT (equilibration buffer): 750 mM NaCl; 50 mM MOPS, pH 7.0; 15% isopropanol; 0.15% Triton X-100, stored at RT.

Buffer QC (wash buffer): 1.0 M NaCl; 50 mM MOPS, pH 7.0; 15% isopropanol, stored at RT.

Buffer QF (elution buffer): 1.25 M NaCl; 50 mM Tris-HCl, pH 8.5; 15% isopropanol, stored at RT.

1.8.2 Solutions for protoplast transformation

Lysostaphin (0.5 mg/ml): Lysostaphin was dissolved in water and filter sterilized. Aliquots of 1 ml are stored at -20°C.

2 x SMM: 1 M Saccharose, 40 mM Maleic acid, 40 mM $MgCl_2$, pH was adjusted to 6.8 with NaOH. Media was filter sterilized.

4 x PAB: 70 g Antibiotic Medium-3 was dissolved in 1l water and autoclaved for 12 min.

5 %BSA-solution: 5 g BSA was dissolved in 100ml water and filter sterilized.

SMMP-B Medium: 75 ml 2 x SMM, 20 ml 4 x PAB, 5 ml 5 % BSA.

DM-3-Agar (protoplast regeneration medium): 5 % Select Agar 500 ml, 1 M Na-succinate (pH adjusted to 7.3 with succinic acid), 100 ml 5 % Select peptone 140, 60

ml 10 % yeast extract, 100 ml 3.5 % K_2HPO_4 + 1.5 % KH_2PO_4 , 10 ml 50 % Glucose, 20 ml 1 M $MgCl_2$, 10 ml 5 % BSA.

Fusogen: 40 g Polyethylen glycol 6000, 50 ml 2 x SMM, 100 ml water. pH was adjusted to 6.5. Solution is autoclaved for 12 min. The components are mixed at a temperature not higher than 50°C. The plates should contain about 25 ml DM-3 agar.

Soft agar: 10 g Select peptone No.140, 10 g Select yeast extract, 6 g NaCl, 4 g Select agar. CY-3-agar is autoclaved for 12 min.

Mix solution: 10 ml of 1 M $MgCl_2$, 5 ml 50 % Glucose, 20 ml Na-β-glycerol phosphate (48.6 g / 100 ml), 5 ml 5 % BSA.

Top agar mix: 5 ml CY-3 medium, 5 ml 1 M Na-Succinate, 0.8 ml Mix, 108 µl chloramphenicol (for pCX19) or tetracycline (for pTX15). CY-3 agar is melted before use and combined at 50°C with the pre-warmed succinate- and mix-solution. 3 ml of top agar mix was poured on one plate.

1.8.3 Agarose gel electrophoresis buffers

50x TAE-buffer: 242 g Tris-base, 57.1 ml Glacial acetic acid 100 ml 0.5 M EDTA (pH 8.0). Water added to 1 liter.

6X Loading Dye: 0.25% Bromophenol blue, 0.25% Xylene cyanol FF, 30% Glycerol dissolved in water.

1.8.4 Buffers for E. coli Competent cell preparations

Buffer TFB1: 100 mM RbCl, 50 mM $MnCl_2$, 30 mM Potassium acetate10 mM $CaCl_2$, 15 % Glycerol. pH 5.8 adjusted with acetic acid, filter sterilized and stored at 4°C.

Buffer TFB2: 10 mM MOPS, 10 mM RbCl, 75 mM CaCl2, 15 % Glycerol. pH 6.8 adjusted with KOH, stored at 4°C.

1.9 Buffers for Protein analysis

1.9.1 Solutions for SDS-PAGE

Separating gel (10%): 30% Acrylamide 1333 µl, 1.5 M Tris (pH 8.8) 1000 µl water 1600 µl, 10% SDS 25 µl, 20% APS 10 µl, TEMED 3 µl.

Stacking gel (4%): 30% Acrylamide 335 µl, 0.5 M Tris (pH 6.8) 625 µl, 10% SDS 40 µl, 20% APS 10 µl, TEMED 3 µl.

Running buffer (5 X): 15 g Tris, 72 g Glycine, 5 g SDS dissolved in 1l and stored at 4°C.

5x SDS-PAGE sample buffer: 0.225 M Tris·Cl; 50% glycerol; 5% SDS; 0.05% Bromophenol blue; 0.25 M DTT, pH 6.8

Coomassie Brilliant Blue staining solution: 0.2% CBB in 45:45:10 % methanol: water: acetic acid.

Destaining buffer: 10% acetic acid.

1.9.2 Western Blotting solutions

Semi-dry transfer buffer: 25 mM Tris base, 150 mM glycine, 10% methanol should be pH 8.3 without adjusting.

TBS buffer: 10 mM Tris·Cl, (pH 7.5); 150 mM NaCl; TBS-Tween buffer: 20 mM Tris·Cl, (pH 7.5); 500 mM NaCl; 0.05% (v/v) Tween 20.

TBS-Tween/Triton buffer: 20 mM Tris·Cl, (pH 7.5); 500 mM NaCl; 0.05% (v/v) Tween 20; 0.2% (v/v) Triton X-100.

Blocking buffer: 3% BSA in TBS buffer.

1.9.3 Affinity purification under native condition

Lysis buffer: 50 mM NaH_2PO_4, 300 mM NaCl, 10 mM imidazole dissolved in 1 l water. pH is adjusted to 8.0 using NaOH.

Wash buffer: 50 mM NaH_2PO_4, 300 mM NaCl, 20 mM imidazole dissolved in 1 l water. pH is adjusted to 8.0 using NaOH.

Elution buffer: 50 mM NaH_2PO_4, 300 mM NaCl, 250 mM imidazole dissolved in 1 l water. pH is adjusted to 8.0 using NaOH.

1.9.4 Affinity purification under denaturing condition

Buffer A (Lysis buffer): 100 mM NaH_2PO_4, 10 mM Tris-HCl, 8 M Urea dissolved in 1 l water. pH is adjusted to 8.0 using NaOH.

Buffer B (wash buffer): 100 mM NaH_2PO_4, 10 mM Tris-HCl, 8 M Urea dissolved in 1 l water. pH is adjusted to 6.3 using NaOH.

Buffer C (elution buffer-I): 100 mM NaH_2PO_4, 10 mM Tris-HCl, 8 M Urea dissolved in 1 l water. pH is adjusted to 5.9 using NaOH.

Buffer D (elution buffer-II): 100 mM NaH_2PO_4, 10 mM Tris-HCl, 8 M Urea dissolved in 1 l water. pH is adjusted to 4.5 using NaOH.

1.9.5 Buffers for X-crystallization setup

Initial crsytal screening buffers contains unique combinations of pH, salts and precipitants. Many of such conditions can promote crystal growth. 50 different buffer solutions were used to identify favourable crystal setup conditions. A list of all buffers are as follows:

Salt	Buffer	Precipitant
1. 0.02 M Calcium Chloride dihydrate	1. 0.1 M Sodium Acetate trihydrate, pH 4.6	1. 30% v/v 2-Methyl-2,4-pentanediol
2. None	2. None	2. 0.26 M Potassium Sodium Tartrate tetrahydrate
3. None	3. None	3. 0.26 M Ammonium dihydrogen phosphate
4. None	4. 0.075 M Tris Hydrochloride pH 8.5	4. 1.5 M Ammonium Sulfate
5. 0.2 M tri-Sodium Citrate dihydrate	5. 0.1 M HEPES - Na pH 7.5	5. 30% v/v 2-Methyl-2,4-pentanediol
6. 0.16 M Magnesium Chloride hexahydrate	6. 0.08 M Tris Hydrochloride pH 8.5	6. 24% w/v Polyethylene Glycol 4000
7. None	7. 0.07 M Sodium Cacodylate pH 6.5	7. 0.98 M Sodium Acetate trihydrate
8. 0.14 M tri-Sodium Citrate dihydrate	8. 0.07 M Sodium Cacodylate pH 6.5	8. 21% v/v iso-Propanol
9. 0.17 M Ammonium Acetate	9. 0.085 M tri-Sodium Citrate dihydrate pH 5.6	9. 25.5% w/v Polyethylene Glycol 4000
10. 0.17 M Ammonium Acetate	10. 0.085 M Sodium Acetate trihydrate pH 4.6	10. 25.5% w/v Polyethylene Glycol 4000
11. None	11. 0.07 M tri-Sodium Citrate dihydrate pH 5.6	11. 0.7 M Ammonium dihydrogen Phosphate
12. 0.18 M Magnesium Chloride hexahydrate	12. 0.09 M HEPES - Na pH 7.5	12. 27% v/v iso-Propanol
13. 0.2 M tri-Sodium Citrate dihydrate	13. 0.1 M Tris Hydrochloride pH 8.5	13. 30% v/v Polyethylene Glycol 400
14. 0.19 M Calcium Chloride dihydrate	14. 0.095 M HEPES - Na pH 7.5	14. 26.6% v/v Polyethylene Glycol 400
15. 0.17 M Ammonium Sulfate	15. 0.085 M Sodium Cacodylate pH 6.5	15. 25.5% w/v Polyethylene Glycol 8000
16. None	16. 0.075 M HEPES - Na pH 7.5	16. 1.125 M Lithium Sulfate monohydrate

17. 0.17 M Lithium Sulfate monohydrate	17. 0.085 M Tris Hydrochloride pH 8.5	17. 25.5% Polyethylene Glycol 4000
18. 0.16 M Magnesium Acetate tetrahydrate	18. 0.08 M Sodium Cacodylate pH 6.5	18. 16% Polyethylene Glycol 8000
19. 0.16 M Ammonium Acetate	19. 0.08 M Tris Hydrochloride pH 8.5	19. 24% v/v iso-Propanol
20. 0.16 M Ammonium Sulfate	20. 0.08 M Sodium Acetate trihydrate pH 4.6	20. 20% w/v Polyethylene Glycol 4000
21. 0.2 M Magnesium Acetate tetrahydrate	21. 0.1 M Sodium Cacodylate pH 6.5	21. 30% v/v 2-Methyl-2,4-pentanediol
22. 0.17 M Sodium Acetate trihydrate	22. 0.085 M Tris Hydrochloride pH 8.5	22. 25.5% w/v Polyethylene Glycol 4000
23. 0.2 M Magnesium Chloride hexahydrate	23. 0.1 M HEPES - Na pH 7.5	23. 30% v/v Polyethylene Glycol 400
24. 0.14 M Calcium Chloride dihydrate	24. 0.07 M Sodium Acetate trihydrate pH 4.6	24. 14% v/v iso-Propanol
25. None	25. 0.07 M Imidazole pH 6.5	25. 0.7 M Sodium Acetate trihydrate
26. 0.2 M Ammonium Acetate	26. 0.1 M tri-Sodium Citrate dihydrate pH 5.6	26. 30% v/v 2-Methyl-2,4-pentanediol
27. 0.14 M tri-Sodium Citrate dihydrate	27. 0.07 M HEPES - Na pH 7.5	27. 14% v/v iso-Propanol
28. 0.17 M Sodium Acetate trihydrate	28. 0.085 M Sodium Cacodylate pH 6.5	28. 25.5% w/v Polyethylene Glycol 8000
29. None	29. 0.065 M HEPES - Na pH 7.5	29. 0.52 M Potassium Sodium Tartrate tetrahydrate
30. 0.17 M Ammonium Sulfate	30. None	30. 25.5% w/v Polyethylene Glycol 8000
31. 0.17 M Ammonium Sulfate	31. None	31. 25.5% w/v Polyethylene Glycol 4000
32. None	32. None	32. 1.5 M Ammonium Sulfate
33. None	33. None	33. 3.6 M Sodium Formate
34. None	34. 0.07 M Sodium Acetate trihydrate pH 4.6	34. 1.4 M Sodium Formate

35. None	35. 0.075 M HEPES - Na pH 7.5	35. 0.6 M Sodium dihydrogen phosphate
36. None	36. 0.065 M Tris Hydrochloride pH 8.5	36. 5.2% w/v Polyethylene Glycol 8000
37. None	37. 0.07 M Sodium Acetate trihydrate pH 4.6	37. 5.6% w/v Polyethylene Glycol 4000
38. None	38. 0.09 M HEPES - Na pH 7.5	38. 1.26 M tri-Sodium Citrate dihydrate
39. None	39. 0.085 M HEPES - Na pH 7.5	39. 1.7% v/v Polyethylene Glycol 400, 1.7 M Ammonium Sulfate
40. None	40. 0.095 M tri-Sodium Citrate dihydrate pH 5.6	40. 19% v/v iso-Propanol, 19% w/v Polyethylene Glycol 4000
41. None	41. 0.085 M HEPES - Na pH 7.5	41. 8.5% v/v iso-Propanol, 17% w/v Polyethylene Glycol 4000
42. 0.04 M Potassium dihydrogen Phosphate	42. None	42. 16% w/v Polyethylene Glycol 8000
43. None	43. None	43. 24% w/v Polyethylene Glycol 1500
44. None	44. None	44. 0.1 M Magnesium Formate
45. 0.16 M Zinc Acetate dihydrate	45. 0.08 M Sodium Cacodylate pH 6.5	45. 14.4% w/v Polyethylene Glycol 8000
46. 0.16 M Calcium Acetate hydrate	46. 0.08 M Sodium Cacodylate pH 6.5	46. 14.4% w/v Polyethylene Glycol 8000
47. None	47. 0.08 M Sodium Acetate trihydrate pH 4.6	47. 1.6 M Ammonium Sulfate
48. None	48. 0.08 M Tris Hydrochloride pH 8.5	48. 1.6 M Ammonium dihydrogen Phosphate
49. 0.8 M Lithium Sulfate monohydrate	49. None	49. 1.6% w/v Polyethylene Glycol 8000
50. 0.4 M Lithium Sulfate monohydrate	50. None	50. 12% w/v Polyethylene Glycol 8000

1.9.6 Solutions for rp-HPLC

Solvent A: Water containing 0.1% TFA.

Solvent B: 30% methanol containing 0.1% TFA or 25% Acetonitrile containing 0.1% TFA.

1.9.7 Other solutions

100 mM Phosphate buffer: 8.9 g Na_2HPO_4, 6.9 g NaH_2PO_4 dissolved in 1 l water, pH 6.8.

100 mM Tris buffer: 12.1 g Trizma base dissolved in 1 l water, pH 7.0.

0.5 M Borate buffer: 30.5 g boric acid dissolved in 1 l water, pH adjusted to 9.0 with NaOH.

Chloroform/ Isoamyl alcohol: 240 ml chloroform, 10 ml isoamyl alcohol in 1 l water.

500 mM EDTA: 186.1 g of EDTA dissolved in 1 l water, pH adjusted to 8.0 with 20 g NaOH.

Methylene blue stain: 0.1% Methylene blue in 100ml water.

Ethidium bromide (10mg/ ml): 1 g EtBr dissolved in 100 ml water.

1M $CaCl_2$: 54 g $CaCl_2.6H_20$ dissolved in 200 ml water and filter sterilized.

8M LiCl: 336 g Lithium chloride dissolved in 1 l water.

10% SDS: 100 g sodium dodecyl sulphate dissolved in 1 l water.

10% APS: 1 g ammonium per sulphate dissolved in 10 ml water.

10% TCA: 100 g Tricholroacetic acid dissolved in 1l water.

Freeze Medium: 25 mM Tris/HCl (pH 8.0), 65% Glycerol, 100 mM $MgSO_4$.

TE buffer: 10 mM Trisma base, 1 mM EDTA (pH 8.0).

Buffers for Gel filtration chromatography: 20 mM Tris, 100 mM NaCl, 1mM EDTA, 0.02 % sodium azide, pH 8.0

IPTG stock (100 mM): 238.3 g isopropyl β-thiogalactopyranoside dissolved in 10 ml water. Filter sterilized and stored in aliquots at -20°C.

50% Xylose: 50 g xylose dissolved in 100 ml water and filter sterilized.

50% Glucose: 50 g glucose dissolved in 100 ml water and filter sterilized.

2. Methods

2.1 Growth conditions

All strains were routinely cultivated at 37°C with shaking at 160 rpm in B-medium except following conditions: *E. coli* cultures were grown at 20°C during over expression of Histidine tagged proteins; *S. aureus* strains were grown at 42°C to facilitate homologous recombination and plasmid curing during knock out mutant construction. Biofilm cells were grown at 37°C under static condition.

2.2 Molecular cloning methods

Standard methods for DNA isolation and manipulation were performed as described in Qiagen manual. Phenol/chloroform extraction and ethanol precipitation were used for purification and concentration of DNA. Quantification of DNA was carried out by using a Thermo spectronic photometer at 260 nm as well as by comparing the fluorescent intensity with DNA markers on agarose gels.

2.2.1 Agarose gel electophoresis of DNA

0.8% - 1.0% (w/v) agarose gels were used to separate DNA fragments. The buffer system employed was 1×TAE buffer. After running the gels, they were stained with the ethidium bromide, detected under the UV light and photographed.1 kb DNA ladder and λ/ HinDIII digest were used as standard markers. DNA fragments were excised and isolated from agarose gels using gel extraction kit according to the protocol described in Qiagen Handbook.

2.2.2 Isolation of plasmids from *E. coli*

Mini-preps employing alkaline lysis were used to isolate recombinant plasmids from *E. coli* for routine screening. 5 ml LB-medium was inoculated with a single colony and grown overnight at 37°C, 160 rpm. 2 ml of this culture was harvested by centrifugation (2,000 ×g, 4°C, 10 min) and resuspended in 250 µl solution P1 by vortexing. The suspension was mixed with 250 µl solution P2 by inversion and

incubated at RT for 5 min. And then 250 µl solution P3 was added and incubated on ice for 10 min. After centrifugation for 30 min (20,000×g, 4°C), the supernatant was transferred into a fresh eppendorf tube. DNA was precipitated by addition of equal volume of isopropanol and centrifugation (20,000×g, 4°C, 30 min). DNA pellet was washed once with 500 µl 70% ethanol, air dried and resuspended in 40 µl TE buffer. Preparative isolation of plasmids from *E. coli* was carried out with DEAE ion-exchange columns (Qiagen) according to the manufacturer's protocol.

2.2.3 Isolation of plasmids from *Staphylococcus*

Plasmids were isolated from *Staphylococcus* sp following the same procedure except lysostaphin was used to lyse the cells. Briefly, cell pellets were suspended in P1 buffer and lysostaphin was added to a concentration of 5-10µg /ml and incubated at 37°C for 15 min. The lysate was mixed with 250 µl solution P2 and then 250 µl solution P3 was added and centrifuged. The supernatant was transferred into a fresh eppendorf tube. DNA was precipitated with isopropanol, washed with 70% ethanol and suspended in TE buffer.

2.2.4 DNA cloning

Insert and Plasmid DNA was digested with restriction enzymes of interest (0.5 to 1µg DNA, 1X restriction buffer, 1U restriction endonuclease and water to 20µl for 6 hours), purified from 1% agarose gel and ligated together. A typical ligation reaction is set up as follows: Component DNAs (0.1–5 µg), 1X Ligase buffer, 20–500 U T4 DNA ligase for 6 h at 22°C.

2.2.5 Preparation of *E. coli* competent cells and transformation

Competent cells were prepared according to the method described in Qiagen Handbook. Briefly, early exponential cells ($O.D._{600nm}$ = 0.5) were centrifuged down and resuspended in equal culture volume of TFB1 buffer. Cells were incubated in ice for 90 minutes and then pelleted down. The pellet was resuspended in 1/100 volume of TFB2 and stored in -75°C. For transformation either plasmid or ligation mixtures were added to the competent cells and kept on ice for another 10 min. Foreign DNA

was introduced using heat shock method (90 sec at 42°C). Cells were mixed with 1 ml B-medium and incubated at 37°C for 1h. Appropriate aliquots were spread on antibiotic selection plates.

2.2.6 Transformation of *Staphylococcus* sp by electroporation

Bacteria were grown to $O.D._{578}$ = 0.5 and centrifuged down. The cells were washed twice with equal culture volume of ice cold 10% glycerol, resuspended in 1:100 culture volume of 10% glycerol, and stored at -70°C. 200 µl of competent cells were mixed with 5 - 8 µl DNA and electroporated. The standard electroporation conditions were: 2 kV, 100 Ω, 25 µF. After electroporation, cells were mixed with 1 ml B-medium and incubated for 1 h at 37°C. Appropriate dilutions were spread on antibiotic selection plates.

2.2.7 Protoplast transformation of *S. carnosus*

2.2.7.1 Preparation of the protoplasts

300 ml BM was inoculated with 1 ml overnight culture of *S. carnosus* TM300. The cells were cultivated on a shaker at 37°C until an absorbance ($O.D._{578}$) of 0.5 was reached. The cells were harvested in an autoclaved centrifuge tube by centrifugation at 8,000 g for 15 min at 4°C. The cell pellet was carefully resuspended in 30 ml SMMP-B, and the cell suspension was transferred to a sterile 100 ml Erlenmeyer flask or to a sterile falcon tube. 40 µl of 0.5 g/ml Lysostaphin was added. The suspension was mixed and incubated overnight (16 hrs) at 30°C without shaking. Protoplast formation was monitored microscopically; the ratio of whole cells and protoplasts should be about 1:1. The cell suspension was centrifuged at RT at 7,000 g for 25 min. The supernatant was discarded and the protoplast pellet washed with 5 ml SMMP-B to remove traces of lysostaphin. The pellet was carefully resuspended in 2 ml SMMP-B and stored at -70°C.

2.2.7.2 Protoplast transformation

0.3 ml of protoplast suspension was thawed at RT. 15 µl of plasmid DNA or 30-40 µl of ligation mixture and 2 ml of Fusogen were added and mixed gently by inversion for

1 min and incubated for an additonal 1 min at RT. 7 ml SMMP-B were added and mixed by inverting the tube. The protoplasts were centrifuged at RT for 25 min at 6,000 g. The supernatant was discarded, and the pellet resuspended in 2 ml SMMP-B. The protoplast suspension (0.5 ml, 0.3 ml, 0.2 ml) was plated undiluted on DM-3 plates. For the phenotypic expression of the antibiotic resistant genes, the DM-3 plates were incubated for 4 - 5 hrs at 37°C. After which 3 ml of soft agar with the respective antibiotic was poured onto the surface of the DM-3 plates. The plates were incubated for 2 days at 37°C.

2.3 Polymerase chain reaction (PCR)

In vitro amplification of DNA was performed using MWG thermocycler. The extension time was usually 1 min/1 kb. For PCR amplification was carried out with Hi fidelity polymerase. The PCR mixture (100µl) contained 20 pmole each primer, 250-500 ng template DNA, 0.2 mM dNTP each and 1× reaction buffer and 1U polymerase. The PCR steps involved denaturation at 95°C for 120 sec, annealing at 48-56 °C for 90 sec and elongation at 72°C 45s/ 1 kb for 30-35 cycle.

2.4 DNA sequencing

DNA sequencing was carried out using LiCOR sequencer using 5' fluorescent-labeled primers.

2.5 Protein methods

2.5.1 Protein purification under denaturing conditions

E. coli M15 harboring either pQE*ami*E and pREP4 were grown overnight in LB medium containing both ampicillin (100 µg/ml) and kanamycin (30 µg/ml). The culture was diluted 1:50 into fresh medium and grown with shaking at 37 °C to an $O.D._{578}$ of 0.5, there after the expression of T7 polymerase was induced by the addition of IPTG to a final concentration of 1 mM. Cells were harvested after 6 h by centrifugation at 8,000 × g. Preliminary experiments revealed that both full-length and truncated amidase enzymes were contained in inclusion bodies, and subsequent purification

steps were therefore carried out under denaturing conditions. The *E. coli* cell sediments were suspended in 50 ml of Buffer A (8M urea, 0.1 M NaH_2PO_4, 0.01 M Tris-HCl, pH 8.0); cells were stirred for 1h at room temperature, insoluble material was removed by centrifugation at 30,000 × g for 20 min. The clear lysate was passed through 5-ml bed volume of nickel nitrilotriacetic acid column (Qiagen). The column was pre-equilibrated with buffer A (8 M urea, 100 mM NaH_2PO_4, 0.01 M Tris-HCl, pH 8) and, after loading with sample; the column was washed with 3 bed volume of Buffer B (8 M urea, 100 mM NaH_2PO_4, 0.01 M Tris-HCl, pH 6.3). Protein was eluted from the column in a pH-dependent manner by a step gradient to 100% elution buffer (8 M urea, 100 mM NaH_2PO_4, 0.01 M Tris-HCl, pH 4.5).

2.5.2 Protein refolding

Proteins were renatured by sequential dialysis steps at 4°C: 1) against 100 mM sodium phosphate (pH 7.0), 1 mM EDTA, 4 M urea, 5% sucrose, 100 mM NaCl, 100 mM KCl, 100 mM l-arginine, 4 mM MgCl2, for 48 h without stirring; 2) against the buffer in step 1 diluted 1:1 with 100 mM phosphate buffer (pH 7.0) for 24 h without stirring; 3) against the buffer in step 2 diluted 1:1 with 100 mM phosphate buffer (pH 7.0) for 12 h without stirring; and 4) against 100 mM phosphate buffer (pH 7.0) for 48 h with very slow stirring. Insoluble protein aggregates were removed by centrifugation. Soluble protein fractions were collected and stored at –20°C.

2.5.3 Protein purification under native conditions

Large scale purification of Histidine tagged proteins were also carried out under native conditions. *E. coli* cells were grown at 20°C overnight. Protein expression were induced using 0.1mM IPTG at $O.D._{600}$ = 0.5. Cells were centrifuged down and suspended in lysis buffer containing 1 mg/ml lysozyme. Cells were incubated in ice for 1 h and broken by five passages in French press. 1 mM PMSF and protease inhibitor cocktail were added to the lysis buffer prior to French press. Broken cells were centrifuged at 15000 rpm for 1 h, the cleared lysate was passed through 0.22 µm filter and proteins were loaded in a Ni-NTA column. Columns were washed with five column volumes of wash buffer and proteins were eluted in step gradient using elution buffer containing increasing amount of immidazole from 50 mM to 300 mM.

The active protein fractions were pooled together and dialyzed against 10 mM Tris containing 100 mM NaCl, 0.02 % sodium azide pH 7 overnight. Insoluble protein aggregates were removed by centrifugation and soluble fractions were concentrated to 5 ml using Millipore 5 kDa cut off centrifugal concentrator. 500 µl of the concentrated protein fractions were loaded in Sephacryl 100 gel filtration column and eluted in a linear gradient of 10 mM Tris containing 100 mM NaCl, 0.02% sodium azide pH7. Eluted protein fractions were analyzed in SDS-PAGE. Fractions containing proteins of interest were pooled together and concentrated using millipore concentrator. PMSF and protease inhibitor cocktails were added in all steps.

2.5.4 X-ray Crystallization of AmiE

Crystallization experiments were carried out with the Hanging Drop Vapor Diffusion method. The detailed procedure for this set-up is as follows:

1. 24 wells reservoir plates were used for Hanging Drop Vapor diffusion method. 1 µl of AmiE (1.9 mg/ml) mixed with 1 µl buffer and applied to the thin bead of cover slide sealant to the upper edge of each of the reservior.

2. Using a clean pipet tip, pipet 1 ml of each Crystal Screen reagent into reservoirs

3.Crystallization setup was performed in duplicate and incubate at 20°C for several weeks in a stable temperature environment, free of vibration.

The drops were observed under a stereo microscope (10 to 100x magnification) once each day for the first week, then once a week there after for another three weeks.

2.5.5 Staphylococcal surface and exoprotein isolation

Staphylococcal cell-wall-associated proteins were extracted with 4% SDS. Briefly cells from overnight cultures were pelleted down, washed twice with 100 mM phosphate buffer and suspended in equal pellet wet weight of 100 mM sodium

phosphate buffer containing 4% SDS. This cell suspension was incubated at 37°C water bath for 10 min. Cells were centrifuged down. Supernatant containing surface proteins were analyzed by Tricine-10% SDS-PAGE, zymograms, and immunoblots. Exoproteins were concentrated by 10% TCA precipitation.

2.5.6 Zymogram

Proteins were analyzed by Tricine-10% SDS-PAGE and zymograms. Bacteriolytic enzyme profiles were obtained with zymograms of polyacrylamide gels containing heat-inactivated *Micrococcus luteus* or *S. aureus* cells. The surface protein and exoproteins were heated for 5 min at 95°C and loaded onto gel containing 0.2% (wt/vol) lyophilized cells. After electrophoresis, gels were washed with water for 30 min and proteins were renatured to detect lytic activity. The gels were incubated with gentle shaking in 100 mM sodium phosphate buffer for 4-6 hours at 37°C. The gels were photographed under dark background.

2.5.7 Determination of protein concentration

The concentration of proteins was measured with the Bradford kit using BSA as standard.

2.6 Microscopy

For electron microscopy, bacterial cells in the stationary phase were harvested, washed twice with 100 mM phosphate buffer (pH 7.0), and fixed using the glutaraldehyde/OsO4 method. After washing, agar blocks were dehydrated in an ethanol series beginning with 50% ethanol and finally placed in water-free acetone. Samples were then embedded in Spurr's resin and polymerized at 60°C for 2 days. Ultrathin sections were cut with an ultramicrotome with a diamond knife. Samples were post-stained with 1% uranyl acetate for 1 h and Reynold's lead citrate for 20 min and examined with a Zeiss EM 109 transmission electron microscope at 80 kV.

2.7 Biofilm assay

Bacterial cells carrying pCtuf-gfp were grown in TSB medium supplemented with 0.5% glucose. Cultures were diluted 1:200 and incubated for 24 h on top of glass slides soaked with medium in a Petri dish. Biofilms on glass slides were viewed using a confocal microscope.

Biofilm formation was also monitored in 96 well microtitre plate, where cells were grown in 200 µl TSB medium containing 0.5% glucose for 24 h, under static condition. Wells were washed with 100 mM phosphate buffer twice; adhered cells were stained with 0.1% safranin.

2.8 Peptidoglycan preparation and binding assay

2.8.1 Isolation of peptidoglycan

S. aureus cells and their different genetically modified mutants were grown to mid-log phase in tryptic soy broth, and culture was chilled to 4 °C on ice. Cells were harvested by centrifugation, suspended in a solution of 4% sodium dodecyl sulfate (SDS), and boiled for 30 min. Cells were centrifuged for 10 min at 30,000 × g and washed six times with water. SDS treatment was used to remove contaminating proteins, non-covalently bound lipoproteins and LPS. The cells were broken with < 100 nm glass beads in a Bead-Beater instrument as described above. Glass beads were removed by centrifugation at 200 × g for 5 min. Broken cell walls were collected by centrifugation at 30,000 × g for 15 min, and the pellet was resuspended in 50 mM Tris-HCl, 10 mM $MgCl_2$, pH 7.5. Walls were treated with DNase (Sigma, 10 µg/ml), and RNase A (Qiagen, 50 µg/ml) for 2 h at 37 °C. $CaCl_2$ was added to a final concentration of 10 mM, and covalently linked proteins were removed from the peptidoglycan by the addition of trypsin (Sigma, 100 µg / ml) and incubating the walls overnight at 37 °C. Peptidoglycan was further treated with 48% hydrofluoric acid for 48hrs at 4°C. This acid hydrolysis allows removal of secondary polysaccharides covalently bound to the peptidoglycan by phosphodiester bonds such as teichoic acid, capsules, poly-(β,1-6 GlcNAc), etc. Peptidoglycans were further treated once with 8 M LiCl, once with 100 mM EDTA, twice with water, and finally with acetone to

remove lipoteichoic acid and any traces of LPS. Walls were suspended in water and stored at 20 °C.

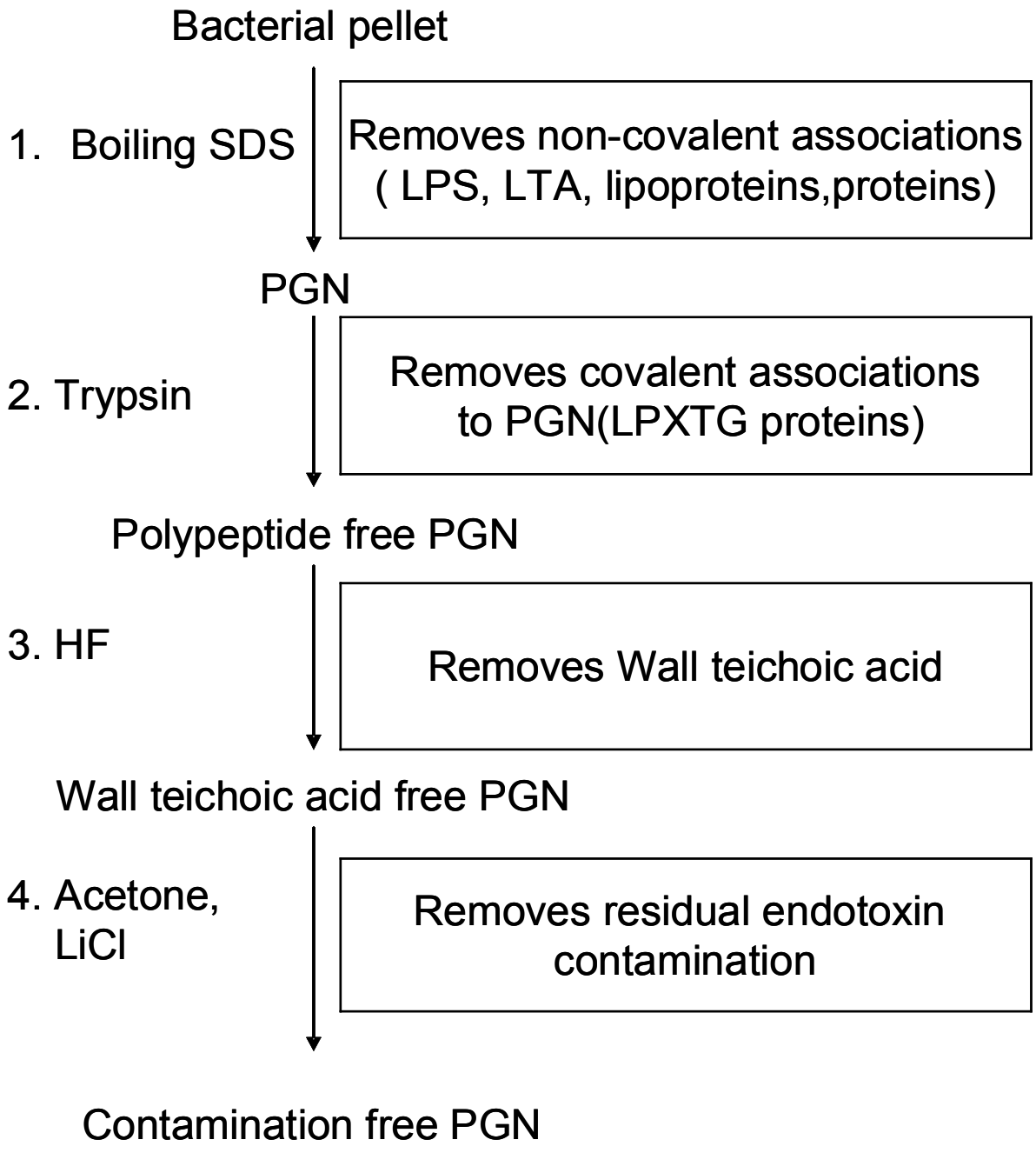

Fig. 4. Schematic representation of peptidoglycan preparation from *S.aureus* strains.

2.8.2 Peptidoglycan preparation and binding assay

PG was isolated from stationary phase cultures of *S. aureus* SA113 and SA113 Δ*tag*O as described above (Bera *et al.*, 2005b; de Jonge *et al.*, 1992). PG binding was assayed at 4°C with 1–2 μg purified (His6)-AmiE, (His6)-AmiE-R1,2, or (His6)-R1,2,3. Ni2+-NTA-purified proteins were mixed with 50 μg of *S. aureus* PG in 500 μl of 100 mM phosphate buffer (pH 7.0) for 10 min at 4°C. Unbound proteins in the supernatant were precipitated with 10% trichloroacetic acid. Bound protein retained in the PG pellet after centrifuging the incubation mixture at 13,000×g for 5 min was washed with 100 mM phosphate buffer (pH 7.0) and then dissolved in SDS sample buffer. Samples were analyzed by electrophoresis in SDS-10% polyacrylamide gels.

2.8.3 HPLC separation of muropeptides

Approximately 2 mg purified PG was digested with either 100 μg (His6)-Ami-R1, 2 or 5 μg lysostaphin or with both enzymes for 16 h in 100 mM phosphate buffer (pH 7.0) in a total volume of 1 ml. Digestions were terminated by heating the samples at 90°C for 5 min. Insoluble muropeptides were removed by centrifugation, and soluble fractions were dried in a rotary evaporator. The dried muropeptides were resuspended in water and reduced with sodium borohydride. Excess borohydride was destroyed by adding 20% phosphoric acid. Digested samples were applied to a Nucleosil 100 C18 column (Grom; 5 μm; 150×4 mm) at room temperature with a water/0.05% TFA : 25% acetonitrile/0.05% TFA gradient for 25 min at flow rate of 0.5 ml/min. Peaks were detected at 206 nm.

For cell signaling experiments peptidoglycan was isolated form seven staphylococcal strains: SA113, SAΔ*srt*A, SAΔ*oat*A, SAΔ*oat*AΔ*tag*O, SAΔ*tag*O, SAΔ*dlt*A and SAΔ*lgt*. Peptidoglycans were digested with mutanolysin or mutanolysin and lysostaphin for 72 h. Insoluble muropeptides were removed by centrifugation. To that equal volume of 0.5 M Borate buffer (pH 7.0) was added and muropeptides were reduced with sodium borohydride ($NaBH_4$) for 15 min. Excess borohydride was destroyed by adding 20% phosphoric acid. Digested samples were applied to a preparative

Reprosil-Pur ODS 3.5µm 250X20mm column (Dr. Masch GmBH) and muropeptides were eluted in a linear gradient of 100% water 10 min; followed by water to 25% Acetonitrile in 30mins and 25% Acetonitrile to 50% acetonitrile in 40min.The major peaks were collected and dried. Individual peaks were further purified using a methanol gradient of 100% water to 50% methanol for 40 min. Pure peaks were collected, dried in a rotary evaporator and suspended in 1 ml water. The amount of purified PGN fragments were quantified using analytical HPLC, using D-Ala-Ala-Ala as a standard. Samples were applied to a Nucleosil 100, C18 column (Grom; 5 μm; 150×4 mm) at room temperature with a water/0.05% TFA to 25% acetonitrile/0.05% TFA gradient for 25 min at flow rate of 2 ml/min. Peaks were detected at 210 nm. Individual peak area was calculated and compaired with the standard. The purified PGN fragments were stored at -20°C.

2.8.4 HPLC-MS

Mass spectroscopy was performed on a Brucker Esquire 3000 plus ion-trap mass spectrometer (Bruker Daltonik, Bremen, Germany) equipped with an atmospheric pressure chemical ionization ion source. The mass spectra were recorded in the positive ion mode in the mass range from m/z 600 to 1000.

2.8.5 MALDI-MS

Dried HPLC fractions containing the peptides of interest were suspended in CH3CN: water:trifluoroacetic acid (50:50:0.1), typically 50 µl per 1.5 absorbance units at 215 nm. MALDI-MS spectra were obtained on a reflectron time-of-flight instrument (Perspective Biosystems Voyager RP) in the linear mode. Samples (0.5 µl) were co-spotted with 0.5 µl of matrix (α-cyano-4-hydroxycinnamic acid, 10 mg/ml in CH3CN:water:trifluoroacetic acid (70:30:0.1)). All samples were externally calibrated to a standard of bovine insulin.

D. RESULTS

1. Sequence analysis

1.1 Sequence analysis of Atl

*atl*A consists of 4007 nucleotides and encodes a deduced protein of 1335 amino acids with a predicted molecular mass of 138 kDa. The *atl* gene product is a bifunctional protein that has a N-terminal N-acetyl L-alanine amidase domain of 62 kDa and a C-terminal ß-N-acetylglucosaminidase domain of 51 kDa. A hydrophobicity plot (**Kyte and Doolittle, 1982**) of amidase and glucosaminidase shows that they are mostly hydrophilic and secreted proteins (**Fig. 5**).

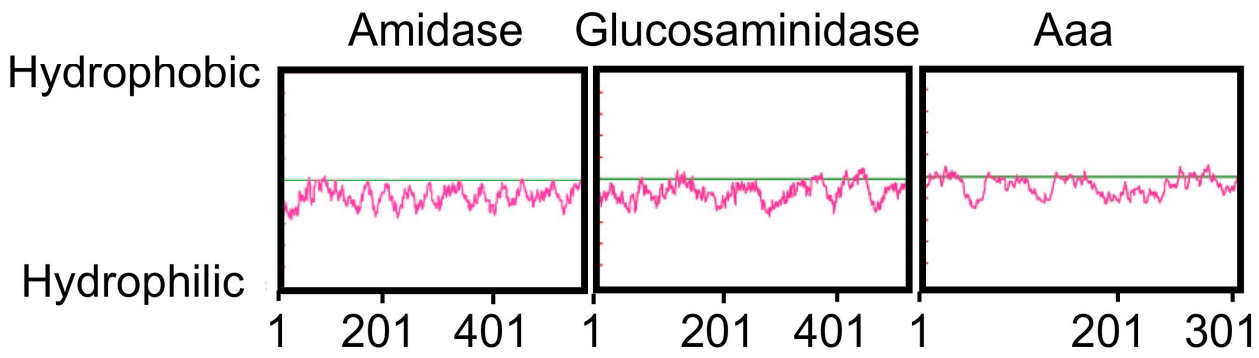

Fig. 5. Hydrophobicity plot of the amino acid sequence of the Atl amidase, glucosaminidase and Aaa (**Kyte and Doolittle, 1982**).

Atl must undergo proteolytic processing during secretion to generate the two extracellular lytic enzymes found in the culture broth of *S. aureus*. The N-terminal part of Amidase shows 40% homology to the N-terminal part of the *Bacillus* cell wall hydrolase (CWLA) and 24% to the pneumoccal EJL bacteriophage amidase.

Atl contains three direct repeat sequences in between the amidase and glucosaminidase domain. The repeats R1 and R2 are present in the C-terminal portion of the amidase and the repetitive sequence R3 in the N-terminal portion of the glucosaminidase domain. The amidase domain of AtlA starts from alanine 199 and

ends at lysine 775, and the glucosamindase domain starts at alanine 776 and ends at lysine 1256. The amidase domain of AtlE starts from valine 303 and ends at leucine 845, whereas the glucosamindase domain starts at threonine 846 and ends at lysine 1335 (**Fig. 6**) (**Heilmann et al., 1997a**).

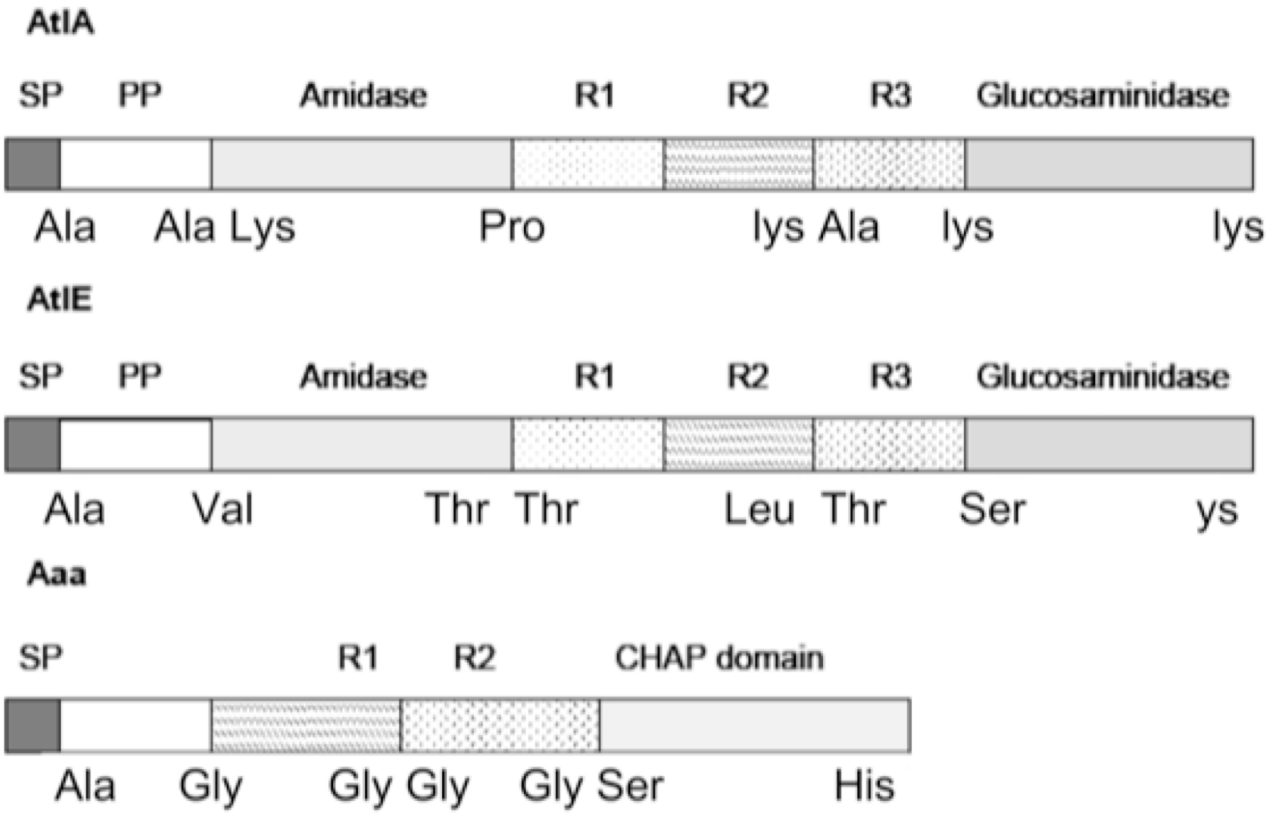

Fig. 6. Model of the structural organization of 138 kDa autolysin Atl from *S. aureus* (A), 148 kDa autolysin AtlE from *S. epidermidis* (B) and 35.8 kDa autolysin Aaa from *S. aureus* (C). Atl is composed of a signal peptide (SP, 3kDa) at the N-terminus followed by a pro-peptide (PP, 18kDa for AtlA and 30kDa for AtlE). The N-terminal catalytic domain of amidase (Ami; 62kDa) is linked with the C-terminal catalytic domain of glucosaminidase (GL; 51kDa) with three direct repeats. Repeats R1 and R2 are located at C-terminal portion of Ami and repeat R3 is located at N-terminal portion of GL. The autolysin/adhesin protein Aaa contains a putative signal peptide in the first 25 amino acids followed by two domains: the N-terminal domain of Aaa contains two direct repeat sequences. The repeats R1 (66 aa, starting at G-89) and R2 (65 aa, starting at G-155) are 65% identical. The Aaa repeats are highly homologous to a consensus sequence that has been termed the LysM domain (for lysin motif). The C-terminal catalytic domain of Aaa is homologous to CHAP (cysteine, histidine-dependent amidohydrolases/ peptidases) domain. This domain is often found in PG hydrolysing enzymes.

1.2 Sequence analysis of Aaa

aaa consists of 1,002 nucleotides and encodes a deduced protein of 334 amino acids with a predicted molecular mass of 35.8 kDa. The hydrophobicity plot analysis using the Kyte-Doolittle program indicates that Aaa mainly consists of hydrophilic amino acids with a strong hydrophobic region at the N-terminus and therefore is a secreted protein (**Fig. 5**). It starts with the start codon GTG and is preceded by a putative ribosome-binding site at a distance of 8 bp. Deduced putative –10 promoter sequence is CATAAT (nucleotides –79 to –84) and –35 sequence is ATGTCA (nucleotides –110 to –104).

Aaa contains a putative signal peptide in the first 25 aa. The predicted *aaa* gene product is composed of 32.4% hydrophobic, 7.5% basic, and 3.3% acidic aa. The theoretical pI value of Aaa is 9.67. The amino acid sequence of Aaa is 100% identical to those of the putative homologous proteins from *S. aureus* strains COL, N315, MW2, NCTC8325, and MSSA476 and shares 97.9% identity with Aaa from strain MRSA252. The sequence similarity between *S. aureus* Aaa and *S. epidermidis* Aae is 75% (**Fig. 7A**).

A sequence comparison of Aaa with known proteins in databases revealed two domains. The N-terminal domain of Aaa contains two direct repeated sequences. The repeats R1 (66 aa, starting at G-89) and R2 (54 aa, starting at G-156) are 65% identical (**Fig. 7B**). The Aaa repeats are highly homologous to a consensus sequence that has been termed the LysM domain. The LysM domain is a part of various cell wall lytic enzymes. The C-terminal catalytic domain of Aaa is homologous to CHAP (cysteine, histidine-dependent amidohydrolases/ peptidases) domain. This domain is often found in PG hydrolysing enzymes (**Fig. 6**).

The N-terminal Aaa repeats are homologous to those of other autolysins that harbor the LysM domain, including the 35 kDa autolysin/adhesin Aae from *S. epidermidis* (three repeats, 71% identity), the 51 kDa cell wall-associated endopeptidase LytF from *Bacillus subtilis* (five repeats, 42% identity), the putative 35 kDa endopeptidase LytE from *B. subtilis* (three repeats, 42% identity), the 70 kDa N-acetylmuramoyl-L-alanine amidase from *Enterococcus faecalis* (five repeats, 37%

identity), and the 50 kDa invasion-associated protein p60 of *Listeria* species (three repeats, 35% identity) .

Fig. 7. Multiple sequence alignment of the deduced amino acid sequences of Aaa from *S. aureus* and Aae from *S. epidermidis* (A). Aaa and Aae amino acid sequences are 75% identical. (B) Alignment between the two repetitive sequences of the Aaa. "*" means that the residues in that column are identical in all sequences in the alignment.":" means that conserved substitutions have been observed.

The C-terminal domain of Aaa shows the highest similarity to the 35 kDa autolysin/adhesin Aae from *S. epidermidis* (87% identical), the secretory, highly antigenic, in vivo-expressed protein SsaA from *S. epidermidis* (56% identical aa), ORF1 from *S. aureus* (55% identical aa) , and the extracellular protein SceB from *Staphylococcus carnosus* (53.6% identical aa).

2. Construction of the *atl*A and *aaa* deletion mutant and complementation

2.1 Construction of SA∆*atlA::spc*

In the genome of *S. aureus* SA113, *atlA* is flanked upstream by genes encoding a proposed autolysin transcription attenuator and a putative acetyl transferase and downstream by a gene encoding a putative transcription regulator.

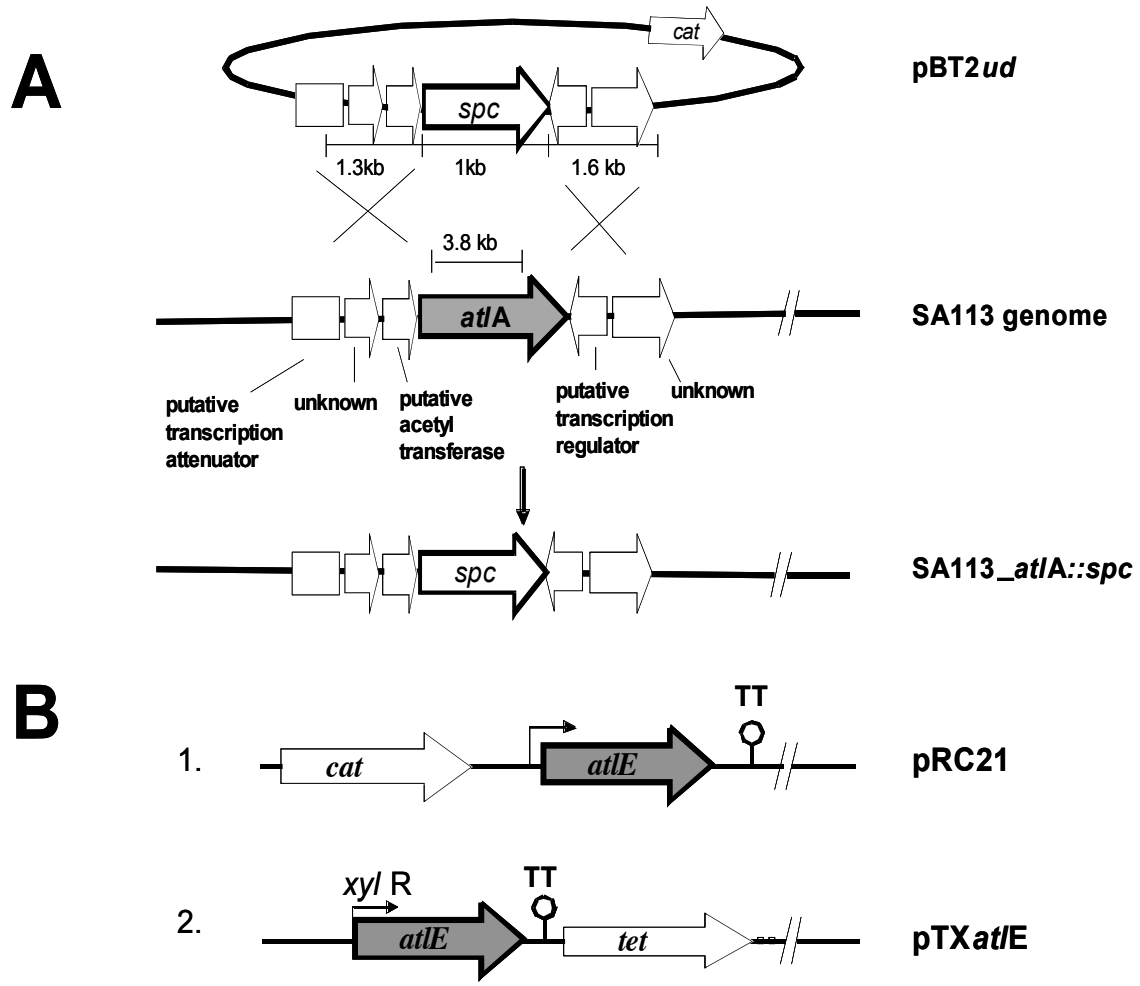

Fig. 8. Allelic replacement of *atlA* in *Staphylococcus aureus* SA113 (A) and of the *atlE* expression vectors (B). The SA113 genomic *atl*A gene was replaced by the spectinomycin (*spc*) resistant cassette of pBT2*ud* by homologous recombination. *spc* in the vector is flanked by 1.3- and 1.6-kb regions found upstream and downstream of the *atlA* gene in the genome. pBT2*ud* was introduced into SA113 by transformation, and clones were screened for allelic replacement (chloramphenicol sensitivity and spectinomycin resistance). (B) Linear map of *atlE* expression vectors. *atlE* is transcribed under its native promoter in pRC21 and from the xylose-inducible promoter in pTX*atlE*.

An *atlA* deletion mutant was constructed by homologous recombination using the plasmid pBT2 (Bruckner, 1997), by cloning a spectinomycin selection marker (*spc)* flanked by upstream and downstream regions of the *atlA* gene in the multiple cloning site of pBT2. The entire genomic *atlA* gene was PCR amplified using the primer pair *atlF Nhe*I and *atlR Eco*RI.

The PCR product was digested with *Eco*RI and *Sph*I (internal site introduced with the primer), and the 1.6 kb downstream fragment (*d*) was cloned in pre-digested pEC2 (Brückner, 1997), generating plasmid pEC2*d*. The upstream flanking region (*u*) was PCR amplified using primers *atlF Nhe*I and *atlR Bam*HI and cloned in pBT2, generating plasmid pBT2*u*. The downstream flanking region was excised from pEC2*u* with *Eco*RI and *Hin*dIII, and the spectinomycin cassette was excised from pIC156 (Steinmetz and Richter, 1994) with *Bam*HI and *Hin*dIII. The two fragments were ligated to each other and with *Bam*HI/*Eco*RI-digested pBT2*d*, generating plasmid pBT2*ud*.

The *atl*A mutant was generated in SA113 by homologous recombination using the temperature-sensitive plasmid pBT2ud, which contains the spectinomycin resistance gene (*spc* cassette) flanked by upstream (u) and downstream regions (d) of atlA (**Fig. 8A**). The plasmid pBTud was electroporated into RN4220 and then in SA113. Mutants were constructed by homologous recombination as described in Material and Methods. Clones were screened for chloramphenicol sensitivity and spectinomycin (for *atlA* deletion) resistance.

2.2 Construction of SA∆*aaa*::*ermB*

aaa consists of 1004 bp nucleotides flanked upstream by ABC transporter protein and downstream by a hypothetical protein. *The* SA∆*aaa* mutant was constructed by replacing the *aaa* gene by the erythromycin cassette (*erm*B) by homologous recombination using temperature sensitive plasmid pBTa. Upstream region genes of 660 bp were amplified using the primer pair *aaa*-BamHI and *aaa*-EcoRI and the downstream region genes using primer pair *aaa*-HindIII and *aaa*-NheI. The *Erm*B cassette was excised from pEC2 (Bruckner, 1997) using the restriction sites BamHI and HindIII. PCR products were digested using the restriction sites as indicated with

the primer name and cloned into the multiple cloning site of pBT2. The resulting plasmid was named pBT2a (**Fig. 9A**). Plasmid pBT2a was electroporated in RN4220 and then in SA113. Mutants were constructed by homologous recombination as described in Material and Methods. Clones were screened for chloramphenicol sensitivity and erythromycin (for *aaa* deletion) resistance.

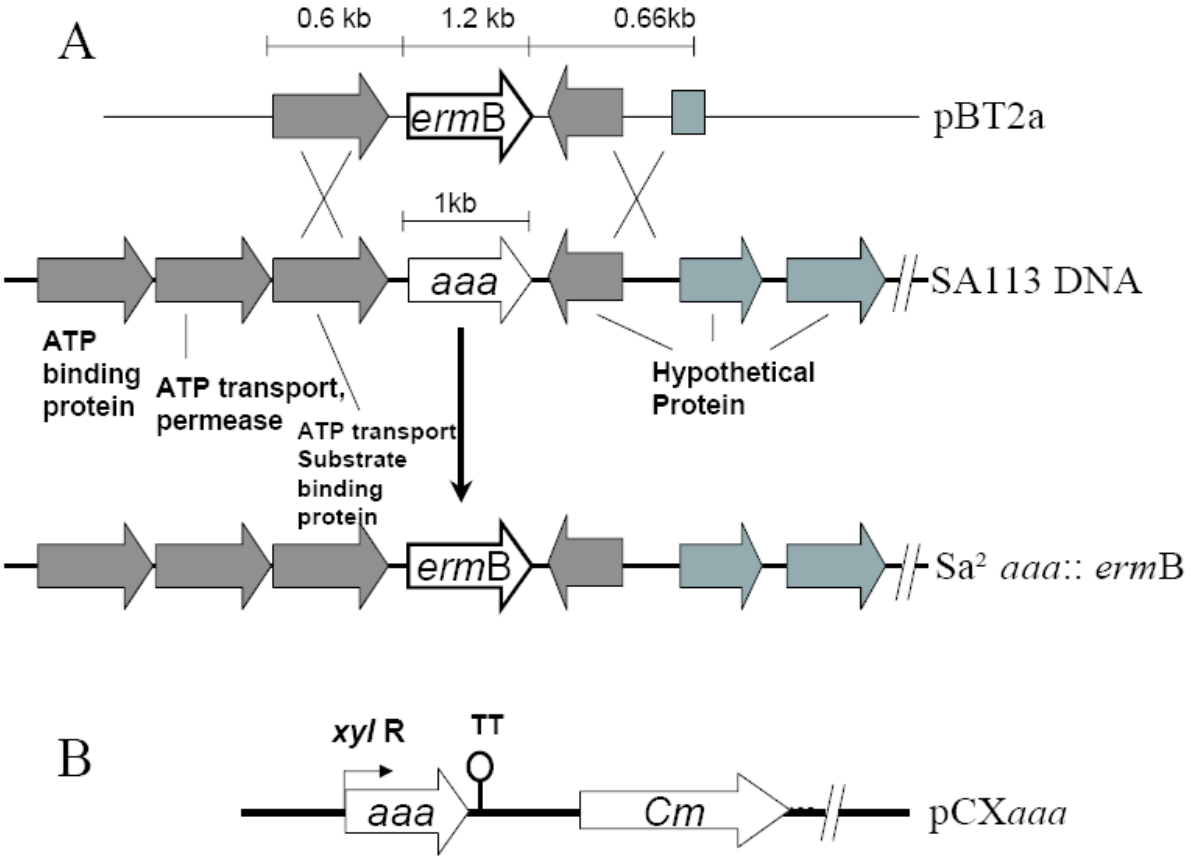

Fig. 9. Allelic replacement of *aaa* in *Staphylococcus aureus* SA113 (A) and construction of the *aaa* expression vector (B). The SA113 genomic *aaa* gene was replaced by the erythromycin (ermB) resistant cassette of pBT2*a* by homologous recombination*. erm*B in the vector is flanked by 0.6- and 0.66-kb regions found upstream and downstream of the *aaa* gene in the genome. pBT2*a* was introduced into SA113 by transformation, and clones were screened for allelic replacement (chloramphenicol sensitivity and erythromycin resistance). (B) Linear map of *aaa* expression vector. *aaA* is transcribed by the xylose-inducible promoter in pCX*aaa.*

2.3 Complementation of ∆*atlA::spc* and ∆*aaa::ermB* mutants

S. aureus SA113 ∆*atl*A::*spc* mutant was complemented by the *S. epidermidis atlE*

gene either in vector pRC21 (Heilmann et al., 1997a) in which the *atlE* gene is under the control of its native promoter (**Fig. 8B**), or in pTX*atlE* in which *atlE* is under the control of the inducible xylose promoter of plasmid pTX15 (Peschel et al., 1996). For cloning in pTX15, the primer pair *atlE-Bgl*II and *atlE-Pst*I was used.

SA∆*aaa*::*erm*B was complemented using plasmid pCX*aaa* (**Fig. 9B**), where aaa is cloned downstream the xylose-inducible promoter in plasmid pCX19, a derivative of pCX15 (Wieland et al., 1995). The *aaa* sequence was amplified from SA113 genomic DNA using primer pair *aaa* BamHI SD 990 and *aaa* SacI 2610. The PCR product was digested with BamHI and ligeated with pCX19 vector which was predigested with BamH1 and SmaI. The resulting plasmid was named pCX*aaa*.

3. Characterization of SA∆*atl*A:: *spc* and SA∆*aaa*:: *erm*B mutants

To analyze the function of AtlA and Aaa in the context of the bacterial cell, we constructed a SA∆*atl*::*spc* and SA∆*aaa*:: *erm*B deficient mutant from *S. aureus* strain SA113 by gene replacement by homologous recombination and compared it with the wild type.

3.1 Confirmation of the *atl* and *aaa* mutant

To verify that the 138 kDa Atl and 35.8 kDa autolysin Aaa was missing from protein preparations of the respective mutants, surface-associated proteins and exoproteins were analyzed by SDS-PAGE, zymogram and Western bloting. A striking feature of the SA∆*atl*A::*spc* mutant is that not only the Atl-derived proteins are missing but also the general content of proteins is significantly decreased (**Fig. 10A and B**). Much more proteins were extracted from the wild-type and the complemented mutant SA113∆*atl*A::*spc* (pCR21) than from the SA113∆*atl*A::*spc* mutant.

The exoprotein and cell wall associated protein pattern of SA113∆*aaa*::*erm*B remains unchanged (**Fig. 11 A**) and comparable with the wild type protein pattern. We assume that protein translocation and secretion is severely hampered in the clump forming SA∆*atl*A::*spc* mutant cells, that were septated but not separated from

each other. The non-covalently linked cell-wall-associated proteins were extracted with 4% SDS and analyzed by SDS-PAGE. The individual deletion of *atl*A (**Fig. 10 C**) and *aaa* (**Fig. 11 B, C**) was confirmed by Western blot analysis.

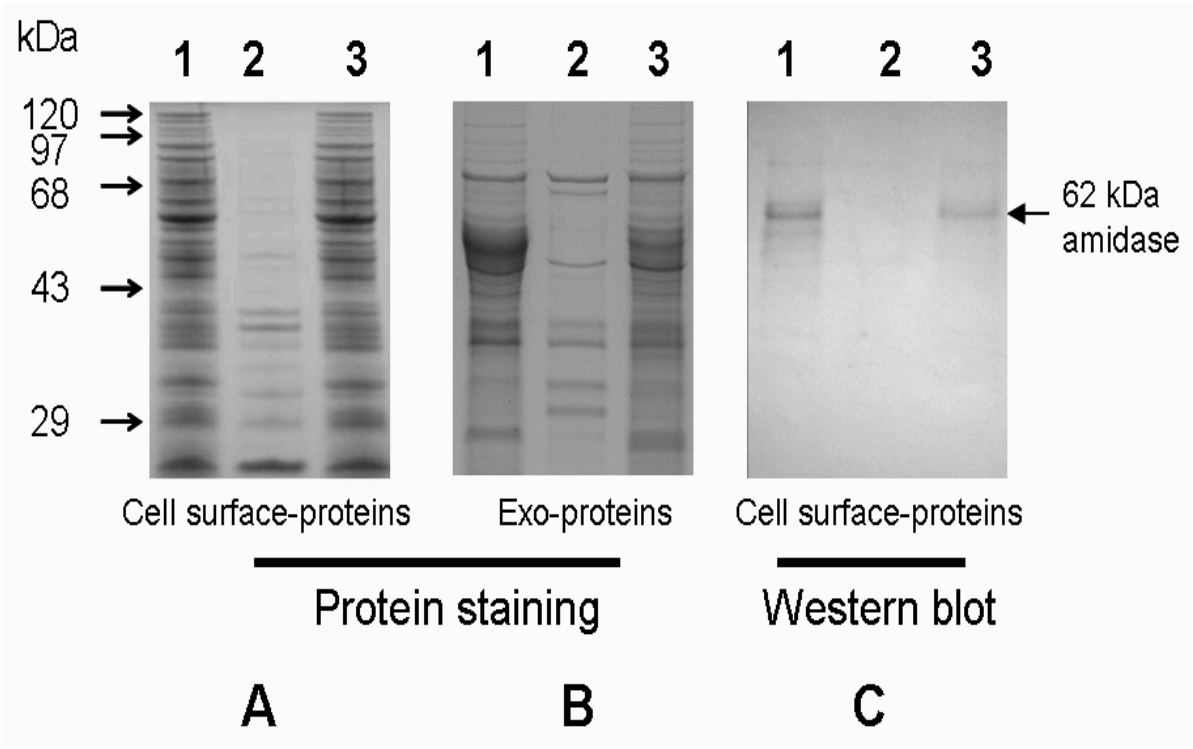

Fig. 10. Analysis of cell surface associated proteins (A), exo-proteins (B) in Tris-tricine SDS 10%Page and Immuno blot(C). SDS-PAGE gels were stained with Coomassie Brilliant-Blue (CBB). Immuno-blot was done using anti-amidase antibody (C) demonstrating the absence of the 62 kDa amidase (C) in the mutant and its restoration in the complemented strain. Molecular masses of standard proteins are indicated on the left. Lane1: Sa113 wt, Lane2: SAΔ*atl*A, Lane3: SAΔ*atl*A (pRC21).

In Western blot analysis, a 35.8 kDa protein that reacted with the anti-Aaa antiserum was detected in protein preparations of the wild-type strain but was missing from protein preparations of the SAΔ*aaa*::*erm*B mutant (**Fig.11 C**). In control experiments, no specific binding of Aaa to the preimmune serum or to the anti-digoxigenin-AP conjugate was observed (**Fig.11 B**). A larger and a smaller protein of around 60 kDa and 40 kDa that reacted with the anti-Aaa antiserum and also with the preimmune serum may represent Eap (also referred to as Map or p70) and its degradation products, respectively, which were reported to have an IgG-binding function (Heilmann et al., 2005).

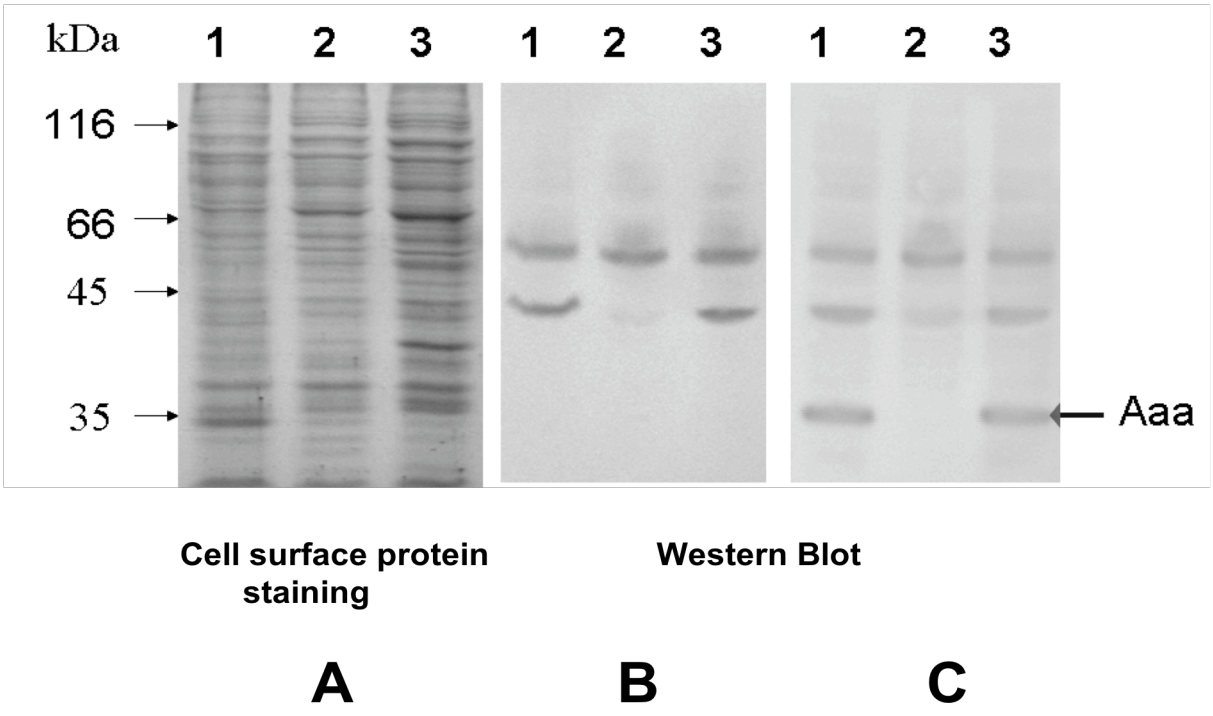

Fig. 11. Analysis of cell surface associated proteins (A) in Tris-tricine SDS 10% Page and Immuno blot (B, C). SDS Page gel (A) was stained with Coomassie Brilliant-Blue (CBB). Immuno-blot was done using pre-immune serum (B) and anti-Aaa serum (C) demonstrating the absence of 36 kDa Aaa in the mutant and its restoration in complemented strain. Molecular masses of standard proteins are indicated on left. Lane1: Sa113 wt, Lane2: SAΔ*aaa*::*erm*B, Lane5: SAΔ*aaa*::*erm*B (pCX*aaa*).

In the zymogram with embedded heat-killed *S. aureus* or *M. luteus* cells, five prominent AtlA-derived lysis bands were observed with samples of the wild-type and the complemented mutant: 138 kDa, pro-Atl; 115 and 80 kDa, intermediates; 62 kDa, amidase; and 51 kDa, glucosaminidase (**Fig. 12**). In the zymogram with embedded *S. aureus* cells (**Fig. 12 A**), an additional lytic band is visible, corresponding to the 36 kDa protein Aaa (Heilmann *et al.*, 2005). This cell wall lytic protein is not a derivative of AtlA, as shown by its presence in the SAΔ*atl*A::*spc* mutant, where it is synthesized at higher levels than in the wild-type. Interestingly, the cell lysis activity appears to be specific for staphylococci; no lysis of *M. luteus* cells was observed (**Fig.12 B**). Moreover, in SAΔ*aaa*::*erm*B the 36 kDa lytic band was missing which was restored in the complemented mutant (**Fig.13**). We observed slight overexpression of the 62 kDa amidase in the Atl derived lytic profile of the SAΔ*aaa*::*erm*B mutant.

Zymographic analysis confirmed that a 35.8 kDa autolysin/adhesin protein (Aaa)

with bacteriolytic activity was present in the *S. aureus* wild type but missing from the Sa∆*aaa*::*erm*B mutant (**Fig. 13**). The larger protein bands with bacteriolytic activity presumably represent the products of proteolytic cleavage from the Atl precursor molecule.

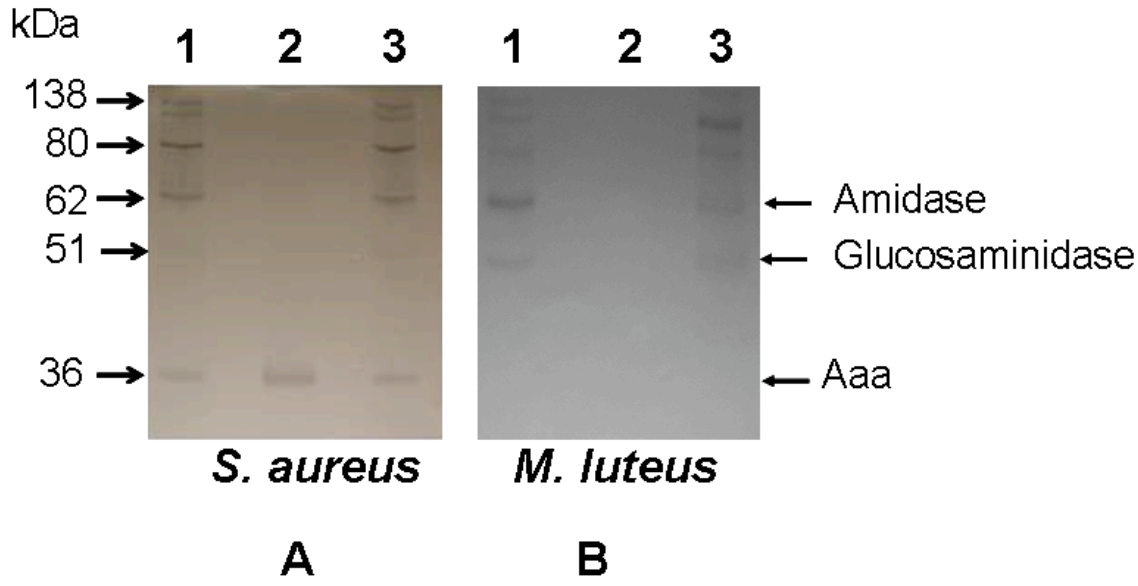

Fig. 12. Bacteriolytic activity profiles of cell surface associated protiens in SDS-PAGE with embedded *S. aureus* (A) and *Micrococcus luteus* (B) cells. Molecular weight standard proteins are indicated on left. Arrow on the right indicates the lytic bands Atl (138kDa), pro-Atl (81kDa), amidase (62 kDa) and glucosaminidase (51 kDa) and 36 kDa AaA.Lane1: SA113, Lane2: SA∆*atl*A, Lane3: SA∆*atl*A (pRC21).

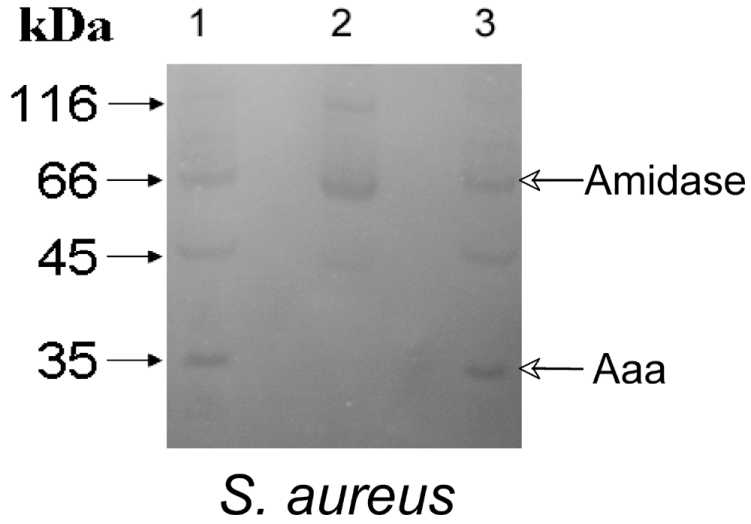

Fig. 13. Bacteriolytic activity profiles of cell surface associated proteins in SDS-PAGE with embedded *S. aureus* cells. Molecular weight standard proteins are indicated on left. Lane1: SA113, Lane2: SA∆*aaa*:: *erm*B, Lane5: SA∆*aaa*::*erm*B (pCXaaa).

3.2 Colony morphology

We found that the colony morphology of the autolysin mutant *S. aureus atlA* differed from that of its wild type. The *atlA* mutant formed rough and dull colonies instead of shiny colonies like the wild type. In contrast, there was no difference in colony morphology phenotypes on TSA plates between the Sa∆*aaa*::*erm*B mutant and its wild type strain SA113.

3.3 Growth in liquid culture and cell aggregation

Autolysins are involved in cell division and cell separation. Therefore, we compared the growth of the SA∆*atl*A::*spc* and SA∆*aaa*::*erm*B mutant with its wild type in liquid culture. The SA∆*atl*::*spc* and SA∆*aaa*::*erm*B mutant revealed the same growth rates in TSB as the wild type, and both strains reached the same end OD_{578} (data not shown). However the SA∆*atl*A::*spc* mutant form large clumps which are septated but not separated from each other. In standing liquid culture the atl mutant precipitates at the bottom of the tube, whereas SA113 and the *aaa* mutant culture remain in suspension (**Fig.14 A**). The SA∆*atl*A:: *spc* mutant formed huge clusters visualized by phase-contrast microscopy (**Fig. 14 B**). When grown overnight without shaking, the mutant cells sedimented in the flask, whereas wild-type cells remained suspended. Cell aggregation is indicative of a loss of an enzyme involved in cell separation .To clarify whether Aaa is involved in cell separation, we observed liquid cultures of the SA∆*aaa*::*erm*B mutant and its wild type in TSB by using phase-contrast microscopy and could not detect any difference in cell cluster formation. With both strains, there were mainly single cells, pairs, and tetrads visible.

3.4 Microscopical studies

The growth rate of the cells was not affected by the SA∆*atl*A::*spc* and SA∆*aaa*::*erm*B mutations. In ultra-thin sections, the SA∆*atl*A::*spc* mutant is distinguished by a rough outer cell surface, particularly near the cell division site. A high proportion of the mutant cells were abnormally tetrameric, which indicates that cell separation was hindered. The cells of SA∆*aaa*::*erm*B exhibit normal cell shape and cell wall architecture when observed under phase construct or electron microscope (**Fig. 15**).

This indicates that in absence of Aaa protein the major autolysin alone is sufficient for cell separtion after cell division.

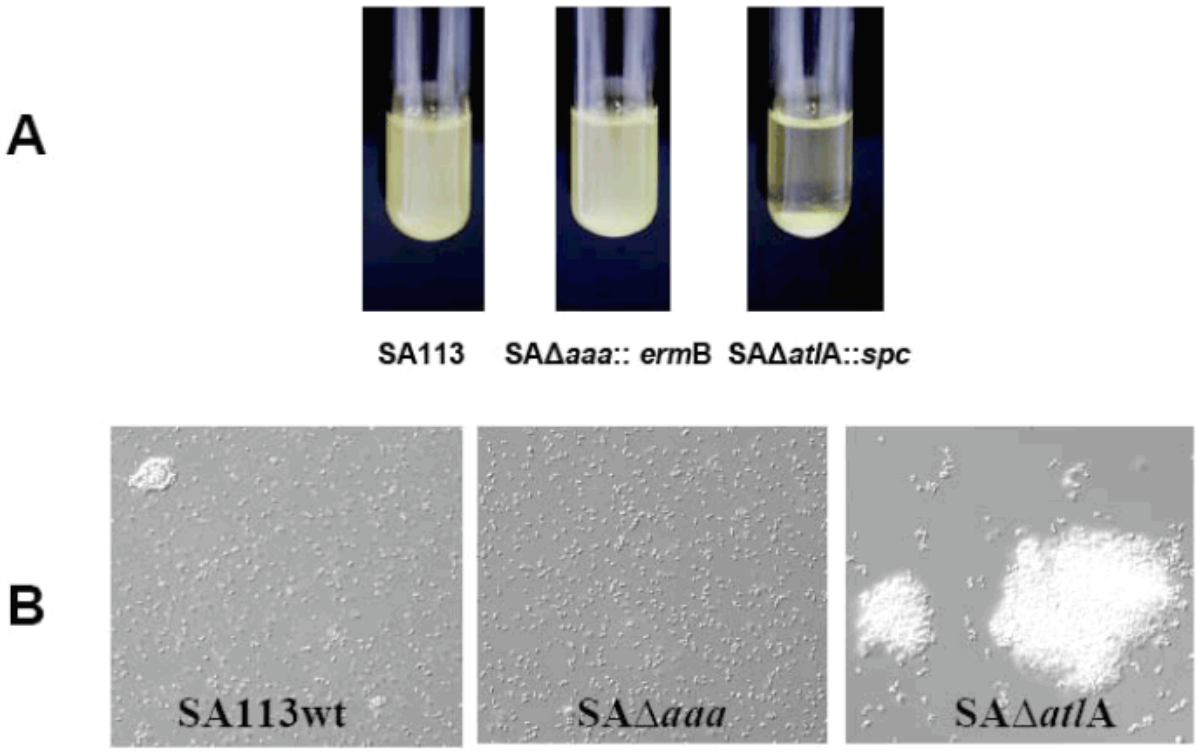

Fig. 14. Comparison of liquid cultures of the SA113 parental strain and its mutants, SAΔ*aaa*::ermB and SAΔ*atl*A:: *spc*. **(A)** In standing liquid culture the *atl* mutant precipitates at the bottom of the tube, whereas Sa113 and *aaa* mutant remains suspended. **(B)** Light micrograph of *S. aureus* wild type, SAΔ*aaa*::ermB and clump forming SAΔ*atl*A:: *spc*.

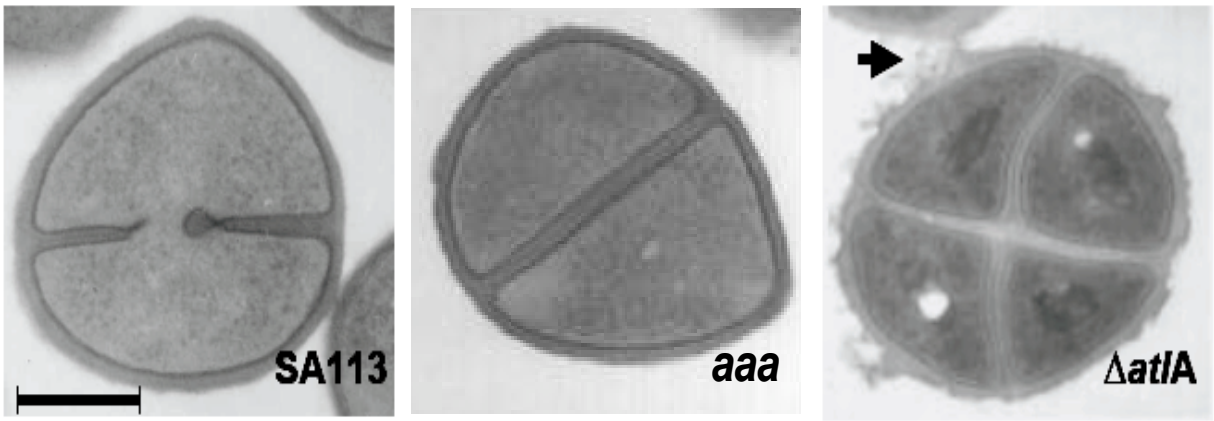

Fig. 15. Transmission electron microscopy of *S. aureus* SA113 and SAΔ*aaa*::ermB and SAΔ*atl*A:: *spc*. The cells of the SAΔ*aaa*::ermB having cell wall arcitecture compariable with the wild type. SAΔ*atl*A::spc mutant possess a very rough

unprocessed cell wall that appears to be interlinked with other cells. Bar indicates 0.5 µm.

A high proportion of the mutant cells were abnormally tetrameric, which indicates that cell separation was hindered. The cells of SAΔ*aaa*::*erm*B exhibit normal cell shape and cell wall architecture when observed under the phase contrust or electron microscope (**Fig. 15**). This indicates that in the absence of Aaa the major autolysin alone is sufficient for cell separation after cell division.

3.5 Role of AtlA and Aaa in initial attachment

The ability to form a biofilm is one of the virulence properties of *S. aureus* which involves two distinct processes: an initial attachment to the surface and the formation of multilayer cell clustering facilitated by the production of a slimy substance called the polysaccharide intercellular adhesin, PIA (Götz, 2002).

The biofilm-forming capacity of the wild-type, the Δ*atl*A::*spc*, the Δ*aaa*::*erm*B mutant and their complemented mutants was compared by cultivating cells on polystyrene (Cramton *et al.*, 2001) or glass surfaces in a biofilm assay using the green fluorescent protein (*gfp*) encoded on plasmid pCtuf-gfp.

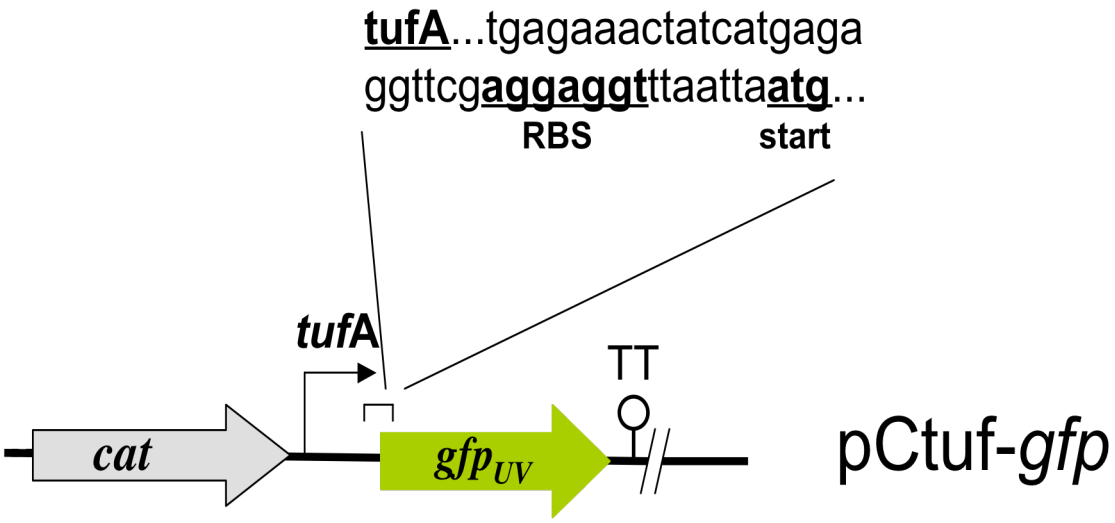

Fig. 16. Genetic map of plasmid pCtuf-gfp. In this vector, the gene encoding the green fluorescent protein, gfp, is transcribed from the tufA promoter, and the ribosomal binding site (RBS) has been altered to AGGAGG for optimal expression in

gram-positive bacteria.

The *gfp* gene was cloned into pCX19 replacing the xylose inducible promoter and the lipase gene. The gfp gene was excised from the vector pgfp-UV (Clontech, Mountain View, Calif., USA) and cloned in pCX19, a derivative of pCX15 in which the *cat* gene has been inverted (Dr. B. Krismer, Genmedics GMBH, Germany). To optimize *gfp* expression, the *tufA* promoter was PCR amplified from SA113 genomic DNA using the primers tufA F and tufA R (nucleotide sequence accession number AF274740) and placed in front of the *gfp* gene. Furthermore, the *gfp* ribosomal binding site was altered to AGGAGG for optimal expression in Gram-positive bacteria. The resulting reporter plasmid pCtuf*gfp* (**Fig. 16**) was used to monitor biofilm formation.

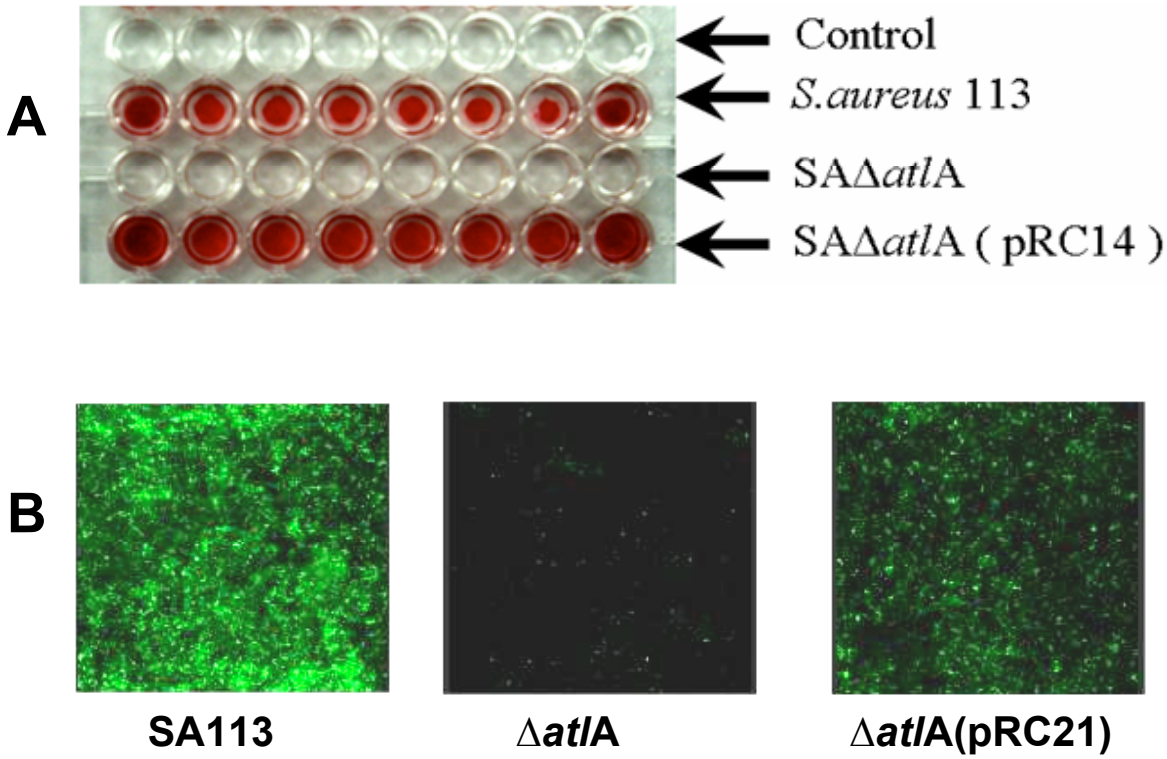

Fig. 17. Biofilm formation monitored using *S. aureus* clones producing green fluorescent protein (A, B). Biofilm formation after 24 h of growth on a microtiter plate and on glass surface of *S. aureus* wild-type SA113, the mutant SAΔ*atl*A::spc, and the mutant complemented with pCR21. Microtiter plate containing biofilms was stained with safranin. Confocal laser scanning microscopy was used to monitor biofilm formation on glass slides.

Homogeneous expression of green fluorescent protein from pCtufgfp was confirmed by FACS analysis (Lalitha Voggu; unpublished data). Cells were grown for 24 h, and cells loosely bound to the surfaces were then washed away with PBS.

Cells adhering to the surfaces of microtiter plate were stained with safranin and green fluorescence of adhered cells on the glass slide was photographed using fluorescence microscopy (**Fig. 17**). The SA∆*atl*A::*spc* mutant was deficient in primary attachment, whereas the wild-type, SA∆*aaa*:: *erm*B mutant and its complemented mutant were not (not shown). This result further supports the role of major autolysin (Atl) in biofilm formation.

4. Molecular cloning of his tag amidase and Aaa in E.coli

4.1 Over-expression of his tag amidase

Since the SA∆*atl*A::*spc* mutant of *S. aureus* could be complemented by DNA encoding the AtlE amidase domain, the atlA and atlE genes and their corresponding enzymes are exchangeable and apparently have similar functions. We used the atlE-derived amidase constructs (Heilmann et al., 1997b) for the remaining studies on the function of the repetitive sequences and biochemical analysis of the cleavage site. The amidase domain of the *atlE* gene was over-expressed with no repeat regions (*ami*E) or with two repeat regions (*ami*E-$R_{1, 2}$), or the three repeat regions alone ($R_{1, 2, 3}$) as N-terminal His-tag fusion proteins in *E. coli* (**Fig. 18**).

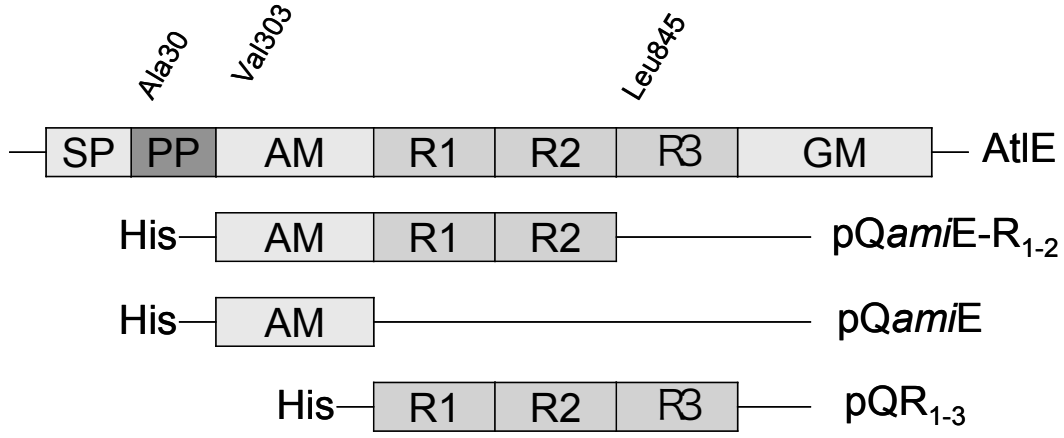

Fig. 18. Construction of vectors expressing various amidase and internal repeat domains of the AtlE precursor protein. *E. coli* expression vectors: pQamiE-$R_{1,2}$ encodes the amidase domain (AM) and the two following repeat sequences (R1 and R2), pQamiE encodes the amidase domain and no repeat sequences, and $pQR_{1,2,3}$ encodes three repeat sequences (R1, R2, R3). All constructs contained an N-terminal His-tag and were located in the cytoplasm.

The amidase domain of the *atlE* gene with no repeat regions (*amiE*) and with two repeat regions (*ami*E-$R_{1,\ 2}$), and the three repeat regions alone ($R_{1,2,3}$) were cloned and expressed as N-terminal His-tag fusion proteins in pQE30 (Qiagen). *ami*E was constructed using the primer pair AM-BglII and AM-PstI amiE-$R_{1,2}$ was PCR amplified from *S. epidermidis* O-47 genomic DNA using the primer pair AM-BglII and AR2-PstI digested with BglII and PstI, and inserted into BamHI/PstI-cleaved pQE30 to generate plasmid pQEamiE. The repeat regions $R_{1,2,3}$ were PCR amplified with the primer pair R1-BglII and AR3-PstI. All constructs were expressed in *E. coli* M15, and the proteins were located in the cytoplasm. Proteins **(Fig. 19)** were purified using Ni-NTA his tag column as described in materials and methods.

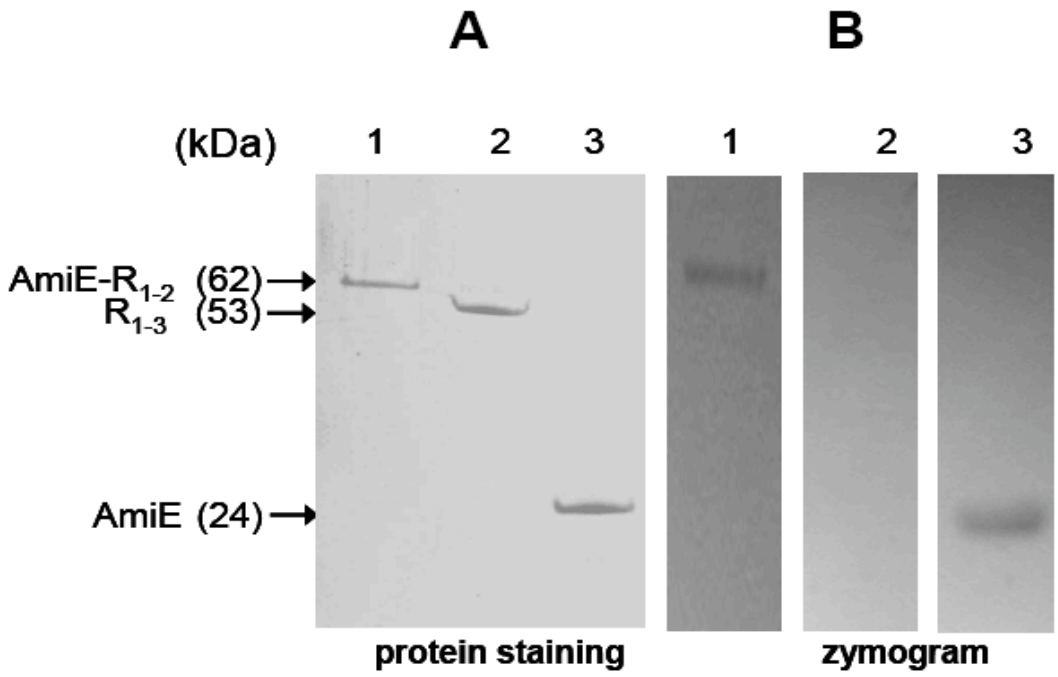

Fig. 19. SDS-PAGE (A) and the corresponding zymogram (B) with embedded heat-killed *S. aureus* cells. AmiE-$R_{1,2}$, R_{1-3} and AmiE was over-expressed in *E. coli*. Proteins were purified by Ni-NTA affinity chromatography. SDS-PAGE gel was stained with coomassie brilliant blue. Lanes: 1) AmiE-$R_{1,2}$ (62 kDa), 2) $R_{1,2,3}$ (53 kDa), and 3) AmiE (24 kDa).

4.2 Turbidometric assay of peptidoglycan

PG was isolated from wild-type SA113 and suspended in 100 mM PBS. O.D. $_{578nm}$ was adjusted to 0.8. PG was digested separately with 100 µg/ml of His tag AmiE-$R_{1,2}$ (62 kDa), $R_{1,2,3}$ (53 kDa), and AmiE (24 kDa) at 37°C. More than 70% of the PG was

digested in 6h with His tag AmiE-$R_{1,2}$. Only 40% PG was digested with His-AmiE. No digestion was observed with His-$R_{1,2,3}$ and in the control sample (Fig. 20). This result indicates that AmiE is also active without its repeat domains and repeat domains contribute little to the lytic activity of amidase.

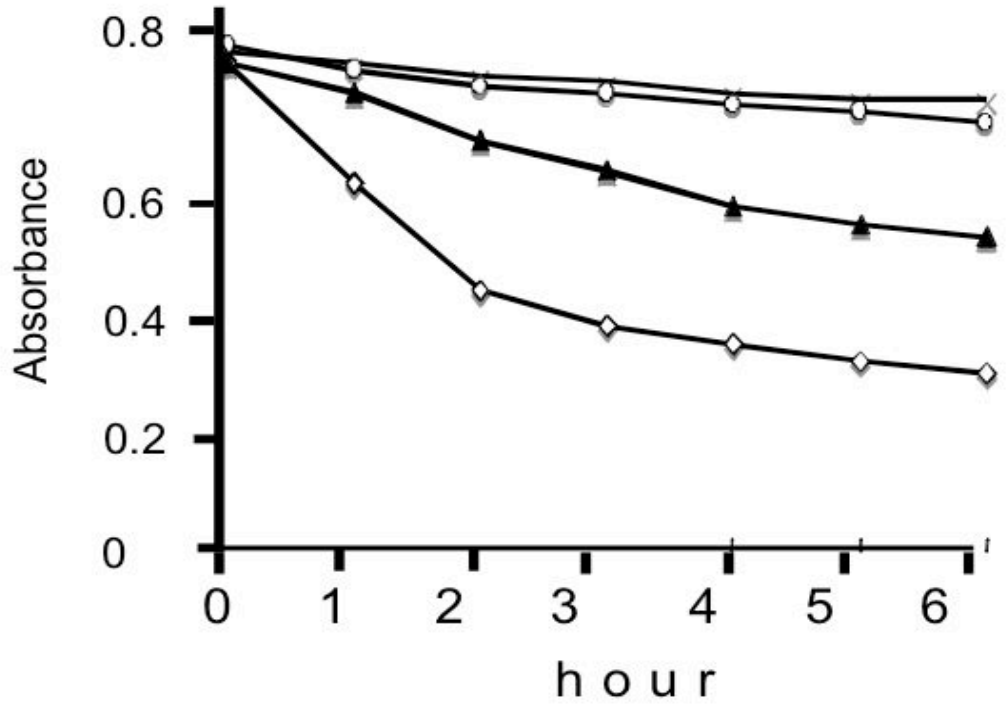

Fig. 20. Amidase induced peptidoglycan lysis. PG was digested with His tag AmiE-$R_{1,2}$ (◊; 62 kDa), $R_{1,2,3}$ (○; 53 kDa), AmiE (▲; 24 kDa) and control (×) for 6 h.

4.3 Purification of AmiE for X-ray crystallography

We attempt to crystallize the catalytic domain of N-acetyl L-alanine amidase (AmiE). Ni-NTA column purified His-AmiE was further purified by gel filtration chromatography (**Fig. 21**). AmiE was purified as a single band as observed in Coomassie stained SDS-PAGE gel.

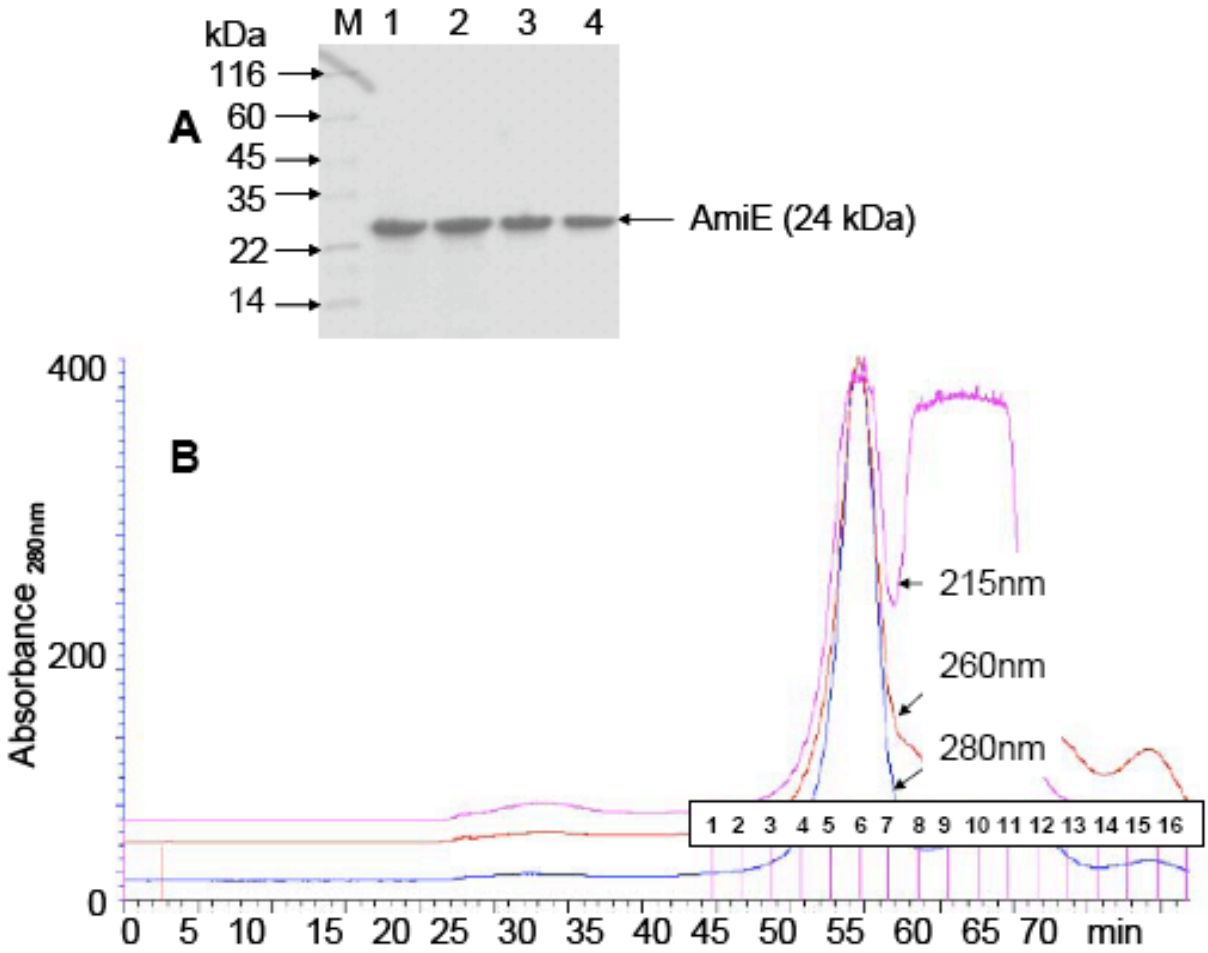

Fig. 21. Purification of His-AmiE by gel filtration chromatography (A) using Sephacryl S-100 high resolution 16/60 (Amarsham Biosciences) column using flow rate 0.5 ml/min with buffer containing 20 mM Tris-HCl, 100 mM NaCl, 0.02% sodium azide (pH 7.0). AmiE (24 kDa) was eluted as a single peak. (B) Insert shows analysis of His-AmiE fractions (4-7) in SDS-PAGE. Molecular weight masses of standard proteins are indicated on the left.The gel was stained with Coomassie Blue.

The estimated protein concentration was 0.5 mg/ ml. We tried to concentrate the protein solution to 10 mg/ml using the Millipore centrifugal protein concentrator (with molecular weight cut off 10 kDa). Higher protein concentrations are necessary to achieve crystalization. However, a protein concentration more that 1.9 mg/ml was not achieved. Above this concentration the protein tended to aggregate and precipitate. However we attempt to crystallize AmiE using this protein concentration. Neverthee less, crystallization expertiments were performed using Hamilton crystal screens. A number of precipitation zones were observed under the microscope with buffer containing PEG, which indicates the possibility of obtaining crystals at higher

protein concentrations. Precipitation was found with buffers number 28, 30,31, 36, 40,43 and 45. The detailed composition of these buffers is listed in Materials and Methods. All the buffers contain either 20% to 30% of polyethylene glycol 8000 or polyethylene glycol 1500.

4.4 Over-expression of His-tag Aaa

The *aaa* open reading frame was cloned in the pET28 (Novagen) vector designed to express proteins as fusions with a His_6-tag at the N-terminus. The insert was PCR-amplified using SA113 genomic DNA as a template and oligonucleotides His Aaa BamHI and Aaa HindIII. The PCR product was digested by BamHI and HindIII and cloned in pET28; the resulting plasmid is designated pET*aaa*.

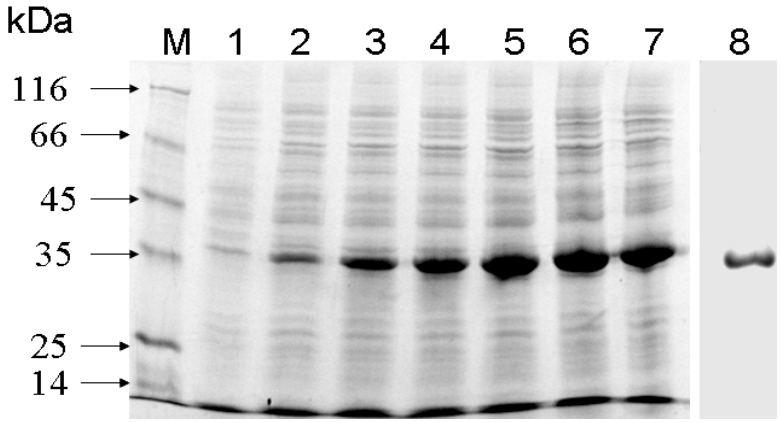

Fig. 22. Expression and purification of His-tagged Aaa. Lane 1, Molecular weight standard; Lane2, *E. coli* BL21 (DE3) / plysS cells containing the pETaaa vector before IPTG induction; lane 3-7, *E. coli* BL21 (DE3) / plysS cells containing the pETaaa vector 1-6 h after IPTG induction; Lane 8, Ni-NTA column purified Aaa protein under denaturing condition.

Overexpression was carried in the *Escherichia coli* strain BL21. Cells were induced with 1 mM IPTG at $O.D._{578\ nm}$= 0.5 and grown for additional 4 h at 37°C. Recombinant proteins were found in inclusion bodies and purified under denaturing conditions, using nickel-nitrilotriacetic acid resin (NTA) (Qiagen), following the manufacturer's instructions **(Fig. 22)**.

5. Determination of the binding capacity of *S. aureus* PG to the repeat domains

To study the interaction of these proteins with PG of *S. aureus*, the proteins were incubated with purified PG in phosphate buffer for 10 min at 4°C. The mixtures were then centrifuged and the content of the three proteins in the supernatants and PG pellets as analyzed by SDS-PAGE (**Fig. 23 A**). AmiE-$R_{1, 2}$ and the $R_{1, 2, 3}$ proteins were recovered in the PG pellet, i.e., they bound to purified PG. AmiE was found only in the supernatant, which indicated that the amidase domain alone has no, or only a very low, PG binding ability.

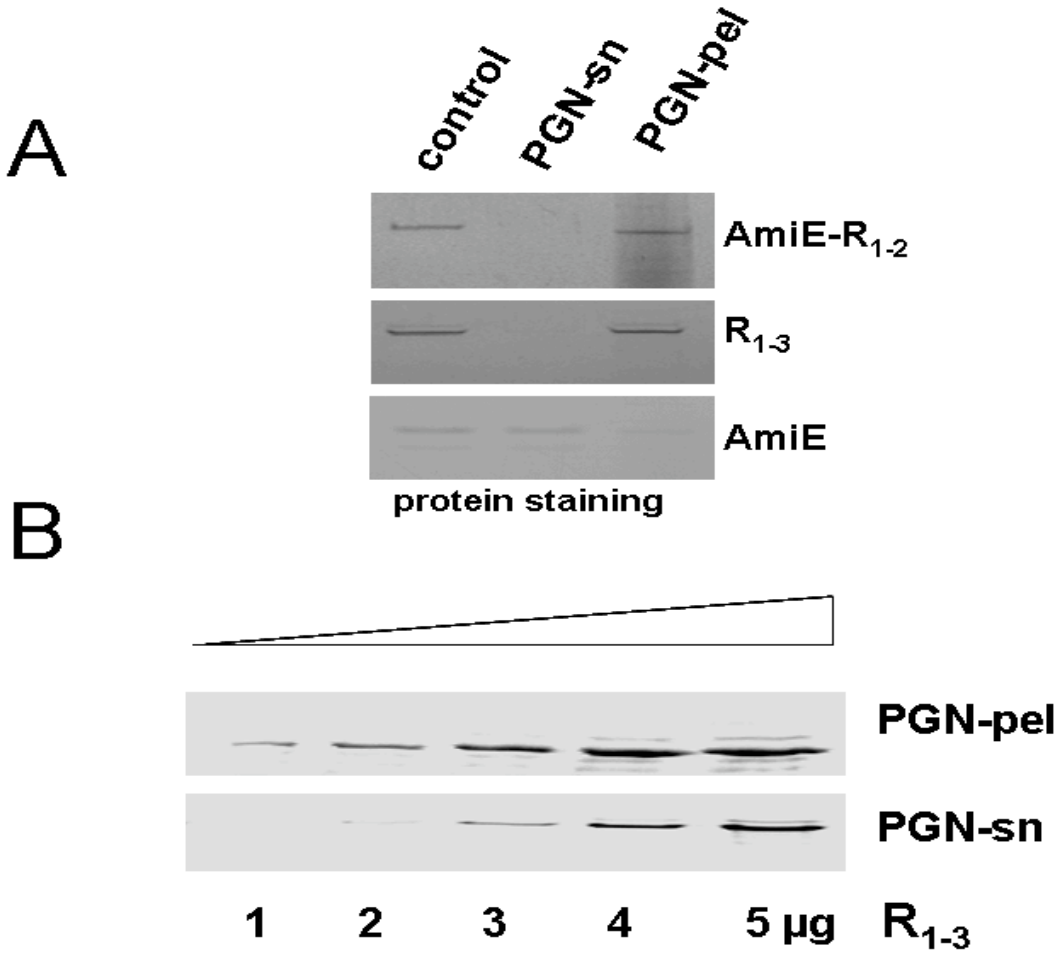

Fig. 23. The role of the repeat sequences in binding to PG. (A) PG binding assay. Approximately 1 µg of AmiE-$R_{1,2}$, $R_{1,2,3,}$ or AmiE was incubated with 50 µg purified PG for 10 min at 4°C in 100 mM phosphate buffer (pH 7.0). After centrifugation, PG-bound (pellet) and unbound proteins (supernatant) were analyzed by SDS-PAGE and stained with Coomassie brilliant blue. The control contained no PG. (B) Dose-dependent binding of $R_{1,2,3}$ to PG lacking cell wall teichoic acid (WTA). PG was isolated from *S. aureus* SA113 Δ*tag*O, a mutant deficient in WTA. PG (50 µg) was mixed with 1, 2, 3, 4, and 5 µg of $R_{1,2,3}$ and analyzed as described above.

To determine the binding capacity of *S. aureus* PG to the repeat domains, a dose-dependent binding assay was carried out with 50 μg purified PG and increasing amounts (1–5 μg) of $R_{1,2,3}$ (**Fig. 23 B**). The binding capacity of 50 μg of PG to the repeat domains was saturated by approximately 2 μg $R_{1,2,3}$; higher concentrations remained more and more unbound and were recovered in the supernatant.

We also investigated whether the presence of cell wall teichoic acid (WTA) plays a role in PG binding. We isolated PG from the *S. aureus* SA113 Δ*tagO* mutant (Weidenmaier et al., 2004), and used it in the same type of dose-dependent binding assay. Essentially the same pattern as for native PG was obtained, ruling out WTA as a binding anchor for the repeat sequences $R_{1,2,3}$.

6. Peptidoglycan hydrolysis activity of His tag AmiE-R1-2 and Aaa

Peptidoglycan hydrolysis activity of cell surface protein extracts from SA113, purified his tag AmiE R1-2 and Aaa was compared in a zymogram gel, as described above. Gels were embedded either with SA113 cells, SAΔ*tag*O cells or *Micrococcus luteus* cells.

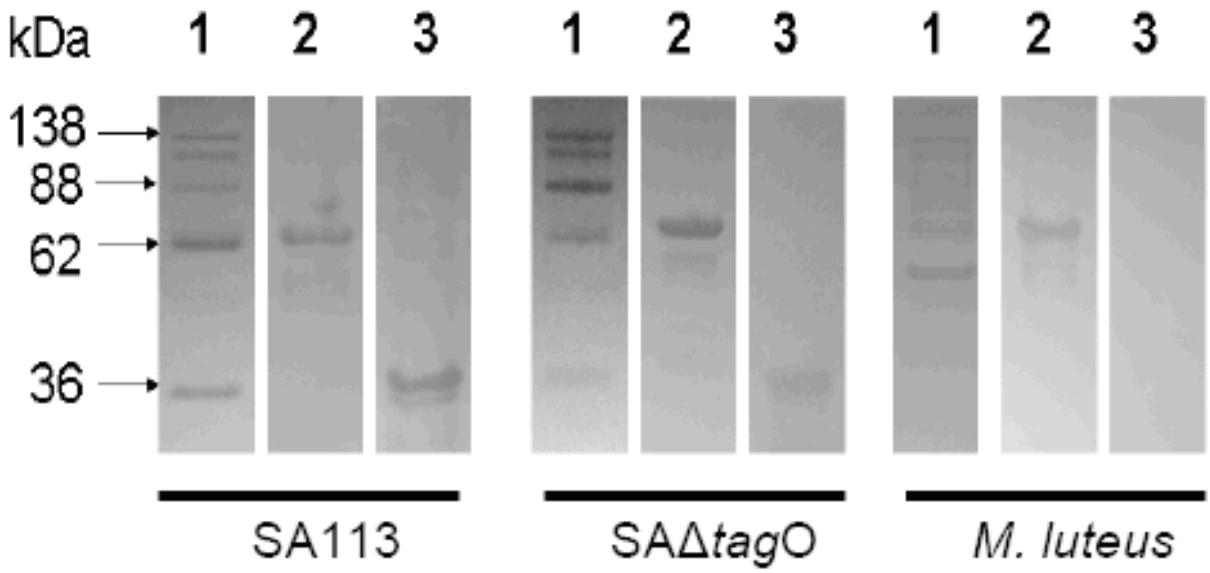

Fig. 24. Bacteriolytic activity of surface associated proteins from SA113 (1), His tag AmiE (2) and His tag Aaa (3) protein in a zymogram gel embedded with SA113 cells, SAΔ*tag*O and *M. luteus* cells. Note that the Aaa protein has no lytic activity against *M. luteus*.

We observed AmiE-R1-2 was equally active against SA113 cells, SAΔ*tag*O cells or *M. Luteus*, whereas Aaa was 50% less active against SAΔ*tag*O cells and possess no activity against *M. luteus* (**Fig. 24**). This indicate the Aaa probably cleaves a peptide bond that is absent in the *M. luteus* peptidoglycan and presence of wall teichoic acid is necessary for the optimum activity of the Aaa protein.

7. Peptidoglycan hydrolysis activity of amidase

S. aureus PG was solubilized with amidase, or lysostaphin, or both. The soluble fractions were recovered, reduced with $NaBH_4$ and analyzed by reversed-phase HPLC (**Fig. 25**). Peaks 1 and 2 in **Fig. 25 C** are products of amidase and lysostaphin double digestion since they were absent in amidase- or lysostaphin-digested samples. These two peaks were individually collected and analyzed by LC-MS and generated ions with m/z of 702.3 and 759.2 (**Fig. 26**).

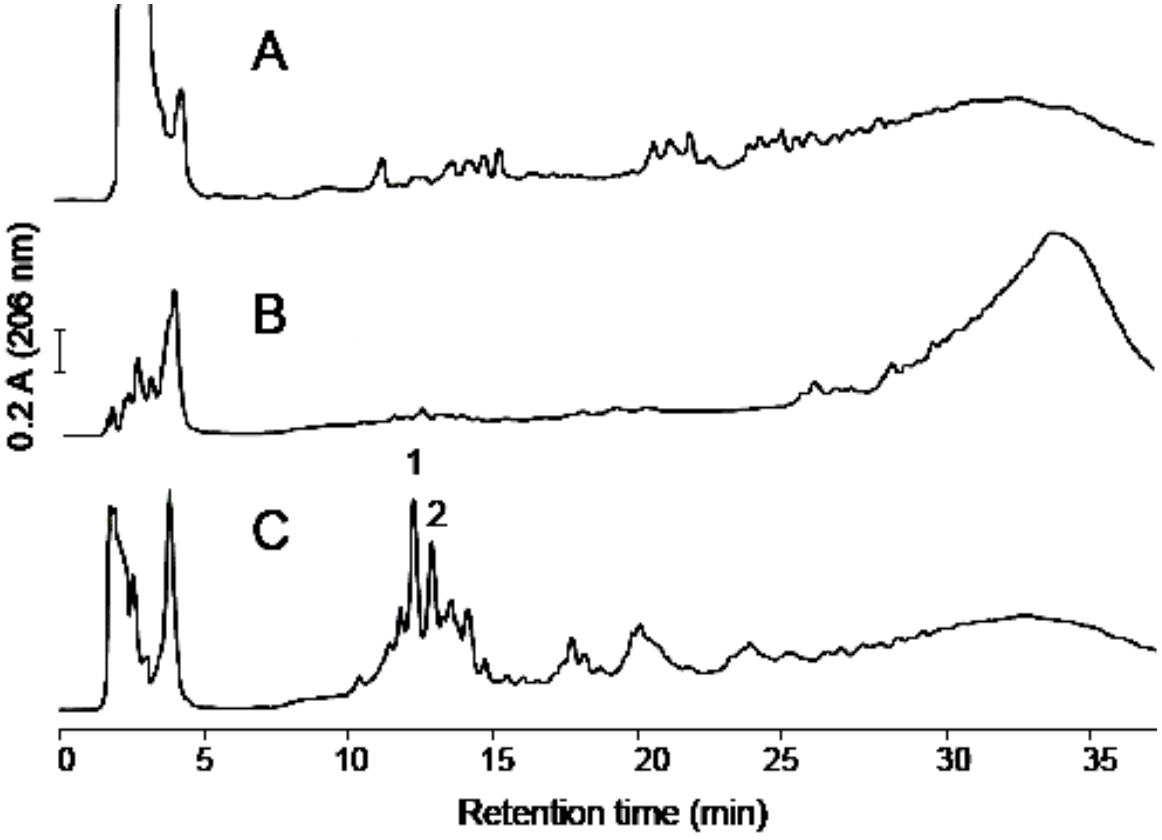

Fig. 25. Reversed-phase HPLC analysis of the soluble muropeptides released from *S. aureus* PG after incubation with AmiE-$R_{1,2}$ (A); lysostaphin (B) or both (C). Digested muropeptides were reduced with sodium borohydride and applied to a C18 nucleosil column. Peptides were eluted with a water/0.05% TFA to 25% acetonitrile/0.05% TFA gradient in 25 min. Peaks were detected by absorbance at

206 nm. Peaks 1 and 2 are the two major peaks generated from amidase-lysostaphin double digestion.

The masses are in close agreement with the peptide subunit structure L-Ala-D-iGln-L-Lys-$(Gly)_Y$-D-Ala-$(Gly)_X$, where X + Y= 5 and 6, respectively. Since lysostaphin cleaves within the glycine pentapeptide bridge (between Gly 2 and Gly 3, and Gly 3 and Gly 4), it is evident that amidase cleaves the amide bond between N-acetylmuramic acid and L-alanine.

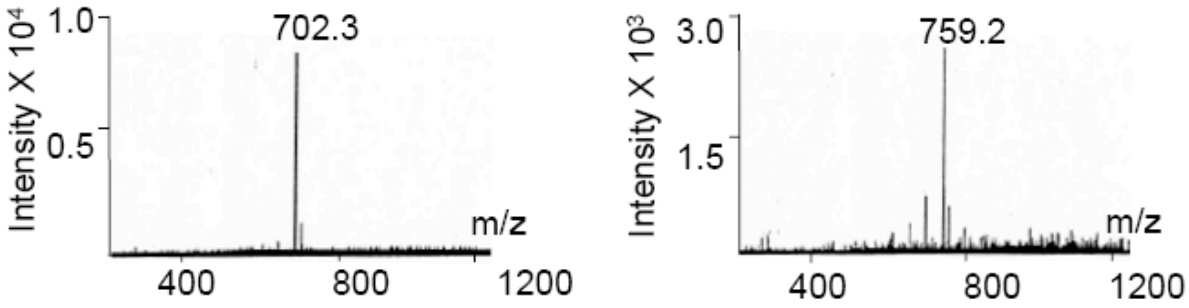

Fig. 26. HPLC fractions containing peaks 1 and 2 were analysed by LC-MS. The observed m/z of the ion signals are 702.3 and 759.2, which indicates the structures L-Ala-D-Gln-L-Lys-$(Gly)_2$-D-Ala-$(Gly)_3$ and L-Ala-D-Gln-L-Lys-$(Gly)_2$-D-Ala-$(Gly)_3$.

8. Isolation of Staphylococcal peptidoglycan fragments

8.1 Quantitative Isolation

To analyse quantitatively the peptidoglycan moiety of the *S. aureus*, it was essential to cleave the peptidoglycan structure by mutanolysin, which cleaves the β1-4 glycosidic bond between N-acetyl glucosamine and N-acetyl muramic acid. *S.aureus* mutanolysin solubilized PGN was reduced with $NaBH_4$ and separated on a reverse phase Prontosil C18 column. **Fig. 28** illustrates the muropeptide pattern of SA113 detected at 210 nm. Isolated peptidoglycan from Staphylococcal strains were digested with mutanolysin and/or lysostaphin. Digested muropeptides were reduced (**Fig. 27**) with sodium borohydride ($NaBH_4$). $NaBH_4$ reduces the glycosidic groups of amino sugars to its corresponding sugar alcohol. Reduced PGN fragments were separated by reverse phase HPLC using C18 column as described in Materials and Methods. Mutanolysin digestion generated muropeptides with different crosslinking,

starting from monomers to heigher oligomers. HPLC techniques were used to separate these oligomers from each other. Standarization of the isolation procedure of soluble PG fragments was essential to achieve more purified and defined peptidoglycan for different host signalling experiments.

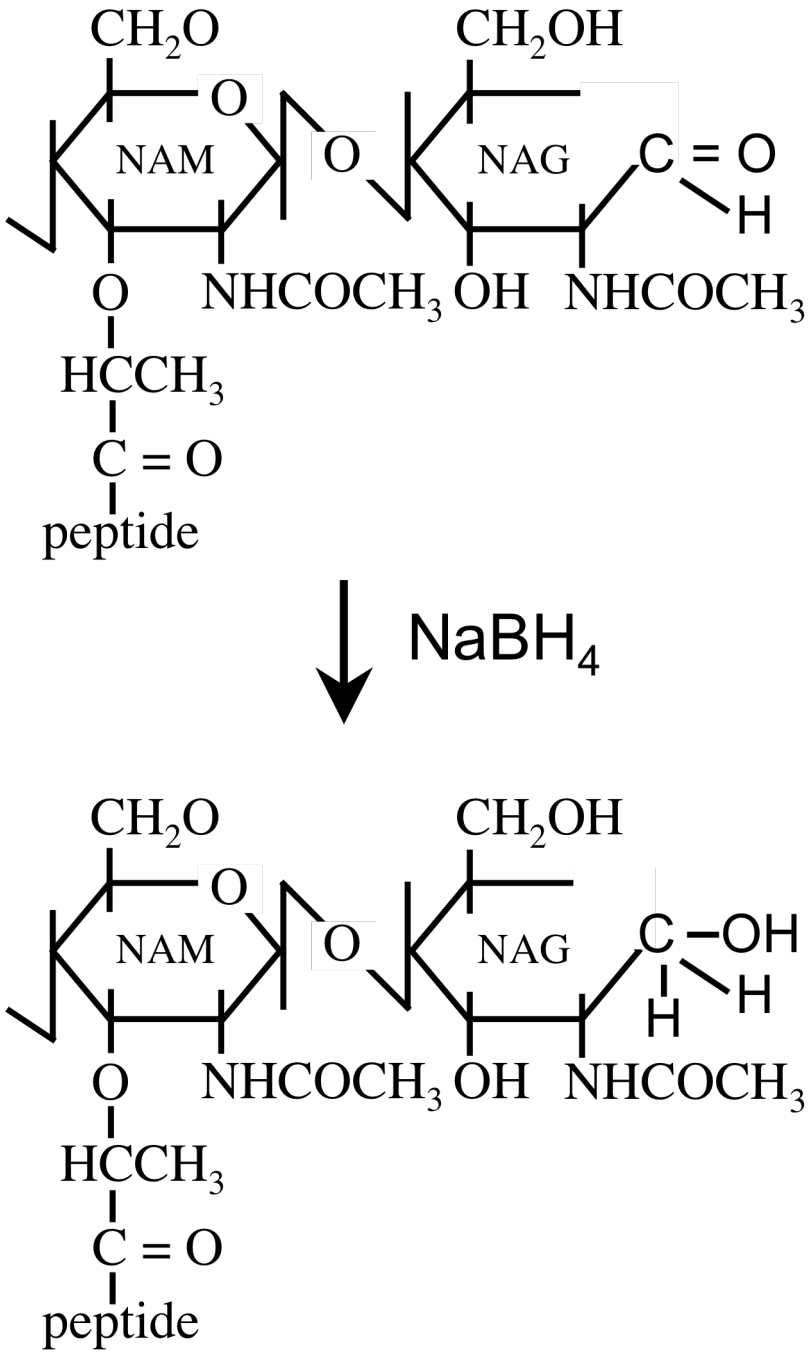

Fig. 27. Reduction of glycosidic groups of amino sugars to its corresponding sugar alcohol with sodium borohydride ($NaBH_4$). Reduction of peptidoglycan were necessary for proper separation of muropeptides by HPLC.

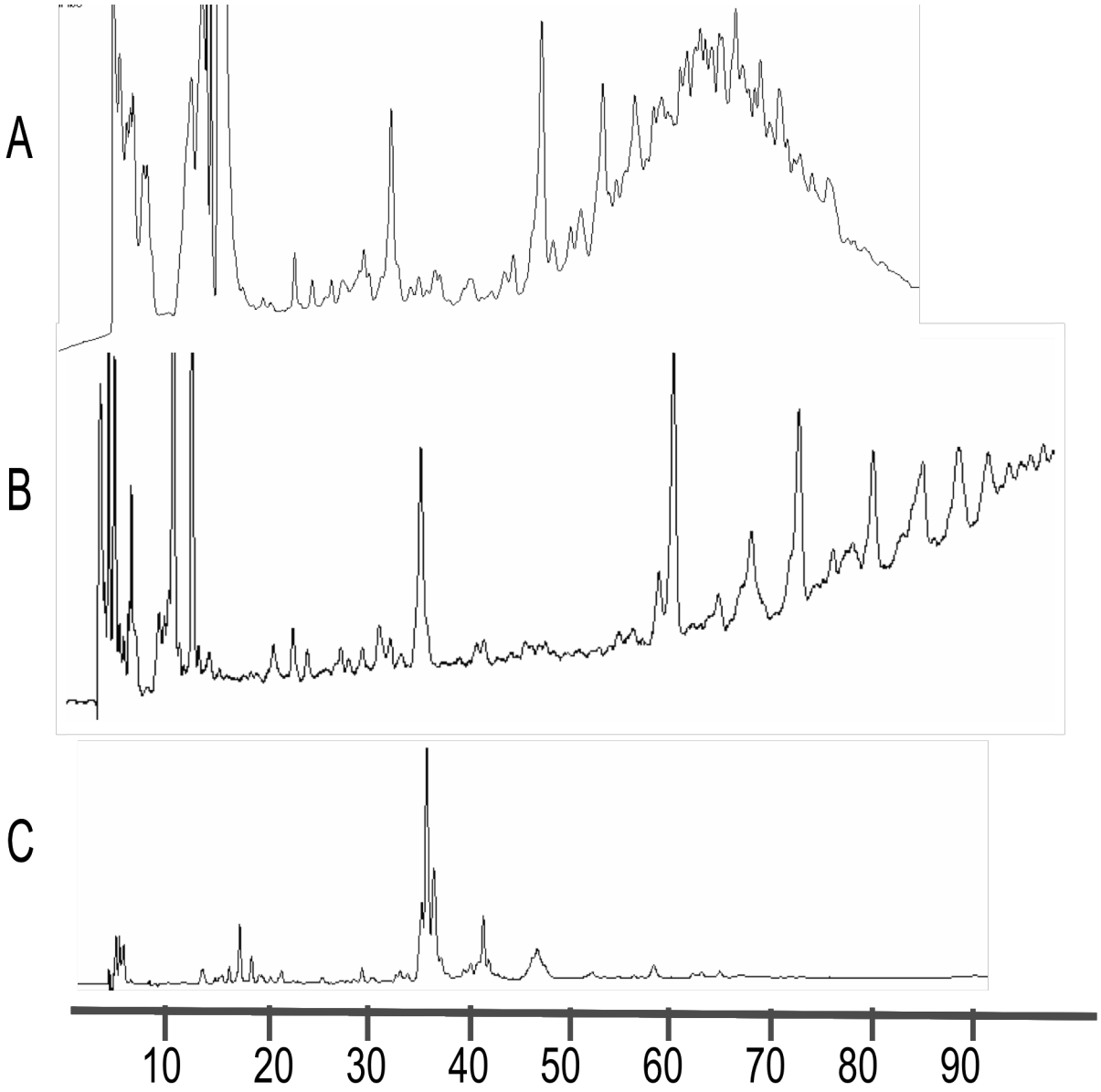

Fig. 28. Separation of staphylococcal cell wall muropeptides by reversed-phase HPLC. PG was obtained from *S. aureus* strain SA113 and digested with mutanolysin (A,B) or mutanolysin and lysostaphin (C). Muropeptides were reduced with $NaBH_4$ and separated using Prontosil C18; 3µ (125X 4.6 mm) column in a linear gradient of water to 25% acetonitrile for 120 mins (A), water to 30% methanol (B,C) using flow rate of 0.5 ml/ min.

However, peptidoglycan preparation can be easily contaminated with different lipoteichoic acids, wall teichoic acids, which cannot be visualized under UV or in the visible spectrum. PG fragments can also be contaminated with minute amounts of peptides or lipopeptides. To solve this problem we used different mutants of

Staphylococcus strains that are deficient in expressing cell wall associated molecules.

A list of mutants used for PG preparation are listed in Table 2:

Table2: List of Staphylococcal strains used for PG isolation.

Strains	**Properties**	**References**
SA113	Wild type strain	(Iordanescu and Surdeanu, 1976)
SAΔ*srt*A	Deficient in covalent linkage of surface proteins to PG	Dr. Günther Thumm, unpublished result
SAΔ*oat*A	Deficient in O-acetylation of the PG	(Bera *et al*., 2005a)
SAΔ*tag*O	Deficient in wall teichoic acid production	(Weidenmaier et al., 2005)
SAΔ*oat*AΔ*tag*O	Deficient in both O-acetylation of the PG and wall teichoic acid production	Agnieszka Bera, munuscript in review
SAΔ*dlt*	Deficient in lipidation of prolipoproteins	(Peschel et al., 1999)
SAΔ*lgt*	Deficient in D-alanylation of teichoic acids	(Stoll et al., 2005)

8.2 Identification of muropeptides

The composition of monomeric muropeptides released from the purified cell wall of the wild type, after mutanolysin /or lysostaphin digestion was determined by HPLC

and MALDI-TOF mass spectrometry (**Fig. 29**).

Peak 1 is comprised of a mixture of monomeric muropeptides with different numbers of glycine residues (**Fig. 29**): [M + Na+] 11047.515 m/z is consistent with GlcNAc-MurNAc-L-Ala-D-Gln-L-Lys-(Gly)-D-Ala-D-Ala, [M + Na+] 1147.52 m/z is consistent with GlcNAc-MurNAc-L-Ala-D-Gln-L-Lys(Gly_x)-D-Ala(Gly_y) with (x + y) = 4, [M + Na+] 1261.5 m/z is consistent with GlcNAc-MurNAc-L-Ala-D-Gln-L-Lys(Gly_x)-D-Ala(Gly_y) with (x + y) = 6, and [M + Na+] 1275.5 m/z is consistent with GlcNAc-MurNAc-L-Ala-D-Gln- L-Lys(Gly_x)- D-Ala(Gly_y)-D-Ala with (x + y) = 5 (**Fig. 29 A**). Peak 2 is comprised of a mixture of dimeric muropeptides with different numbers of glycine residues (**Fig. 29 B**): [M + Na+] 2368.012 and [M + Na+] 2440. [M + Na+] 2368.012 m/z is consistent with GlcNAc-MurNAc-L-Ala-D-Gln-L-Lys-(Gly_5-D-Ala-L-Lys(Gly_5)-D-Gln-L-Ala-MurNAc-GlcNAc)-D-Ala, [M + Na+] 2440.085 m/z is consisted with GlcNAc-MurNAc-L-Ala-D-Gln-L-Lys-(Gly_5-D-Ala-L-Lys(Gly_5)-D-Gln-L-Ala-MurNAc-GlcNAc)-D-Ala-D-Ala. We failed to detect the mass of higher oligomeric muropeptides.

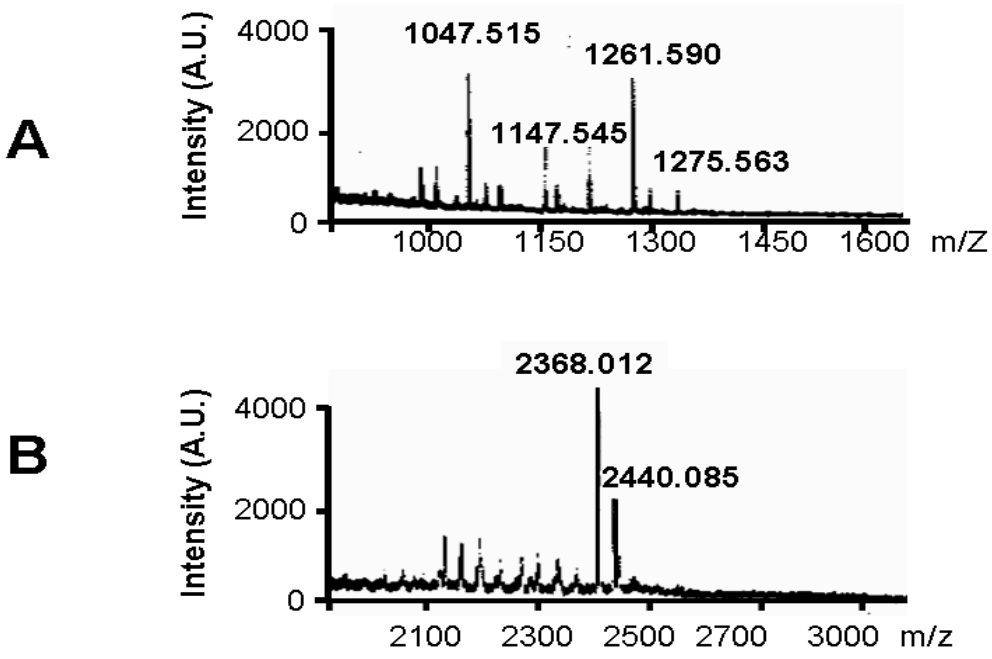

Fig. 29. MALDI-MS spectra of peak 1 (A) and 2 (B) generated by mutanolysin digestion.

Table. 3. MALDI-MS results indicating the observed mass and their proposed structures generated by mutanolysin-lysostaphin digested SA113 peptidoglycan.

Ion	m/z observed	proposed structure: GlcNAc-MurNAc-L-Ala-D-Gln-L-Lys(Gly_x)-D-Ala(Gly_Y)
M+H	1068.7	x+y=3
M+Na	1090.6	x+y=3
M+H	1125.7	x+y=4
M+Na	1147.7	x+y=4
M+H	1182.6	x+y=5
M+Na	1204.6	x+y=5
M+H	1239.6	x+y=6
M+Na	1261.6	x+y=6

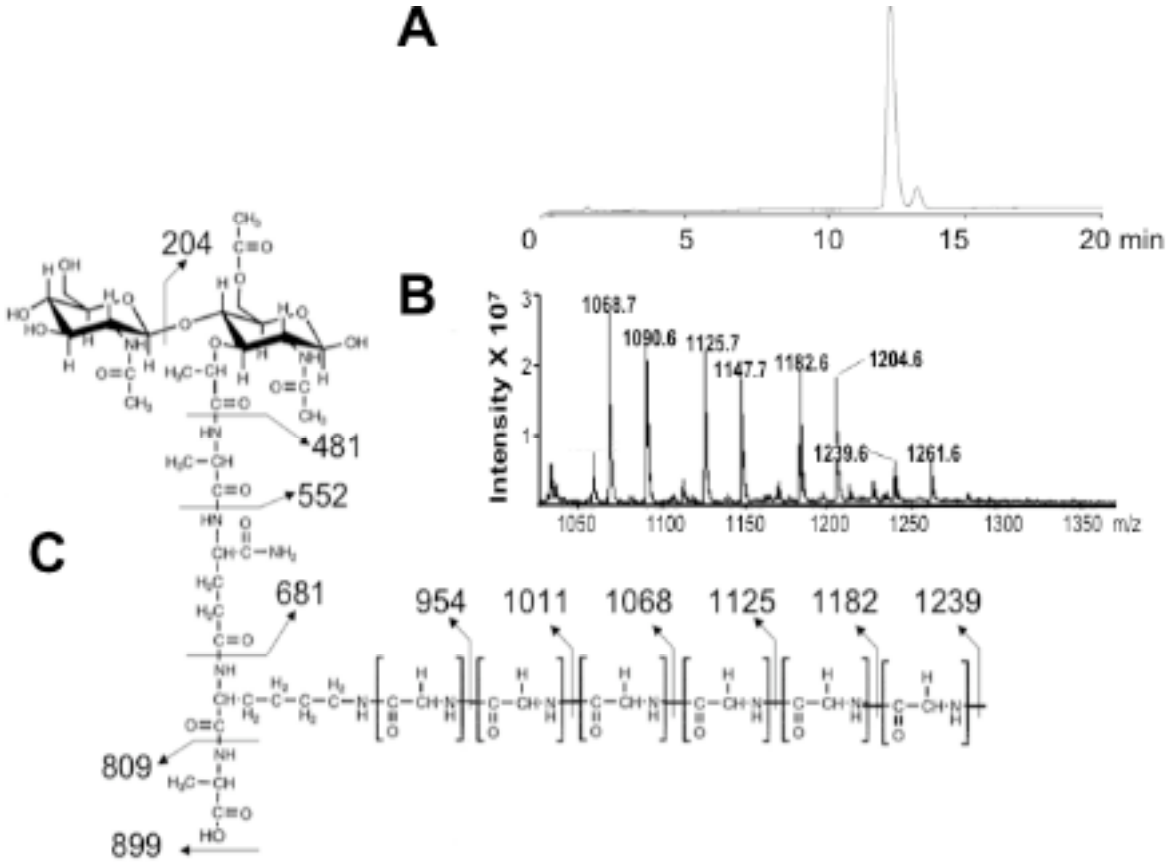

Fig. 30. HPLC analysis of mutanolysin-lysostaphin digested muropeptide (A) and MADI-MS (B) analysis. Proposed structure of the lysostaphin-solubilized compound generated after double digestion with mutanolysin and Lysostaphin (C).

When mutanolysin digested muropeptides were further digested with lysostaphin we got an enrichment of monomeric muropeptides. This monomeric PG

fragments were separated by HPLC using water-methanol gradient. Single monomeric peak was collected, dried and analysed by MALDI-MS. MALDI-MS results indicate that a single monomeric peak is a mixture of GlcNAc-MurNAc-pentapeptide, containing either different glycine residues or one extra alanine **(Fig. 30).** The structures predicted from the obtained masses are listed in Table 3.

E. DISCUSSION

We have constructed *atl*A and *aaa* deletion mutants by homologous recombination. The mutants can be complemented with plasmids encoding the corresponding genes (**Fig. 8, 9**). The major Atl amidase is curious in so far as the *atl* null mutant is affected in many respects and still its growth is hardly decreased in complex medium. The mutant cells form huge cell clusters (**Fig. 14**), and are defective in cell separation, form tetrad-shaped multicells that were septated but not separated from each other (**Fig. 15**), are unable to properly adhere to various surfaces that is responsible for their biofilm-negative phenotype (**Fig. 17**), and they produce much lower amounts of secreted and cell-wall bound proteins (**Fig. 10**). Apparently, whenever the major amidase gets mutated (Sugai *et al.*, 1995; Takahashi *et al.*, 2002) or attacked, abnormal cluster formation occurs. For example the addition of protease to exponentially growing cultures of *S. haemolyticus* that degrades the major amidase led to the formation of tetrad-shaped staphylococcal multicells (Yabu *et al.*, 1997).

The SAΔ*aaa*::*erm*B mutant did not differ from the wild type in its colony morphology (**Fig. 14**), growth rate, and cell cluster formation (**Fig. 15**), suggesting that Aaa does not play a major role in cell separation or, more probably, that the function of Aaa in cell separation may have been taken over by other autolysins, among them is the major autolysin Atl, which seemed to be more strongly expressed in the SAΔ*aaa*::*erm*B mutant than in the wild type (**Fig. 13**).

The question is why does such a multiple disadvantage of an SAΔ*atl*A::*spc* null mutant has ultimately so little impact on growth. It is thought that the other cell wall hydrolase, Aaa, (autolysin/adhesin from *S. aureus*) counterbalances to some extent the deleterious effect in the SA∆*atl*A::*spc* mutant. This is corroborated by the results observed with the zymogram where the lytic activity of Aaa is increased in the *atl* mutant, which is again decreased in the complemented strain (SA∆*atl*A::spc,pRC21). This illustrates that staphylococci are able to cope with the loss of Atl by up regulation of the Aaa expression. How this regulation occurs is unknown, but it appears to be a general phenomenon as it was also observed in the *atlE* mutant of *S. epidermidis*. However, Aaa up regulation is not sufficient to prevent cell aggregation, tetrad formation or to bring back the ability of biofilm formation. It appears that up regulation of Aaa is a regime for the extreme emergency; it allows survival but does

not cure the severe consequences of an atl mutation. After several trials we failed to construct a double mutant of SAΔ*atl*/*aaa* indicating that genetic deletion of both *aaa* and *atl* is probably lethal for the cell.

Involvement of multiple peptidoglycan hydrolases in cell separation has been reported in a number of other bacteria. For instance, three amidases, AmiA, B and C, are involved in cell separation of *E. coli* (Heidrich *et al.*, 2001). In *S. pneumoniae*, LytA and LytB are shown to be involved in cell separation (Severin *et al.*, 1997; Yother *et al.*, 1998) and further, in *Bacillus subtilis* LytF and CwlF are involved in cell separation (Ohnishi *et al.*, 1999). In these cases a single mutation has little effect on cell separation and the double or triple mutants showed a phenotypically impaired cell separation with extraordinarily long chain formation (Heidrich *et al.*, 2001; Ohnishi *et al.*, 1999). However, constructing a mutant lacking all the cell wall hydrolases was never possible.

We also attempted to determine the role of the three repetitive sequences located between the amidase and the glucosaminidase domains of the autolysins. Since AtlA and AtlE show essentially the same genetic organization, we chose AtlE for further studies. We have previously shown that an extracellular protease cleaves the two catalytic domains at valine-303 and leucine-845 in such a way that the amidase contains two repeat sequences (R1 and R2) at its C-terminus, and the glucosaminidase contains the R3 repeat at its N-terminus (Heilmann *et al.*, 1997b). It has been suggested that the repeat domains direct the 62-kDa amidase and 51-kDa glucosaminidase to a specific receptor at the equatorial surface ring of staphylococci, thereby allowing localized PG hydrolysis and separation of the dividing cells.

Here, we investigated PG binding and lytic activity of the amidase with and without the repeats (**Fig. 19**). Slight differences in lytic activity was observed in zymogram and in liquid assays (**Fig. 20**). Therefore, the repeat domains contribute little to the lytic activity. However, the repeat sequences play a role in PG binding (**Fig. 23**). Since both amidase and glucosaminidase are preferentially located at the equatorial surface ring, it is speculated that the repeat sequences $R_{1,2,3}$ probably have a higher affinity to premature PG structures. The cell wall targeting function of repeat sequences from autolysin/adhesin protein Aas of *Staphylococcus*

saprophyticus has been previously studied and similar results were obtained (Hell *et al.*, 1998).

We also addressed the question whether the Ami or Ami-$R_{1,2}$ show different activities with PG that lacks either wall teichoic acid, O-acetylation, or both. *S. aureus* PG is modified during the course of its biosynthesis. One modification comprises the linkage of cell wall teichoic acid; the other modification is the O-acetylation of the muramic acid residues at the C_6 position. Both modification steps were thought to be carried out extracellularly. Here we used isolated PG lacking O-acetylation or cell wall teichoic acid for binding studies with $R_{1,2,3}$ and found no evidence for preferential binding of either of these unmodified PG structures. Also no difference was observed in lysis activity. Therefore, cell wall teichoic acids apparently does not act as a binding anchor for the repeat sequences as was speculated earlier. The question by what particular cell wall structure or component Atl proteins are attached to the equatorial surface ring is still unanswered.

The Atl-derived amidase has been referred to as a N-acetylmuramyl-l-alanine amidase. However, no clear biochemical proof has been carried out. The designation was based on sequence similarity of its N-terminus with the N-terminus of the *Bacillus subtilis* cell wall hydrolase CwlA and the pneumococcal EJL bacteriophage amidase (Diaz *et al.*, 1992; Kuroda and Sekiguchi, 1990). We biochemically determined the exact cleavage site of amidase. The obtained masses of the two cleavage products obtained (**Fig. 26**) matched precisely with the sizes expected when PG is cleaved between N-acetylmuramic acid and L-alanine.

This study shows that the Atl derived amidase is necessary to cleave the amide bond that links the peptide subunit to the muramic acid residues in the glycan strands of the murein netting. As this is one of the crucial stress-bearing bonds in the murein sacculus, amidases are potentially autolytic enzymes. The specific function of Atl is the splitting of the septum during cell division to allow the separation of the daughter cells. Consequently, mutants deficient in *atl* are growing in large cell clusters. If one considers the multiple phenotypic alterations associated with the *atl* mutants, particularly the difficulties in the separation of daughter cells after cell division, it is surprising that growth and virulence were not affected much in these mutants.

We also attempted to study the peptidoglycan cleavage site of Aaa. After several attempts we failed to refold His tagged Aaa from the inclusion bodies. Aaa can be purified also under native conditions by growing the cells at 25°C. The native protein was soluble but misfolded. However, his-tagged Aaa was active in zymogram gel containing heat killed *S. aureus* cells. Surprisingly, Aaa was inactive against *M.luteus* cells in the zymogram gel. This result indicate that Aaa probably cleaves a peptide bond which is present in *Staphylococcus* but absent in *Micrococcus*. The major difference between *Staphylococcus* and *Micrococcus* peptidoglycan is the peptide cross bridges (**Fig. 31**) (Li *et al.*, 2000). In *Staphylococcus* muropeptides were cross-linked by penta glycin bridge, whereas in *Micrococcus* peptide cross-bridges were formed by D-Ala-L-lys-D-Glu-L-Ala.

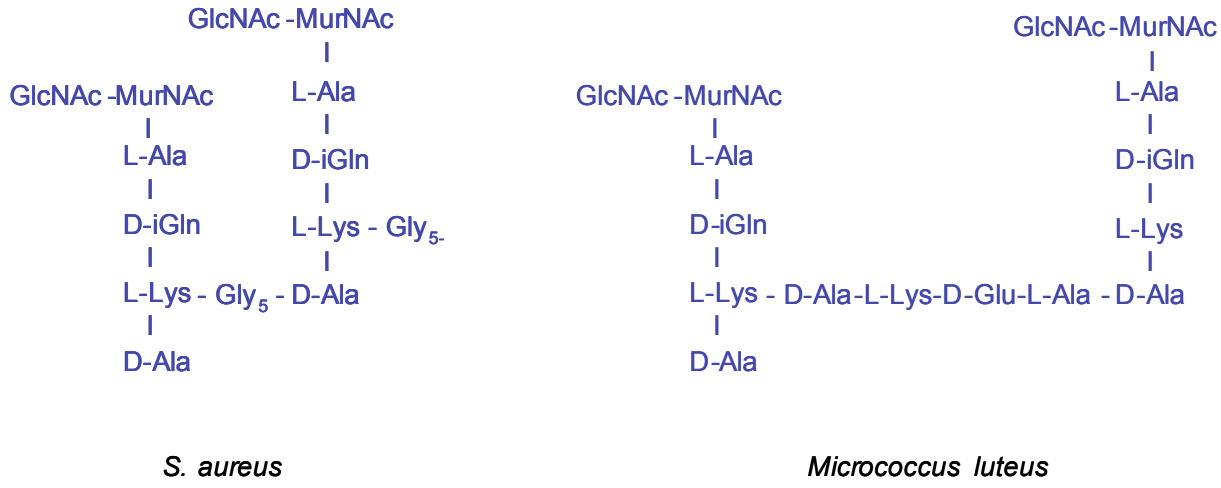

Fig. 31. Structure of *S. aureus* and *M. luteus* peptidoglycan. In *Staphylococcus* glutamate is amidated and peptides are cross-linked by a penta glycin bridge, whereas in *Micrococcus* glutamic acid is linked with one glycine and peptides are cross linked by D-Ala-L-lys-D-Glu-L-Ala (Li *et al.*, 2000).

Moreover, the glutamic acid of *Staphylococcus* peptidoglycan is amidated, whereas in *Micrococcus* peptidoglycan glutamic acid is linked with glycine. It is speculated that

Aaa either cleaves the peptide bond either in the cross bridges or between Ala-Gln/ Gln-lys. This speculation needs further experimental support.

Crystallization of AmiE (24 kDa) using vapour diffusion method was not successfull. One reason is the too low concentration of AmiE proteins. At higher concentrations AmiE tends to aggregate. A crystal is formed by numerous copies of a molecule becoming arranged in a tightly packed repeating motif. Well-ordered protein crystals are difficult to grow because proteins are large, irregularly shaped molecules that do not readily come together in a repeating pattern. The formation of a crystal is critically dependent on a number of factors, including pH, temperature, protein concentration, the nature of the solvent, the precipitant used, etc. Crystals form when molecules are slowly precipitated from solutions. With AmiE we observed a number of precipitaion zone with buffers containing polyethylene glycol. However, we did not observe any clear crystal. This result indicates that it could be possible to get the crystal at higher protein concentration. It is known that a His tag often decreases protein solubility. In order to acheive more concentrated protein we are now purifying amidase from pTX*atl*E (**Fig. 8**). This work is in progress.

We characterized the amidase from *Staphylococcus* and provide an extra tool for cleaving Staphylococcal peptidoglycan. Defined peptides structure can be isolated using amidase and can be used to study their role in eukaryotic cell signaling. It was shown earlier times that amidase digested *Streptococcus pneumoniae* walls displays proinflammatory activity (Majcherczyk *et al.*, 1999). To study the mechanism of peptidoglycan-induced inflammation, different types of Gram-positive wall materials were utilized. On the one hand large molecules such as insoluble cell walls and soluble peptidoglycan released from penicillin-treated staphylococci peptidoglycan structure carrying immunomodulatory activity. However, while very useful, these compounds might not be ideal for solving the structure-activity relationship between the wall degradation products occurring in the nature and their cytokine-releasing capacity. First, molecules such as insoluble peptidoglycan are very large and might be too complicated for refined analysis (Dziarski, 1991). Second, muramoyl dipeptide is not a natural product of wall degradation, and it has only limited cytokine-stimulatory power *in vitro* (Dokter *et al.*, 1994). To further explore this question, we attempted to isolate and characterize

amidase from *Staphylococcus*, so that we can mimic the natural condition of infection where small peptidoglycan fragments get released near the site of infection which mimics the digestion of Staphylococcal walls by their native autolysins, thereby liberating products of digestion that are likely to be found *in vivo*. Specifically, Staphylococcus contains a major autolytic enzyme, *N*-acetylmuramoyl-L-alanine amidase, which hydrolyzes the bonds between the glycan chain and the stem peptides that is mainly responsible for both wall solubilization and cell lysis during the stationary growth phase or during β-lactam treatment. Mutanolysin, lysostaphin and Amidase digested soluble fragments can be separated by reverse phase high pressure chromatography (HPLC). Individual fractions can be tested for their cell signalling activity.

By releasing murein products into the host, autolysins may also play a major role during infection. Indeed, *in vivo*, innate immunity to microbial pathogens relies on the specific detection of pathogen associated molecular patterns by specific host receptors. Recent finding suggest that the immune system of vertebrates uses a family of membrane receptors involved in the ‘ outside-in’ signalling (TLRs) and another set of cytoplasmic proteins that could be responsible for ‘ inside-in’ signalling. Toll like receptors recognize several pathogen associated molecules including lipoproteins, lipopolysaccharide, lipoteichoic acids and peptidoglycans. Nod factors sense bacterial peptidoglycans of intracellular invasive bacteria. After detection of bacterial products, these receptors induce the activation of proinflamatory signalling pathways. In this scheme, Atl and Aaa could contribute to the pathogenicity of *Staphylococcus* sp by controlling bacterial peptidoglycan structure and/ or release of more or less immunologically active cell wall components.

F. REFERENCES

Akira, S., and Sato, S. (2003) Toll-like receptors and their signaling mechanisms. *Scand J Infect Dis* **35**: 555-562.

Barton, G.M., and Medzhitov, R. (2002) Toll-like receptors and their ligands. *Curr Top Microbiol Immunol* **270**: 81-92.

Bauer, S., Kirschning, C.J., Hacker, H., Redecke, V., Hausmann, S., Akira, S., Wagner, H., and Lipford, G.B. (2001) Human TLR9 confers responsiveness to bacterial DNA via species-specific CpG motif recognition. *Proc Natl Acad Sci U S A* **98**: 9237-9242.

Bera, A., Herbert, S., Jakob, A., Vollmer, W., and Gotz, F. (2005a) Why are pathogenic staphylococci so lysozyme resistant? The peptidoglycan O-acetyltransferase OatA is the major determinant for lysozyme resistance of *Staphylococcus aureus*. *Mol Microbiol* **55**: 778-787.

Bera, A., Herbert, S., Jakob, A., Vollmer, W., and Götz, F. (2005b) Why are pathogenic staphylococci so lysozyme resistant? The peptidoglycan O-acetyltransferase OatA is the major determinant for lysozyme resistance of *Staphylococcus aureus*. *Mol Microbiol* **55**: 778-787.

Boneca, I.G. (2005) The role of peptidoglycan in pathogenesis. *Curr Opin Microbiol* **8**: 46-53.

Bruckner, R. (1997) Gene replacement in *Staphylococcus carnosus* and *Staphylococcus xylosus*. *FEMS Microbiol Lett* **151**: 1-8.

Brückner, R. (1997) Gene replacement in *Staphylococcus carnosu*s and *Staphylococcus xylosus*. *FEMS Microbiol Lett* **151**: 1-8.

Cabanes, D., Dussurget, O., Dehoux, P., and Cossart, P. (2004) Auto, a surface associated autolysin of *Listeria monocytogenes* required for entry into eukaryotic cells and virulence. *Mol Microbiol* **51**: 1601-1614.

Carlin, G., and Viitanen, E. (2005) In vitro pyrogenicity of the diphtheria, tetanus and acellular pertussis components of a trivalent vaccine. *Vaccine* **23**: 3709-3715.

Chamaillard, M., Girardin, S.E., Viala, J., and Philpott, D.J. (2003) Nods, Nalps and Naip: intracellular regulators of bacterial-induced inflammation. *Cell Microbiol* **5**: 581-592.

Chuang, T.H., Lee, J., Kline, L., Mathison, J.C., and Ulevitch, R.J. (2002) Toll-like receptor 9 mediates CpG-DNA signaling. *J Leukoc Biol* **71**: 538-544.

Cramton, S.E., Gerke, C., and Götz, F. (2001) In vitro methods to study staphylococcal biofilm formation. *Methods Enzymol* **336**: 239-255.

Crozat, K., and Beutler, B. (2004) TLR7: A new sensor of viral infection. *Proc Natl Acad Sci U S A* **101**: 6835-6836.

Dangl, J.L., and Jones, J.D. (2001) Plant pathogens and integrated defence responses to infection. *Nature* **411**: 826-833.

de Jonge, B.L., Chang, Y.S., Gage, D., and Tomasz, A. (1992) Peptidoglycan composition of a highly methicillin-resistant *Staphylococcus aureus* strain. The role of penicillin binding protein 2A. *J Biol Chem* **267**: 11248-11254.

Diaz, E., Lopez, R., and Garcia, J.L. (1992) EJ-1, a temperate bacteriophage of *Streptococcus pneumoniae* with a Myoviridae morphotype. *J Bacteriol* **174**: 5516-5525.

Dokter, W.H., Dijkstra, A.J., Koopmans, S.B., Stulp, B.K., Keck, W., Halie, M.R., and Vellenga, E. (1994) G(Anh)MTetra, a natural bacterial cell wall breakdown product, induces interleukin-1 beta and interleukin-6 expression in human monocytes. A study of the molecular mechanisms involved in inflammatory cytokine expression. *J Biol Chem* **269**: 4201-4206.

Dziarski, R. (1991) Demonstration of peptidoglycan-binding sites on lymphocytes and macrophages by photoaffinity cross-linking. *J Biol Chem* **266**: 4713-4718.

Dziarski, R. (2004) Peptidoglycan recognition proteins (PGRPs). *Mol Immunol* **40**: 877-886.

Dziarski, R., and Gupta, D. (2005) *Staphylococcus aureus* peptidoglycan is a toll-like receptor 2 activator: a reevaluation. *Infect Immun* **73**: 5212-5216.

Esen, N., and Kielian, T. (2006) Central Role for MyD88 in the Responses of Microglia to Pathogen-Associated Molecular Patterns. *J Immunol* **176**: 6802-6811.

Felix, G., Duran, J.D., Volko, S., and Boller, T. (1999) Plants have a sensitive perception system for the most conserved domain of bacterial flagellin. *Plant J* **18**: 265-276.

Felix, G., and Boller, T. (2003) Molecular sensing of bacteria in plants. The highly conserved RNA-binding motif RNP-1 of bacterial cold shock proteins is recognized as an elicitor signal in tobacco. *J Biol Chem* **278**: 6201-6208.

Fitzgerald, K.A., Rowe, D.C., Barnes, B.J., Caffrey, D.R., Visintin, A., Latz, E., Monks, B., Pitha, P.M., and Golenbock, D.T. (2003) LPS-TLR4 signaling to

IRF-3/7 and NF-kappaB involves the toll adapters TRAM and TRIF. *J Exp Med* **198**: 1043-1055.

Ghuysen, J.M., and Strominger, J.L. (1963a) Structure of the Cell Wall of *Staphylococcus aureus*, Strain Copenhagen. I. Preparation of Fragments by Enzymatic Hydrolysis. *Biochemistry* **2**: 1110-1119.

Ghuysen, J.M., and Strominger, J.L. (1963b) Structure of the Cell Wall of *Staphylococcus aureus*, Strain Copenhagen. Ii. Separation and Structure of Disaccharides. *Biochemistry* **2**: 1119-1125.

Girardin, S.E., Travassos, L.H., Herve, M., Blanot, D., Boneca, I.G., Philpott, D.J., Sansonetti, P.J., and Mengin-Lecreulx, D. (2003) Peptidoglycan molecular requirements allowing detection by Nod1 and Nod2. *J Biol Chem* **278**: 41702-41708.

Götz, F. (2002) *Staphylococcus* and biofilms. *Mol Microbiol* **43**: 1367-1378.

Grundling, A., and Schneewind, O. (2006) Cross-linked peptidoglycan mediates lysostaphin binding to the cell wall envelope of *Staphylococcus aureus*. *J Bacteriol* **188**: 2463-2472.

Guerout-Fleury, A.M., Shazand, K., Frandsen, N., and Stragier, P. (1995) Antibiotic-resistance cassettes for *Bacillus subtilis*. *Gene* **167**: 335-336.

Hadley, J.S., Wang, J.E., Foster, S.J., Thiemermann, C., and Hinds, C.J. (2005) Peptidoglycan of *Staphylococcus aureus* upregulates monocyte expression of CD14, Toll-like receptor 2 (TLR2), and TLR4 in human blood: possible implications for priming of lipopolysaccharide signaling. *Infect Immun* **73**: 7613-7619.

Hanahan, D. (1983) Studies on transformation of *Escherichia coli* with plasmids. *J Mol Biol* **166**: 557-580.

Heidrich, C., Templin, M.F., Ursinus, A., Merdanovic, M., Berger, J., Schwarz, H., de Pedro, M.A., and Holtje, J.V. (2001) Involvement of N-acetylmuramyl-L-alanine amidases in cell separation and antibiotic-induced autolysis of *Escherichia coli*. *Mol Microbiol* **41**: 167-178.

Heilmann, C., Gerke, C., Perdreau-Remington, F., and Götz, F. (1996) Characterization of *Tn*917 insertion mutants of *Staphylococcus epidermidis* affected in biofilm formation. *Infect Immun* **64**: 277-282.

Heilmann, C., Hussain, M., Peters, G., and Gotz, F. (1997a) Evidence for autolysin-mediated primary attachment of *Staphylococcus epidermidis* to a polystyrene surface. *Mol Microbiol* **24**: 1013-1024.

Heilmann, C., Hussain, M., Peters, G., and Götz, F. (1997b) Evidence for autolysin-mediated primary attachment of *Staphylococcus epidermidis* to a polystyrene surface. *Mol Microbiol* **24**: 1013-1024.

Heilmann, C., Thumm, G., Chhatwal, G.S., Hartleib, J., Uekotter, A., and Peters, G. (2003) Identification and characterization of a novel autolysin (Aae) with adhesive properties from *Staphylococcus epidermidis*. *Microbiology* **149**: 2769-2778.

Heilmann, C., Hartleib, J., Hussain, M.S., and Peters, G. (2005) The multifunctional *Staphylococcus aureus* autolysin aaa mediates adherence to immobilized fibrinogen and fibronectin. *Infect Immun* **73**: 4793-4802.

Hell, W., Meyer, H.G., and Gatermann, S.G. (1998) Cloning of aas, a gene encoding a *Staphylococcus saprophyticus* surface protein with adhesive and autolytic properties. *Mol Microbiol* **29**: 871-881.

Hirschfeld, M., Kirschning, C.J., Schwandner, R., Wesche, H., Weis, J.H., Wooten, R.M., and Weis, J.J. (1999) Cutting edge: inflammatory signaling by *Borrelia burgdorferi* lipoproteins is mediated by toll-like receptor 2. *J Immunol* **163**: 2382-2386.

Huard, C., Miranda, G., Wessner, F., Bolotin, A., Hansen, J., Foster, S.J., and Chapot-Chartier, M.P. (2003) Characterization of AcmB, an N-acetylglucosaminidase autolysin from *Lactococcus lactis*. *Microbiology* **149**: 695-705.

Iordanescu, S., and Surdeanu, M. (1976) Two restriction and modification systems in *Staphylococcus aureus* NCTC8325. *J Gen Microbiol* **96**: 277-281.

Janssens, S., and Beyaert, R. (2003) Role of Toll-like receptors in pathogen recognition. *Clin Microbiol Rev* **16**: 637-646.

Jayaswal, R.K., Lee, Y.I., and Wilkinson, B.J. (1990) Cloning and expression of a *Staphylococcus aureus* gene encoding a peptidoglycan hydrolase activity. *J Bacteriol* **172**: 5783-5788.

Kirschning, C.J., and Schumann, R.R. (2002) TLR2: cellular sensor for microbial and endogenous molecular patterns. *Curr Top Microbiol Immunol* **270**: 121-144.

Kreiswirth, B.N., Lofdahl, S., Betley, M.J., O'Reilly, M., Schlievert, P.M., Bergdoll, M.S., and Novick, R.P. (1983) The toxic shock syndrome exotoxin structural gene is not detectably transmitted by a prophage. *Nature* **305**: 709-712.

Kuroda, A., and Sekiguchi, J. (1990) Cloning, sequencing and genetic mapping of a *Bacillus subtilis* cell wall hydrolase gene. *J Gen Microbiol* **136**: 2209-2216.

Kyte, J., and Doolittle, R.F. (1982) A simple method for displaying the hydropathic character of a protein. *J Mol Biol* **157**: 105-132.

Li, S., Norioka, S., and Sakiyama, F. (2000) Purification, characterization, and primary structure of a novel cell wall hydrolytic amidase, CwhA, from *Achromobacter lyticus*. *J Biochem (Tokyo)* **127**: 1033-1039.

Liu, C., Xu, Z., Gupta, D., and Dziarski, R. (2001) Peptidoglycan recognition proteins: a novel family of four human innate immunity pattern recognition molecules. *J Biol Chem* **276**: 34686-34694.

Majcherczyk, P.A., Langen, H., Heumann, D., Fountoulakis, M., Glauser, M.P., and Moreillon, P. (1999) Digestion of *Streptococcus pneumoniae* cell walls with its major peptidoglycan hydrolase releases branched stem peptides carrying proinflammatory activity. *J Biol Chem* **274**: 12537-12543.

Mattsson, E., Herwald, H., Bjorck, L., and Egesten, A. (2002) Peptidoglycan from *Staphylococcus aureus* induces tissue factor expression and procoagulant activity in human monocytes. *Infect Immun* **70**: 3033-3039.

Navarre, W.W., Ton-That, H., Faull, K.F., and Schneewind, O. (1999) Multiple enzymatic activities of the murein hydrolase from staphylococcal phage phi11. Identification of a D-alanyl-glycine endopeptidase activity. *J Biol Chem* **274**: 15847-15856.

Ohnishi, R., Ishikawa, S., and Sekiguchi, J. (1999) Peptidoglycan hydrolase LytF plays a role in cell separation with CwlF during vegetative growth of *Bacillus subtilis*. *J Bacteriol* **181**: 3178-3184.

Oshida, T., Sugai, M., Komatsuzawa, H., Hong, Y.M., Suginaka, H., and Tomasz, A. (1995) A *Staphylococcus aureus* autolysin that has an N-acetylmuramoyl-L-alanine amidase domain and an endo-beta-N-acetylglucosaminidase domain: cloning, sequence analysis, and characterization. *Proc Natl Acad Sci U S A* **92**: 285-289.

Perry, A.M., Ton-That, H., Mazmanian, S.K., and Schneewind, O. (2002) Anchoring of surface proteins to the cell wall of *Staphylococcus aureus*. III. Lipid II is an in vivo peptidoglycan substrate for sortase-catalyzed surface protein anchoring. *J Biol Chem* **277**: 16241-16248.

Peschel, A., Ottenwalder, B., and Gotz, F. (1996) Inducible production and cellular location of the epidermin biosynthetic enzyme EpiB using an improved staphylococcal expression system. *FEMS Microbiol Lett* **137**: 279-284.

Peschel, A., Otto, M., Jack, R.W., Kalbacher, H., Jung, G., and Gotz, F. (1999) Inactivation of the dlt operon in *Staphylococcus aureus* confers sensitivity to

defensins, protegrins, and other antimicrobial peptides. *J Biol Chem* **274**: 8405-8410.

Pucci, M.J., Thanassi, J.A., Ho, H.T., Falk, P.J., and Dougherty, T.J. (1995) *Staphylococcus haemolyticus* contains two D-glutamic acid biosynthetic activities, a glutamate racemase and a D-amino acid transaminase. *J Bacteriol* **177**: 336-342.

Schindler, C.A., and Schuhardt, V.T. (1964) Lysostaphin: a New Bacteriolytic Agent for the Staphylococcus. *Proc Natl Acad Sci U S A* **51**: 414-421.

Schleifer (1982) Description of a new species of the genus staphylococcus: *Staphylococcus carnosus*. *Int J Sys Bacteriol* **32**: 153-156.

Severin, A., Horne, D., and Tomasz, A. (1997) Autolysis and cell wall degradation in a choline-independent strain of *Streptococcus pneumoniae*. *Microb Drug Resist* **3**: 391-400.

Steinmetz, M., and Richter, R. (1994) Plasmids designed to alter the antibiotic resistance expressed by insertion mutations in *Bacillus subtilis*, through in vivo recombination. *Gene* **142**: 79-83.

Stoll, H., Dengjel, J., Nerz, C., and Gotz, F. (2005) *Staphylococcus aureus* deficient in lipidation of prelipoproteins is attenuated in growth and immune activation. *Infect Immun* **73**: 2411-2423.

Strober, W., Murray, P.J., Kitani, A., and Watanabe, T. (2006) Signalling pathways and molecular interactions of NOD1 and NOD2. *Nat Rev Immunol* **6**: 9-20.

Strominger, J.L., and Ghuysen, J.M. (1967) Mechanisms of enzymatic bacteriaolysis. Cell walls of bacteri are solubilized by action of either specific carbohydrases or specific peptidases. *Science* **156**: 213-221.

Sugai, M., Komatsuzawa, H., Akiyama, T., Hong, Y.M., Oshida, T., Miyake, Y., Yamaguchi, T., and Suginaka, H. (1995) Identification of endo-beta-N-acetylglucosaminidase and N-acetylmuramyl-L-alanine amidase as cluster-dispersing enzymes in *Staphylococcus aureus*. *J Bacteriol* **177**: 1491-1496.

Swaminathan, C.P., Brown, P.H., Roychowdhury, A., Wang, Q., Guan, R., Silverman, N., Goldman, W.E., Boons, G.J., and Mariuzza, R.A. (2006) Dual strategies for peptidoglycan discrimination by peptidoglycan recognition proteins (PGRPs). *Proc Natl Acad Sci U S A* **103**: 684-689.

Takahashi, J., Komatsuzawa, H., Yamada, S., Nishida, T., Labischinski, H., Fujiwara, T., Ohara, M., Yamagishi, J., and Sugai, M. (2002) Molecular characterization of an *atl* null mutant of *Staphylococcus aureus*. *Microbiol Immunol* **46**: 601-612.

Takeuchi, O., Hoshino, K., Kawai, T., Sanjo, H., Takada, H., Ogawa, T., Takeda, K., and Akira, S. (1999) Differential roles of TLR2 and TLR4 in recognition of gram-negative and gram-positive bacterial cell wall components. *Immunity* **11**: 443-451.

Takeuchi, O., and Akira, S. (2001) Toll-like receptors; their physiological role and signal transduction system. *Int Immunopharmacol* **1**: 625-635.

Tallant, T., Deb, A., Kar, N., Lupica, J., de Veer, M.J., and DiDonato, J.A. (2004) Flagellin acting via TLR5 is the major activator of key signaling pathways leading to NF-kappa B and proinflammatory gene program activation in intestinal epithelial cells. *BMC Microbiol* **4**: 33.

Tipper, D.J., Katz, W., Strominger, J.L., and Ghuysen, J.M. (1967) Substituents on the alpha-carboxyl group of D-glutamic acid in the peptidoglycan of several bacterial cell walls. *Biochemistry* **6**: 921-929.

Tipper, D.J., Tomoeda, M., and Strominger, J.L. (1971) Isolation and characterization of 1,4-N-acetylmuramyl-N- acetylglucosamine and its O-acetyl derivative. *Biochemistry* **10**: 4683-4690.

Travassos, L.H., Girardin, S.E., Philpott, D.J., Blanot, D., Nahori, M.A., Werts, C., and Boneca, I.G. (2004) Toll-like receptor 2-dependent bacterial sensing does not occur via peptidoglycan recognition. *EMBO Rep* **5**: 1000-1006.

Wang, Q., Dziarski, R., Kirschning, C.J., Muzio, M., and Gupta, D. (2001) Micrococci and peptidoglycan activate TLR2-->MyD88-->IRAK-->TRAF-->NIK-->IKK-->NF-kappaB signal transduction pathway that induces transcription of interleukin-8. *Infect Immun* **69**: 2270-2276.

Weidenmaier, C., Kokai-Kun, J.F., Kristian, S.A., Chanturiya, T., Kalbacher, H., Gross, M., Nicholson, G., Neumeister, B., Mond, J.J., and Peschel, A. (2004) Role of teichoic acids in *Staphylococcus aureus* nasal colonization, a major risk factor in nosocomial infections. *Nat Med* **10**: 243-245.

Weidenmaier, C., Peschel, A., Xiong, Y.Q., Kristian, S.A., Dietz, K., Yeaman, M.R., and Bayer, A.S. (2005) Lack of wall teichoic acids in *Staphylococcus aureus* leads to reduced interactions with endothelial cells and to attenuated virulence in a rabbit model of endocarditis. *J Infect Dis* **191**: 1771-1777.

Wieland, K.P., Wieland, B., and Gotz, F. (1995) A promoter-screening plasmid and xylose-inducible, glucose-repressible expression vectors for *Staphylococcus carnosus*. *Gene* **158**: 91-96.

Yabu, K., Nishiyama, Y., and Ochiai, T. (1997) Protease-induced multicell formation in *Staphylococcus haemolyticus*. *Microbiol Immunol* **41**: 799-803.

Yamamoto, M., Yamazaki, S., Uematsu, S., Sato, S., Hemmi, H., Hoshino, K., Kaisho, T., Kuwata, H., Takeuchi, O., Takeshige, K., Saitoh, T., Yamaoka, S., Yamamoto, N., Yamamoto, S., Muta, T., Takeda, K., and Akira, S. (2004) Regulation of Toll/IL-1-receptor-mediated gene expression by the inducible nuclear protein IkappaBzeta. *Nature* **430**: 218-222.

Yoshimura, A., Lien, E., Ingalls, R.R., Tuomanen, E., Dziarski, R., and Golenbock, D. (1999) Cutting edge: recognition of Gram-positive bacterial cell wall components by the innate immune system occurs via Toll-like receptor 2. *J Immunol* **163**: 1-5.

Yother, J., Leopold, K., White, J., and Fischer, W. (1998) Generation and properties of a *Streptococcus pneumoniae* mutant which does not require choline or analogs for growth. *J Bacteriol* **180**: 2093-2101.

Acknowledgements

As I stand at the threshold of earning my doctorate, I am overwhelmed when I recall all the people who have helped me get this far. First and foremost, I would like to thank my Ph.D. advisor, Professor Friedrich Götz, for his constant support, guidance, and inspiration. Professor Götz is a truly remarkable advisor who grants students a lot of freedom to explore new ideas, but at the same time interacts closely with them. I have greatly benefited both from his excellent technical advice and from his role-model as a successful team leader and researcher. I look forward to continuing my association with him in the future. I am indebted to Dr. Günther Thumm and Dr. Bernhard Krismer for introducing me to Molecular Biological techniques. I would like to thank Mulugeta Nega for providing me generous support, beginning from the first day of my Phd. I would like to thank Dr. Andreas Peschel, Dr.Waldemar Vollmer, Profesor Dr. Volkmar Braun for critical remarks. My graduate student career has also been enriched by interactions with several researchers including Dr. Ralf Rosenstein, Dr. Silvia Herbert, Christiane Zell, Timo Birkenstock, Agnieszka Bera, Steffen Schlag, Till Albrecht, Regine Stemmler and Qiang Gao. I would like to thank them all. This work was supported primarily by the DFG: Graduate College "Infection biology" (GKI 685) and Forschergruppe (FOR 449/1).

Many thanks to my friends Julia Buschmann and Melani Kull for every help they provided during last few years. I would like to thank all my teachers, from elementary school through graduate school, for providing me with an excellent education. I am particularly indebted to my professors at the Madurai Kamaraj University, particularly Prof Dr. S. Krishnaswamy for giving me a solid foundation in Biological Sciences.

Most important of all, I would like to express my gratitude to my family for being an unstinting source of support and encouragement. My grandparents have inspired me through their courage in overcoming the challenges of life. My parents have taught me the value of education and have worked hard to provide me the very best of it. They have always been there when I have needed them.

Curriculum Vitae

Name	Raja Biswas
Date of birth	06.01.1975
Place of birth	Bishnupur, West Bengal
Nationality	Indian

Education

1991	Board of Secondary School Education, Behala Aryya Vidya Mandir, Calcutta, West Bengal, India
1991-1993	Board of Intermediate Education, St. Xavier´s College, Calcutta, West Bengal, India
1993-1997	**Bachelor of Science**, Bidhan Chandra Krishi Viswavidyalaya,Nadia, West Bengal, India
1998-2000	**Master of Science** (Biotechnology), Madurai Kamaraj University, Madurai, Tamil Nadu, India **Thesis**: Purification and characterization of OmpC from *E. coli*. **Supervisor**: Prof Dr. S. Krishnaswamy
2002-2006	**Ph.D.**, Institute of Microbial Genetics. University of Tuebingen, Tuebingen. **Dissertation**: **Characterization of Staphylococcal peptidoglycan hydrolases and isolation of defined peptidoglycan structures.** **Supervisor:** Prof. Dr. F. Götz